Two-Dimensional Hydrodynamic Simulation of Surface-Water Flow and Transport to Florida Bay through the Southern Inland and Coastal Systems (SICS)

By Eric D. Swain, Melinda A. Wolfert, Jerad D. Bales, *and* Carl R. Goodwin

U.S. Geological Survey

Water-Resources Investigations Report 03-4287

Prepared as part of the

U.S. Geological Survey Priority Ecosystem Science Program and the

National Park Service Critical Ecosystem Studies Initiative

Tallahassee, Florida
2004

U.S. DEPARTMENT OF THE INTERIOR
GALE A. NORTON, Secretary

U.S. GEOLOGICAL SURVEY
Charles G. Groat, Director

Use of trade, product, or firm names in this publication is for descriptive purposes only and does not imply endorsement by the U.S. Geological Survey.

For additional information write to:

U.S. Geological Survey
2010 Levy Avenue
Tallahassee, FL 32310

Copies of this report can be purchased from:

U.S. Geological Survey
Branch of Information Services
Box 25286
Denver, CO 80225-0286
888-ASK-USGS

Additional information about water resources in Florida is available on the internet at **http://fl.water.usgs.gov**

CONTENTS

Abstract 1
Introduction 2
- Purpose and Scope 2
- Description of Study Area 4
- Previous Studies 6

Approach 8
- Model Selection and Required Enhancements 8
- Data 9
  - Topography 10
  - Vegetation 10
  - Water Level, Currents, and Discharge 11
  - Salinity 11
  - Rainfall, Wind and Solar Radiation 11
- Process Studies in Support of Model Development 15
- Model Construction, Calibration, Testing, and Application 16

Description of Model Structure 16
- Governing Equations 17
- Numerical Solution Technique 18
- Model Input Requirements 18
- Enhancements for Everglades Application 20
  - Rainfall as a Time-Varying Point Source 20
  - Spatially Detailed Evapotranspiration Calculations 20
  - Wind-Sheltering Coefficient 21
  - Computational Cells Adjacent to Flow Barriers 21
  - Other Code Modifications 21

Construction, Calibration, Testing, and Application of Flow and Transport Model 22
- Computational Model Domain 22
- Boundary Conditions 22
  - Water-Surface Boundary 22
  - Lateral Boundaries 25
- Model Parameters 28
  - Computational Control Parameters 28
  - Wind Coefficients 29
  - Evapotranspiration 29
  - Frictional Resistance — Vegetation 30
  - Flow Coefficient — Coastal Creeks 30
  - Dispersion Coefficient 33
- Calibration 33
- Testing 36
  - Verification 36
  - Sensitivity Analysis 40
- Model Application Examples 44
  - Flow Estimates at Unmeasured Locations 44
  - Water Ponding and Salinity Distribution for Different Inflow and Wind Conditions 47
  - Using SICS Model for Restoration Testing 48

Conclusions 50
References Cited 50
Appendix I—SWIFT2D Subroutines Modified for Southern Inland and Coastal Systems (SICS) 55
Appendix II—Excerpt from Input File Highlighting Areal Gains and Losses 56

PLATES [in back pocket]

1. Maps showing water levels and unit discharges for verification simulation
2. Plots showing water-level time series at field stations for verification simulation
3. Map of wetland flow velocities for verification simulation, July 29-31, 1997
4. Maps showing salinity distribution in verification simulation
5. Maps showing effects of wind and Taylor Slough bridge flows on water levels
6. Maps showing effects of wind and Taylor Slough bridge flows on salinity

FIGURES

1-6. Maps showing:
1. Southern Inland and Coastal Systems (SICS) study area and selected data-collection sites 3
2. Discharge, conductivity, and water-level data-collection sites within the study area 5
3. Apparent resistivity in the Southern Inland and Coastal Systems (SICS) study area at 5-meter depth below land surface 7
4. Vegetation features in the Southern Inland and Coastal Systems (SICS) study area 12
5. Location of acoustic Doppler velocimeter measurements in the Southern Inland and Coastal Systems (SICS) study area 14
6. Map showing rainfall data-collection sites 15
7. Space-staggered grid used in SWIFT2D 19
8-10. Maps showing:
8. Model grid, location of embankment barriers, and location of creeks in the study area 23
9. Land-surface elevation in grid cells 24
10. Model boundaries and data-collection sites used to determine discharge, conductivity, and water-level boundary conditions 26
11-13. Graphs showing spectral function of stage:
11. Downstream of structure S-21 27
12. At McCormick Creek 28
13. At Trout Creek 28
14. Map showing Manning's *n* values used in the model 31
15. Time-series plots showing measured and computed salinities at coastal creeks for calibration simulation in September 1997 34
16. Maps showing salinity distributions from the calibration simulation 35
17. Time-series plots showing measured and computed flows at coastal creeks for calibration simulation in September 1997 37
18. Map of wetland flow velocities for calibration simulation, September 22, 24, and 25, 1997 38
19-21. Graphs showing:
19. Measured and computed creek flows for verification simulation, August 1996 to July 1997 39
20. Model-computed flows at each section for verification simulation and map showing flow cross sections for Joe Bay 45
21. Model-computed flows at selected coastal creeks for verification simulation, August 1996 to July 1997 46
22. Hydrograph showing differences in computed flow at Trout Creek with and without wind effects for verification simulation 47
23. Hydrographs showing measured and estimated daily mean flows for Taylor Slough bridge, 1989-99 49

TABLES

1. Hydrologic and meteorological data-collection sites for the Southern Inland and Coastal Systems (SICS) study 13
2. Summary of studies and research investigations used to develop the Southern Inland and Coastal Systems (SICS) model 16
3. Stream friction terms and lengths and Manning's *n* 32
4. Results of sensitivity analysis 42
5. Summary of sensitivity tests for coastal creeks 44

CONVERSION FACTORS, DATUMS, ABBREVIATIONS, AND ACRONYMS

Multiply	By	To obtain
meter (m)	3.281	foot
meter per second (m/s)	3.281	foot per second
meter squared per day (m^2/d)	10.76	foot squared per day
meter squared per second (m^2/s)	10.76	foot squared per second
cubic meter per second (m^3/s)	35.31	cubic foot per second
kilometer (km)	0.6214	mile
square kilometer (km^2)	0.3861	square mile
centimeter (cm)	3.281×10^{-2}	foot
centimeter per second (cm/s)	3.281×10^{-2}	foot per second

Vertical coordinate information is referenced to the National Geodetic Vertical Datum of 1929 (NGVD 29) and the North American Vertical Datum of 1988 (NAVD 88); horizontal coordinate information is referenced to the North American Datum of 1983 (NAD 83).

Other Units of Abbreviations

g/L	gram per liter
ppt	part per thousand
$s/m^{1/3}$	second per meter cube root
W/m^2	watt per square meter

Acronyms

ADI	Alternating-direction implicit
ATLSS	Across Tropic Level Systems Simulation
CERP	Comprehensive Everglades Restoration Plan
CESI	Critical Ecosystem Studies Initiative
ENP	Everglades National Park
GIS	Geographic information system
GPS	Global positioning system
HSE	Hydrologic Simulation Engine
MAD	Mean absolute difference
MD	Mean difference
NOAA	National Oceanic and Atmospheric Administration
NPS	National Park Service
PES	Priority Ecosystem Science
RMSD	Root mean square difference
SFRSM	South Florida Region Simulation Model
SFWMD	South Florida Water Management District
SFWMM	South Florida Water Management Model
SICS	Southern Inland and Coastal Systems
SWIFT2D	Surface-water integrated flow and transport in two dimensions
TBA	Turning bands algorithm
USGS	U.S. Geological Survey

Two-Dimensional Hydrodynamic Simulation of Surface-Water Flow and Transport to Florida Bay through the Southern Inland and Coastal Systems (SICS)

By Eric D. Swain, Melinda A. Wolfert, Jerad D. Bales, *and* Carl R. Goodwin

ABSTRACT

Successful restoration of the southern Florida ecosystem requires extensive knowledge of the physical characteristics and hydrologic processes controlling water flow and transport of constituents through extremely low-gradient freshwater marshes, shallow mangrove-fringed coastal creeks and tidal embayments, and near-shore marine waters. A sound, physically based numerical model can provide simulations of the differing hydrologic conditions that might result from various ecosystem restoration scenarios. Because hydrology and ecology are closely linked in southern Florida, hydrologic model results also can be used by ecologists to evaluate the degree of ecosystem restoration that could be achieved for various hydrologic conditions.

A robust proven model, SWIFT2D, (Surface-Water Integrated Flow and Transport in Two Dimensions), was modified to simulate Southern Inland and Coastal Systems (SICS) hydrodynamics and transport conditions. Modifications include improvements to evapotranspiration and rainfall calculation and to the algorithms that describe flow through coastal creeks. Techniques used in this model should be applicable to other similar low-gradient marsh settings in southern Florida and elsewhere.

Numerous investigations were conducted within the SICS area of southeastern Everglades National Park and northeastern Florida Bay to provide data and parameter values for model development and testing. The U.S. Geological Survey and the National Park Service supported investigations for quantification of evapotranspiration, vegetative resistance to flow, wind-induced flow, land elevations, vegetation classifications, salinity conditions, exchange of ground and surface waters, and flow and transport in coastal creeks and embayments.

The good agreement that was achieved between measured and simulated water levels, flows, and salinities through minimal adjustment of empirical coefficients indicates that hydrologic processes within the SICS area are represented properly in the SWIFT2D model, and that the spatial and temporal resolution of these processes in the model is adequate. Sensitivity analyses were conducted to determine the effect of changes in boundary conditions and parameter values on simulation results, which aided in identifying areas of greatest uncertainty in the model. The parameter having the most uncertainty (most in need of further field study) was the flow coefficient for coastal creeks. Smaller uncertainties existed for wetlands frictional resistance and wind. Evapotranspiration and boundary

inflows indicated the least uncertainty as determined by varying parameters used in their formulation and definition.

Model results indicated that wind was important in reversing coastal creek flows. At Trout Creek (the major tributary connecting Taylor Slough wetlands with Florida Bay), flow in the landward direction was not simulated properly unless wind forcing was included in the simulation. Simulations also provided insight into the major influence that wind has on salinity mixing along the coast, the varying distribution of wetland flows at differing water levels, and the importance of topography in controlling flows to the coast. Slight topographic variations were shown to highly influence the routing of water.

A multiple regression analysis was performed to relate inflows at the northern boundary of Taylor Slough bridge to a major pump station (S-332) north of the SICS model area. This analysis allows Taylor Slough bridge boundary conditions to be defined for the model from operating scenarios at S-332, which should facilitate use of the SICS model as an operational tool.

INTRODUCTION

The National Park Service (NPS) is charged with the task of conserving and protecting Everglades National Park (ENP), which includes the Southern Inland and Coastal Systems (SICS) that connect the Taylor Slough and C-111 wetlands with Florida Bay (fig. 1). Preservation of this ecosystem requires a hydrologic regime that approximates natural hydrologic conditions. At stake are thousands of acres of invaluable wilderness habitat and wildlife that the habitat supports (U.S. Army Corps of Engineers, 1992). Recent studies suggest that the SICS area is under great ecological stress with dwindling populations of many freshwater and saltwater animal species (Van Lent and others, 1998). Fifteen species found in the area are either threatened or endangered with extinction (Beccue, 1999). Gradual reductions over time in freshwater flow from north to south in the SICS area are thought to have contributed to the northward encroachment of salt-tolerant mangrove vegetation into the former domain of freshwater marsh vegetation (Smith, 1998). These reductions in freshwater are the result of modifications to the natural flow regime that divert water for other uses.

Physical characteristics and hydrologic processes within canals, wetlands, and subtidal embayments of the southern Florida ecosystem are being defined and investigated by the U.S. Geological Survey (USGS) in projects supported through the Priority Ecosystem Science (PES) Program and through the NPS Critical Ecosystem Studies Initiative (CESI). Investigations have been undertaken to better understand important wetland processes such as vegetative resistance to flow, evapotranspiration, ground-water/surface-water exchanges, quantity and distribution of flow in creeks and marshes, canal/wetland interactions, saltwater intrusion, and wind-induced flow (Schaffranek and others, 1999). Considerable effort has also been expanded to precisely measure land-surface elevations in the wetlands and along the mangrove fringe and coastal embankment to determine the bathymetry of subtidal embayments and tidal creeks in northeastern Florida Bay. Additional data have been collected on coastal creek discharges, flow velocities in Taylor Slough, and water levels throughout the system.

Most of these investigations focused on individual topics and, in many cases, results were limited to a finite number of points at limited locations and for a short time. To better describe SICS area hydrology on larger temporal and spatial scales, results of these studies needed to be integrated. Moreover, current understanding of the SICS area needs to be used to evaluate changes that might occur in response to various water-management scenarios. In 1996, the USGS initiated a study to determine the effects of relevant physical characteristics and hydrologic processes on the flow regime in the SICS area. The USGS surface-water integrated flow and transport in two dimensions (SWIFT2D) hydrodynamic/transport model was adapted to this mixed sheetflow, stream, and tidal regime using findings from the PES and CESI investigations (Swain, 1999). The model has the capability to simulate both current conditions (throughout the SICS area) as well as possible future conditions.

Purpose and Scope

The purpose of this report is to describe the development, testing, and application of a flow and transport simulation model for the SICS area, a critically important and threatened ecosystem of southeastern ENP. The report summarizes the extensive research efforts that resulted in better definition and understanding of major physical features and processes in the

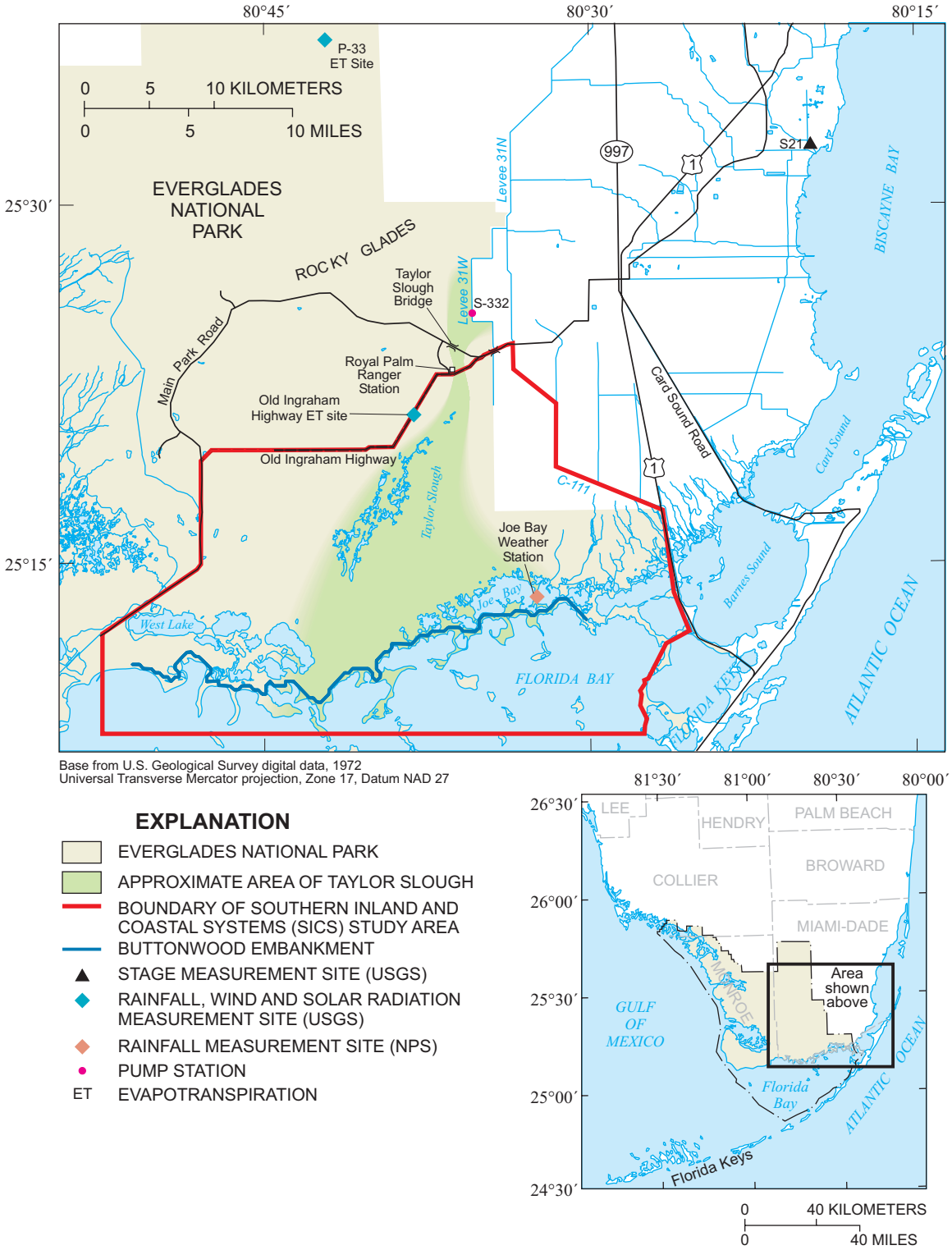

Figure 1. Southern Inland and Coastal Systems (SICS) study area and selected data-collection sites. (USGS, U.S. Geological Survey; NPS is National Park Service)

SICS area and that were used in the development of the model. Studies were conducted to better describe and document topography, distribution of vegetation, vegetative resistance to water flow, water levels, currents, flow, salinity, meteorology, ground- and surface-water interactions, and evapotranspiration. The report also describes the structure, characteristics, capabilities, requirements, and limitations of the SWIFT2D numerical flow and transport simulation model and also discusses several enhancements made to the code to improve simulations for the SICS area.

The construction, calibration, testing, and application of the SWIFT2D model to the SICS study area are documented. This report describes incorporation of physical and hydrologic data into the model, the reliability of the hydrologic simulations, results of some model applications, and some general ways the model might be used to help evaluate hydrologic responses to proposed Everglades restoration alternatives.

The model was adapted to the study area using information on land-surface elevations, topographic features, vegetation characteristics, and bathymetry. The model was then calibrated and verified using data on flow rates and salinity measured at key outflow points along the mangrove fringe. Additionally, concurrent set measurements that defined mass fluxes at strategic transect locations within the wetlands and continuously measured water levels in the wetlands were used for comparison and verification of model results. The model was calibrated using data from September 1-30, 1997, and was verified using data from August 1, 1996, to July 31, 1997. The sensitivity of model results to changes in critical model parameters and boundary data was evaluated, both to establish error bounds for simulation results and to identify critical factors controlling flow dynamics and transport properties throughout the SICS study area. Numerical simulations that represent past and current hydrologic conditions were made using available data or estimated values, where no data existed, to establish baseline conditions. Through further application of the calibrated model, these baseline conditions can be used to evaluate the effects of future hydrologic changes within the SICS ecosystem. The SICS model version 1.2, described in this report, simulates time-varying information on surface-water level, flow velocity, salinity, and conservative material transport at a relatively detailed spatial scale.

Description of Study Area

The study area, referred to hereafter as the SICS area, encompasses about 900 km^2. Within the study area are the Taylor Slough drainage basin of southeastern ENP, wetlands southwest of the C-111 Canal, part of northeastern Florida Bay, and several natural drainage features, including Alligator Creek, McCormick Creek, Taylor River, East Creek, Mud Creek, Trout Creek, Shell Creek, and West Highway Creek. Also included in the area are shallow coastal embayments, such as Joe Bay and Little Madeira Bay (fig. 2). A cluster of inland lakes are present in the southwestern corner of the study area, including West Lake, Cuthbert Lake, Seven Palm Lake, Monroe Lake and several smaller lakes (fig. 2). The study area boundary follows the ENP Main Park Road and then Old Ingraham Highway to the bridge over Taylor Slough and finally southeastward along part of the C-111 Canal. Flows from the very flat study area through the creeks and into Florida Bay have a large controlling influence on salinity concentrations and distribution in the bay (Nuttle, 1995).

The SICS area is a small but prominent ecosystem that is somewhat hydraulically isolated south of a northeasterly trending topographic high of several centimeters called the Rocky Glades (fig. 1). Natural water flow to the SICS area occurs during times of high water level through a north-south trending depression known as Taylor Slough. As water has been drained from the Everglades over the last 60 years for urban and agricultural development, flows to Taylor Slough have diminished. This natural source of freshwater to the SICS area has been supplemented with water deliveries from the extensively managed canal system in southern Florida—through pump station S-332 to Taylor Slough, through Levee 31W Canal (Rose and others, 1981), and through C-111 Canal (fig. 1). The Levee 31W Canal lies northeast of Taylor Slough and brings water from the north, terminating just southeast of Taylor Slough bridge. Farther to the east, the C-111 Canal forms the northeastern boundary of the SICS area; farther south, the canal crosses US-1 and discharges into Barnes Sound.

Old Ingraham Highway is a substantial obstruction to flow along the northwestern and western parts of the study area. However, the road does not completely block flow, especially during high-water periods (Craighead and Holden, 1965). Although overtopping of Old Ingraham Highway has been observed during high-water events, volumes of water moving

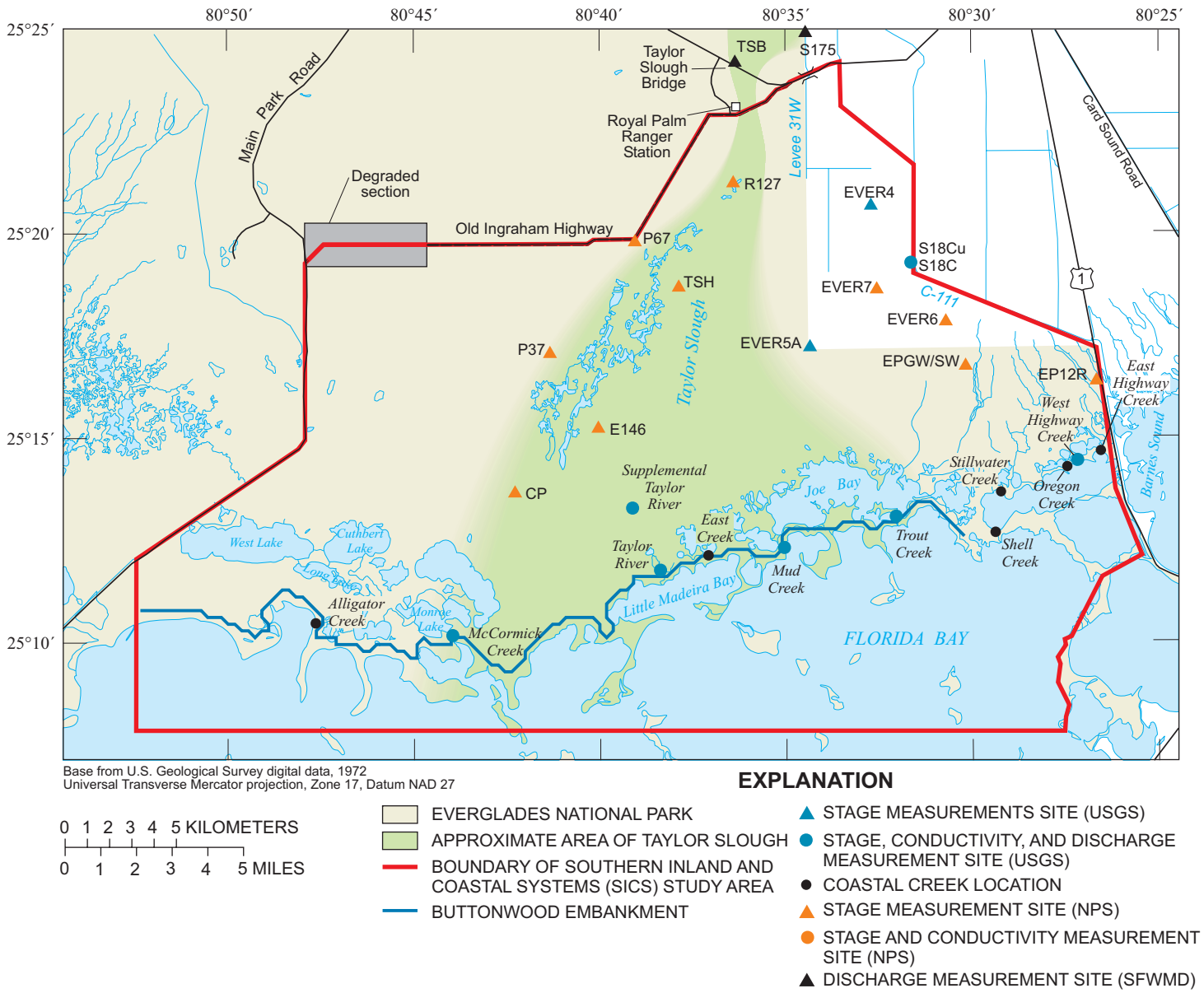

Figure 2. Discharge, conductivity, and water-level data-collection sites within the study area (USGS, U.S. Geological Survey; NPS, National Park Service; SFWMD South Florida Water Management District).

over the road have not been measured. About 5.5 km of the 14-km east-west section of Old Ingraham Highway (fig. 2) have been degraded, and this segment is where overland flow most often occurs.

The NPS has studied hydrologic conditions within the SICS area for quite some time. Continuous measurements of stage or stage and conductivity were made at 10 sites within the SICS domain (fig. 2) by the NPS. These sites contain shallow wells so that stage measurements can continue, in conjunction with several sites operated by the USGS, when levels are below land surface.

Ground-water inflow into the SICS area was investigated by Fitterman (1996), who described the location of the ground-water interface between saltwater and freshwater in the SICS study area. During the investigation, a helicopter-based instrument pod was used for measuring the electromagnetic response of the ground at differing frequencies to determine the apparent resistivity of the underlying formation (Fitterman and Deszcz-Pan, 1999). The resistivity is highly inversely correlated to the salinity of the shallow ground water. The apparent resistivity map (fig. 3), for a depth of 5 m (meters) below land surface, indicates a relatively sharp transition between more resistive (lower salinity) ground water on the north side of western Old Ingraham Highway to higher salinity on the south side of the highway. To the east, the transition zone is closer to Florida Bay in the vicinity of Taylor Slough, but the transition zone then trends northeasterly toward US-1 (Fitterman and Deszcz-Pan, 1998). The general south-southeast direction of fresh ground-water flow (Swain and others, 1996) is forced by buoyancy to move upward as the freshwater approaches the saltwater interface. The region where upwelling of fresh ground water into the surface-water regime should occur is just landward of the saltwater-freshwater interface shown in figure 3. Evidence also suggests that saltwater has apparently intruded eastward adjacent to the degraded section along Old Ingraham Highway.

Additional evidence of ground-water flow into the study area is from geochemical tracer measurements conducted to determine the locations of ground-water discharge to surface water in wetland areas (Harvey and others, 2000a; 2000b). The area just south of the central bend at Old Ingraham Highway near site P67 (fig. 2) has been identified as a primary source of ground-water seepage to surface waters of the SICS area. Overland flow is most likely to occur west of this area, which includes the degraded section of Old Ingraham Highway.

The southern boundary of the SICS study area is well south of the Florida Bay shoreline. Florida Bay is a shallow saline water body semi-enclosed from the Atlantic Ocean by the Florida Keys archipelago (fig. 1). The northeastern part of Florida Bay has negligible diurnal or semidiurnal tidal forcing, but water levels can fluctuate 10 to 30 cm during sustained frontal type wind events (Smith, 2001).

One of the most hydrologically significant features of the SICS area is a higher elevation feature along the coast called the Buttonwood Embankment (fig. 1). This ridge is estimated to be on the order of 15 cm higher than the surrounding marsh (Holmes and others, 2000). The existence of the Buttonwood Embankment is thought to be related to either build-up of organic matter from the overlying mangrove forest or deposition of sediment near the shore that is eroded from Florida Bay during periodic hurricanes and tropical storms (Holmes and others, 2000). Several creek channels cut through this ridge and drain into northeastern Florida Bay. The ridge itself forms a partial low-head dam to overland flow from the SICS wetlands into Florida Bay, and the incised channels concentrate the flow into a small number of creeks. The ridge itself rarely is overtopped (Hittle, 2000).

Previous Studies

Numerous studies of Everglades hydrology have been conducted in recent years, and several models of the southern Florida region have been developed. Few models have been applied to the coastal Everglades (none focusing on the SICS area). This section summarizes some of the previous modeling efforts in the Everglades.

To implement the Comprehensive Everglades Restoration Plan (CERP) (U.S. Army Corps of Engineers, 1999), numerous natural resource management decisions must be made with less than complete information on the probable impacts of the decisions on hydrology, habitat, wildlife, and millions of southern Florida residents. Because numerical simulation models are capable of reasonably integrating many complex and interacting processes, models are finding greater use in southern Florida for evaluation of the effects of possible future management scenarios. It is increasingly important, therefore, that all such models be as reliable as possible.

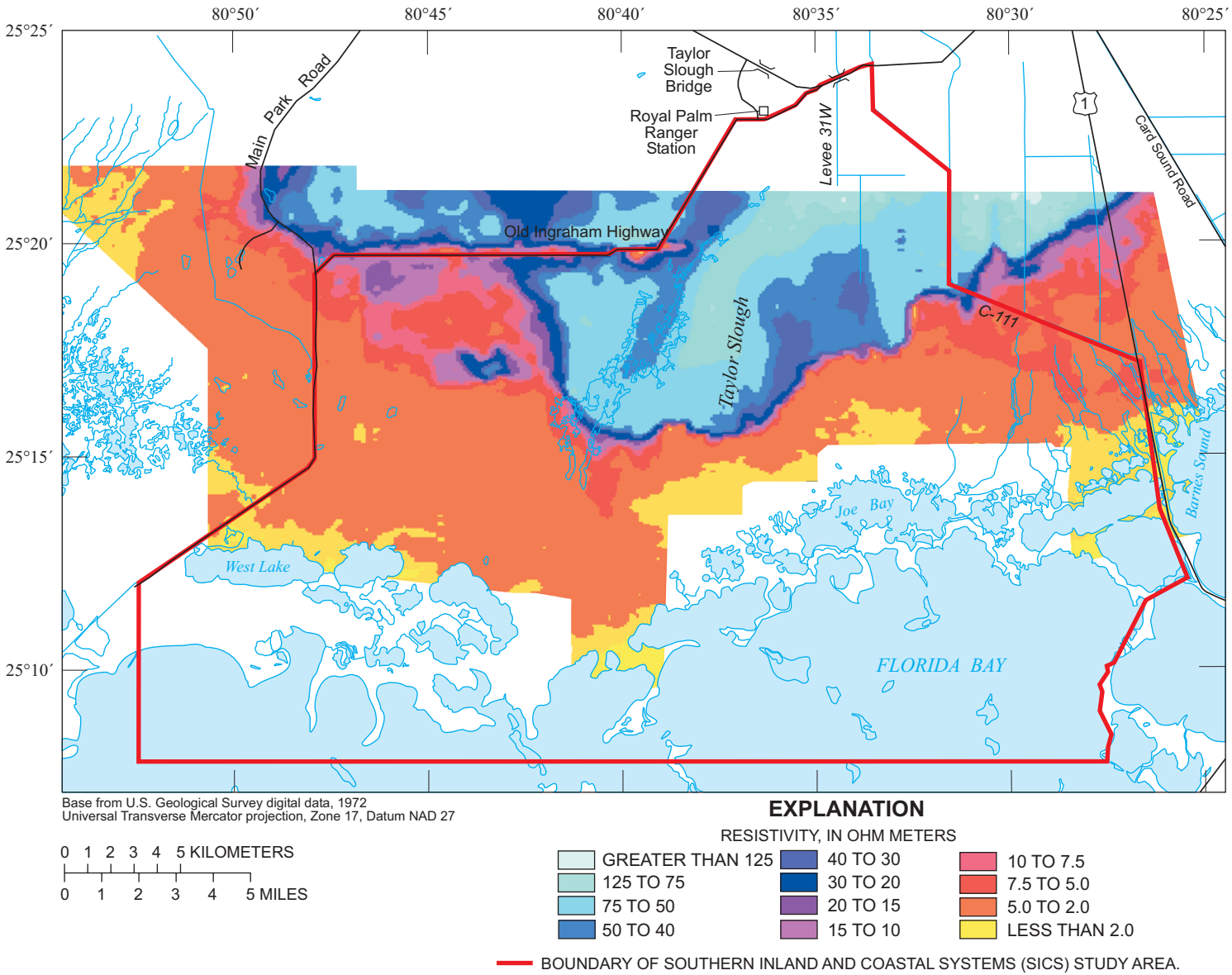

Figure 3. Apparent resistivity in the Southern Inland and Coastal Systems (SICS) study area at 5-meter depth below land surface (from Fitterman and Deszcz-Pan, 1998).

One key model now being applied to the SICS and other southern Florida areas is the Across Trophic Level Systems Simulation (ATLSS) model (Deangelis, 2000). The ATLSS model is used to compare the relative effects of differences between alternative hydrologic scenarios on several key indicator species (alligator, snail kite, Florida panther, white-tailed deer, and Cape Sable seaside sparrow) within the ecosystem using linked species models. The ATLSS model requires very detailed and accurate water-level, flow, and salinity information from a hydrologic model in order to simulate realistic population changes for these species in response to restoration options (DeAngelis, 2000). Improved hydrologic input to ATLSS should result in better ecological simulations.

Southern Florida hydrologic conditions have been simulated by the South Florida Water Management Model (SFWMM) for more than 15 years (MacVicar and others, 1984). This model has undergone numerous improvements since its inception and is relied upon to provide regional information at coarse spatial resolution. The Hydrologic Simulation Engine (HSE) for the next generation SFWMM, called the South Florida Region Simulation Model (SFRSM), has been tested in the Everglades region (Brion and others, 2000). The overland flow algorithm in the HSE, as in the SFWMM, neglects inertial forces, and analysis indicates that these models are more reasonable in their representation of water level than flow volumes (Bales and others, 1997). The SFWMM has been used to simulate coastal flows into Florida Bay as part of a hydrodynamic modeling effort (McAdory and Kim, 1998). In this application, simulated coastal flows were much greater than field measurements (Hittle, 2000), resulting in simulated Florida Bay salinities that were much lower than measured values. Another large regional model was attempted with the FEMWATER123 code (Lin and others, 2000). This included one-dimensional canal flow, two-dimensional overland flow, and three-dimensional finite-element ground-water flow. The combined model was very computationally intensive which restricted its usage.

The need for greater accuracy and finer spatial resolution of hydrologic model input to ecological models as well as the need for better information on freshwater flows that can be used in Florida Bay models highlight the importance of an improved flow model of the SICS coastal region. Such a model should substantially improve the reliability of information available for resource management decision making in support of Everglades restoration.

APPROACH

The approach for this study included selection, enhancement, and application of a numerical model capable of simulating flow and solute transport within the SICS area and into Florida Bay. Data were obtained from several sources to apply, calibrate, and test the model. Additionally, results from ongoing or recently completed process studies were used to develop the model. The approach used for model selection and enhancement, model development, application of process studies in support of model development, and model calibration, testing, and application are described in this section.

Model Selection and Required Enhancements

A numerical model was needed to accurately simulate water movement and solute transport through the SICS area to Florida Bay for a range of existing and possible future conditions, given natural or imposed changes in inflows. Selection of the model for the study was governed by the anticipated application of the model and by the controlling physical characteristics and governing hydrologic/hydraulic processes in the SICS area.

Numerous physical characteristics and processes affect flow in the SICS area. Hydraulic gradients are very small—less than 2 cm per kilometer (Lee and others, 2000a; 2000b). Water movement into Florida Bay from the SICS area is strongly affected by the coastal Buttonwood Embankment as well as the coastal creeks that breach the embankment, water levels in Florida Bay and the Everglades, wind conditions, evapotranspiration, and the frictional resistance to flow by vegetation. With such low hydraulic gradients, rainfall and exchanges with ground water are also important factors in the total water budget. The transition from freshwater in the Everglades to saltwater in Florida Bay and the location and size of this transition zone also affect water movement and solute transport. Although some parts of the SICS area are continuously inundated, other parts vary between inundated and dry (water level at or below land surface) conditions.

Small creeks also are present throughout the SICS area, particularly in the southeastern part of the study area (fig. 2), and these creeks play a major role in the movement of water and solutes into Florida Bay.

Given these characteristics, the model selected for this study needed the capability to simulate: (1) time-varying, two-dimensional, depth-averaged overland flow through spatially varying topography; (2) the effects of wind on flow; (3) drying and rewetting within the study area; (4) dynamic transport of salt including the coupling between density and flow; (5) one-dimensional flow through creeks at a smaller spatial scale than for overland flow; and (6) the effects of rainfall and evapotranspiration on water balance and flow.

The SWIFT2D model (Leendertse, 1987), described in some detail later, was selected for this study because the model: (1) includes many of the capabilities required for the SICS application, (2) is easily modified, (3) is a nonproprietary and freely obtained code, (4) runs on a personal computer, and (5) has been successfully applied to other systems in Florida and elsewhere. The model solves the hydrodynamic equations of mass continuity and momentum conservation in two horizontal dimensions. Drying and rewetting of the land surface are simulated. The model also includes algorithms that describe flow at various types of structures; this feature was particularly important for the simulation of flow in tidal creeks and through the Buttonwood Embankment. The creeks are much smaller than the size of the computational grid cell, and thus, are represented in SWIFT2D as notches in a barrier. Time-varying transport of constituents is simulated, and the transport equation is coupled to the flow equations through density effects.

Many previous applications of the SWIFT2D model were for tidally driven systems with hydraulic gradients generally greater than those of the SICS area. Many of these applications, however, included selected areas having lower hydraulic gradients, such as in tidal flats, similar to the SICS area. Slight modifications to the SWIFT2D model were sometimes needed in previous applications. For instance, the SWIFT2D model was used to design the Dutch Delta Works (Leendertse and others, 1981), and modifications to the model subsequently were made to evaluate mixing and chaotic stirring in the Dutch Wadden Sea (Ridderinkhof and Zimmerman, 1992). In a report on a model of the Eastern Scheldt estuary in the Netherlands (Leendertse, 1988), an evaluation of the effects of the advection terms on tidal propagation was conducted. These experiments illustrated the importance of the timestep size, grid size, roughness estimation, depth measurement accuracy, turbulence closure, and horizontal momentum exchange in obtaining accurate simulations. Lee and others (1989; 1994) demonstrated the effects of highway crossings and embankments on the circulation and flow within an estuarine system that consisted of narrow channels and extensive tidal flats that became exposed at low tide. Using a nested computational grid, Schaffranek and Baltzer (1988) used SWIFT2D to evaluate hydraulic effects of modifications to wetlands in the Port Royal Sound area of South Carolina. Bales and Robbins (1995) and Robbins and Bales (1995) characterized flow, circulation, and solute transport in the Pamlico and Neuse River estuaries in North Carolina using the SWIFT2D model. Those studies included detailed field measurement programs and calibration and testing of the SWIFT2D model.

Other studies have simulated the effects of dredging and alternative spoil placement options on tidal flow, circulation, and flushing within several estuaries in Florida, including Tampa Bay (Goodwin, 1987) and Hillsborough Bay (Goodwin, 1977; 1991). Application of SWIFT2D to Charlotte Harbor (Goodwin, 1996) and the Loxahatchee River (Russell and Goodwin, 1987) provided insight into tidal flow and mixing characteristics and how they might change with proposed future alterations to causeways and bridges. Schaffranek (1986) and Schaffranek and Baltzer (1990) illustrated horizontal density-gradient effects on estuarine flushing and circulation in the upper Potomac estuary and the effect of bathymetric grid density on model results using the SWIFT2D model.

The SWIFT2D model, in its standard form, satisfies the hydrodynamic requirements for the SICS application. Several enhancements were required, however, to represent hydrologic processes such as evapotranspiration and rainfall. The computational algorithms for wind and flow at barriers also were enhanced.

Data

Data served the following distinct purposes in the study: (1) to characterize the model area, (2) to provide model boundary conditions, (3) to assist in model performance testing, and (4) to estimate model parameters. Most data used to characterize the model area were developed by field studies associated with

this modeling effort. Boundary conditions and data for model performance testing were derived from numerous projects conducted by the USGS, South Florida Water Management District (SFWMD), and ENP. Data from all of these sources are available on a database that can be accessed at http://sofia.usgs.gov.

Results from field studies were used to estimate model parameters. Most parameters are constrained to values close to field measurements, and confidence in these parameter values is high. This approach for determining parameters is in contrast to the typical approach for parameter determination in model studies. Typically, during model calibration, parameters are set to nominal values obtained from the literature and adjusted over a wide range until model simulation results are in reasonable agreement with available data. In contrast, the SICS model parameters are largely derived from process studies and are physically based. Hence, the chance of nonunique solutions, in which similar simulation results are obtained with different combinations of parameter values, is less likely to occur than with a model calibrated using the typical approach. In some cases, values measured in the field at a few points may not always be the best representation for a parameter in a model due to scale effects; the model represents an effective value as applying over an entire grid cell, whereas measurements sometimes apply to a point. Nonetheless, field measured values typically define model parameters more accurately than values obtained from other indirect sources including the literature and model tuning. Methods used for obtaining data for this study are described in the following sections.

Topography

Topographic data included land-surface elevations, embayment bathymetry, Buttonwood Embankment elevations, and the widths and bottom elevations of tidal creeks. The USGS used a helicopter-mounted global positioning system (GPS) unit and weighted line to measure land-surface elevations (Desmond and others, 2000) in the Everglades wetlands. Land-surface elevations were measured on a grid with about 400-m spacing (Henkle, 1996).

The bathymetries of Joe Bay and Florida Bay were measured by the USGS (Hansen and DeWitt, 1998), using a boat with a depth finder and a GPS unit. More than 30,000 individual depth measurements along boat track lines were made in Joe Bay (fig. 2). The bathymetries of other subembayments and Florida Bay were determined from nautical charts developed from National Oceanic and Atmospheric Administration (NOAA) data. The USGS Florida Bay data coincided well with the nautical charts, while providing a much more refined representation of the embayment bathymetry than was previously available. The bathymetries of West Lake and associated lakes were estimated from depth measurements made by USGS personnel in September 1999. All bathymetric and topographic elevations were referenced to the North American Vertical Datum of 1988 (NAVD 88).

The location of the Buttonwood Embankment was derived from 1:24,000 scale USGS topographic maps. Based on observations by USGS personnel, the bottom elevations of tidal creeks at the location where the creeks cut through the embankment are all at an elevation of about 1.5 m below NAVD 88. The creek widths are as follows: (Eduardo Patino, U.S. Geological Survey written commun., 1998):

Creek name	Width (meters)
McCormick Creek	16.8
Taylor River	6.7
East Creek	12.2
Mud Creek	12.2
Trout Creek	36.6
Shell Creek	12.2
Stillwater Creek	9.1
Oregon Creek	4.6
East Highway Creek	15.2
West Highway Creek	21.3

Channels connecting the lakes in the southwestern part of the study area (West Lake area) were estimated to be about 24 m wide.

Vegetation

Aerial- and land-based vegetation surveys (Carter and others, 1999; Jones, 1999) were conducted, and results were compiled into a geographic information system (GIS) database (Stewart, 1997). The aerial surveys were conducted to determine regional vegetation types by using spectral reflectivity and visual onsite observations for ground truthing. These data were compared with data previously collected for the area, such as the 68-class 1993-94 Landsat vegetation map and a 20-class Landsat thematic mapper image (February 2000). The vegetation in the study area was categorized into eight classes at a horizontal resolution

of 30 m (fig. 4). Although vegetative density is not indicated by this classification system, the system does identify areal distribution of vegetation types for correlation to hydrologic parameters, and the information is adequate for hydrodynamic modeling.

Water Level, Currents, and Discharge

Water-level, current, and discharge data were collected at 23 sites in the study area and 1 site (P33) north of the study area (fig. 2 and table 1). Data used for this study were collected by the SFWMD, USGS, and NPS through existing monitoring networks and research projects.

Gage datums at the continuous water-level recording stations were established relative to the National Geodetic Vertical Datum of 1929 (NGVD 29). The model was developed, however, using topographic data referenced to NAVD 88. Therefore, gage datum adjustments were made at all water-level stations. The CORPSCON datum adjustment routine (North Carolina Geographic Information Coordinating Council, 1999) was used to adjust datums from NGVD 29 to NAVD 88 at all stations except R127, TSH, P37, E146, and CP. At these stations, reference marks relative to NAVD 88 were established during land-surface elevation surveys (Gordon Shupe, U.S. Geological Survey, written commun., 1999). Subsequent surveys determined the differences between the NAVD 88 reference marks and previously established NGVD 29 datums. Adjustments to correct NGVD 29 gage datums to NAVD 88 elevations are as follows:

Station	Datum adjustment (meters)
R127	-0.5200
TSH	- .4916
P37	- .4801
E146	- .3734
CP	- .5288

A unique aspect of this study involved the measurement of flow velocities (currents) in the wetlands (Tillis, 2001). This type of data is seldom available, but is invaluable for testing model performance. Flow velocity, depth, and water-quality constituents (water temperature, dissolved-oxygen concentration, specific conductance, and pH) were measured within the study area at 137 locations (fig. 5), including along three approximately east-west transects in the wetlands (Schaffranek and others, 1999). Acoustic Doppler velocimeters were used to make point velocity measurements at various depths in the water column, and depth-averaged velocities were calculated at each measurement location for use in model evaluation. The data were collected between July 1997 and July 1998. Data from the first two measurement sessions were used in this study.

Salinity

Salinity measurement stations in the study area are shown in figure 2 (as conductivity locations) and presented in table 1. These stations are located at the mouths of coastal creeks. Specific conductance sensors were deployed at multiple vertical positions in the water column to detect any vertical stratification. Little vertical variation in salinity occurred except at brief intervals during flow reversals (Hittle, 2000). The specific conductance measured at these locations was converted to salinity by the following relation (Riley and Skirrow, 1975):

$$s = 0.4081 C_s^{1.121}, \qquad (1)$$

where s is salinity, in parts per thousand; and C_s is specific conductance, in microsiemens per centimeter at 25 °C. The standard USGS method for converting specific conductance to salinity was given by Miller and others (1988, p. 14). The maximum specific conductance measured at Trout Creek in 1996 was 42.238 microsiemens per centimeter, which converts to a salinity of 27.08 ppt using equation 1 and to a salinity of 27.11 ppt using the equation by Miller and others (1988). The differences are very small (0.1 percent) compared to potential measurement error in the field. In addition to the data from the coastal creek stations, salinity from NPS-operated stations in Florida Bay were used to define the southern salinity boundary.

Rainfall, Wind, and Solar Radiation

Initial applications of the SICS model (version 1.1) used rainfall data collected at the Old Ingraham evapotranspiration site and the Joe Bay weather station (fig. 1). Data for the model domain were interpolated from these two sites. This approach proved to be unsatisfactory, considering the large spatial variations in southern Florida rainfall. For example, from July 1996 to February 1997, rainfall was 107.2 cm at the Old Ingraham site and 68.1 cm at the Joe Bay site.

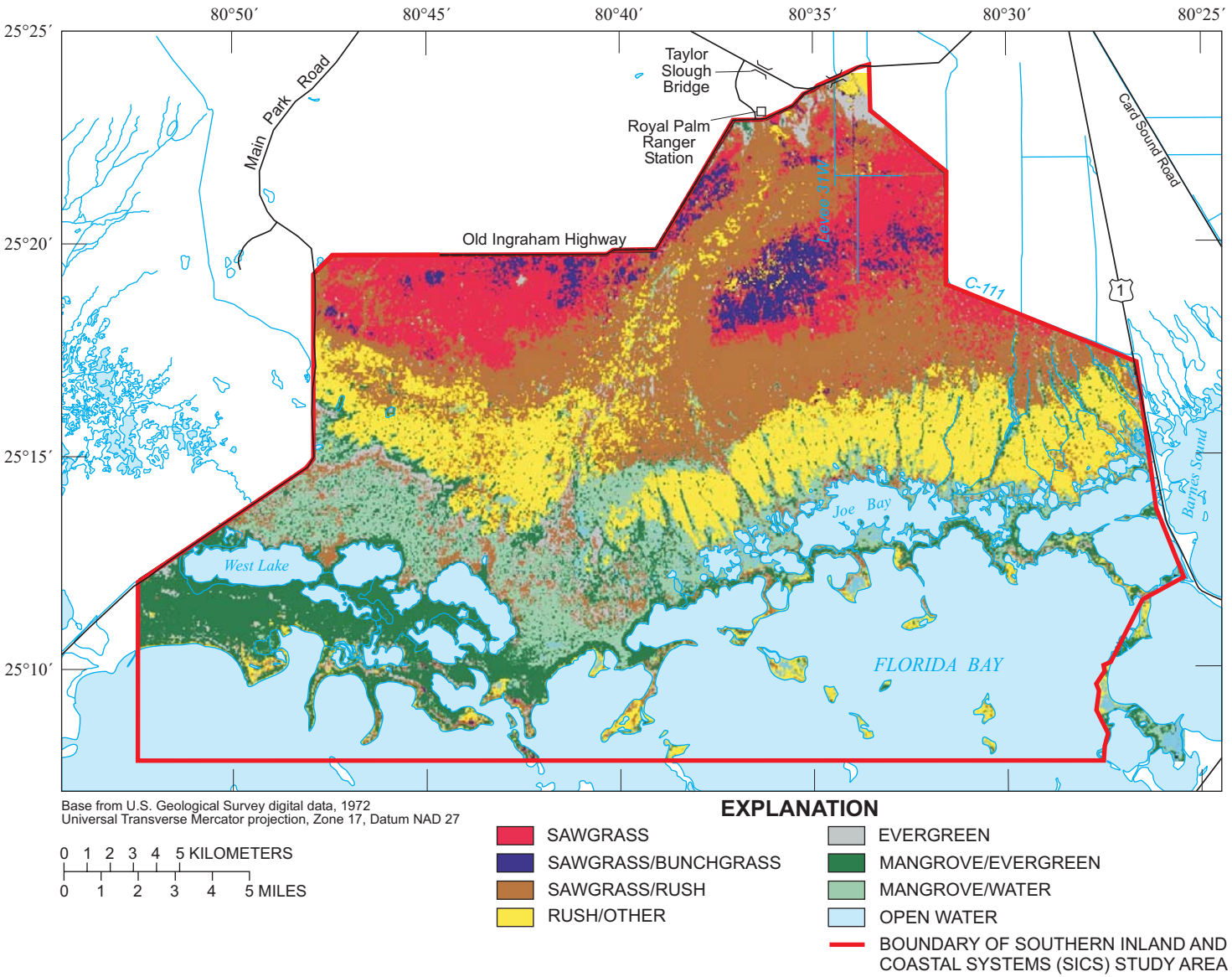

Figure 4. Vegetation features in the Southern Inland and Coastal Systems (SICS) study area.

Table 1. Hydrologic and meteorological data-collection sites for the Southern Inland and Coastal Systems (SICS) study

[The P-33, Old Ingraham Highway, and Joe Bay sites are shown in figure 1; the sites used for rainfall data are shown in figure 6; the sites used for boundary conditiona are shown in figure 10. All remaining sites are shown in figure 2. Data: C, conductance; D, discharge; ET, evapotranspiration; S, stage; R, rainfall; WL, water level. Agency: NPS, National Park Service; SFWMD, South Florida Water Management District; USGS, U.S. Geological Survey. Purpose: BC, boundary condition; MF, model formulation; MPT, model performance testing]

Site name	Map identifier	Latitude	Longitude	Data	Reporting interval	Period of record	Agency	Purpose
Sites shown in figure 1								
Joe Bay weather station	Joe Bay weather station	25°13′28″	80°32′24″	R	Daily	1991-Present	NPS	BC
Old Ingraham Highway	Old Ingraham Highway ET site	25°21′12″	80°38′07″	ET,WL,R,W	15 minutes	1995-Present	USGS	BC,MF
P-33	P-33	25°36′55″	80°42′11″	ET	Hourly	1995-Present	USGS	MF
Sites shown in figure 2								
Craighead Pond	CP	25°13′44″	80°42′15″	WL	Daily	1978-Present	NPS	MPT
E-146	E146	25°15′18″	80°40′01″	WL	Daily	1994-Present	NPS	MPT
Everglades 4	EVER4	25°20′43″	80°32′44″	WL	Daily	1985-Present	USGS	MPT
Everglades 5A	EVER5A	25°17′16″	80°34′21″	WL	Daily	1985-Present	USGS	MPT
Everglades 6	EVER6	25°17′54″	80°30′43″	WL	Daily	1991-Present	NPS	MPT
Everglades 7	EVER7	25°18′35″	80°32′34″	WL	Daily	1991-Present	NPS	MPT
Everglades Park 12R	EP12R	25°16′26″	80°26′43″	WL	Daily	1988-Present	NPS	MPT
Everglades Park ground-water/surface-water station	EPGW/SW	25°16′49″	80°30′12″	WL	Daily	1986-Present	NPS	MPT
P-37	P37	25°17′08″	80°41′19″	WL	Daily	1953-Present	NPS	MPT
P-67	P67	25°19′50″	80°39′02″	WL	Daily	1962-Present	NPS	MPT
R-127	R127	25°21′15″	80°36′24″	WL	Daily	1984-Present	NPS	MPT
Taylor Slough Hilton	TSH	25°18′44″	80°37′52″	WL	Daily	1994-Present	NPS	MPT
Sites shown in figure 6								
Everglades 8	NP-EV8	25°20′46″	80°28′44″	R	15 minutes	1992-Present	NPS	BC
Flamingo	NP-FLA	25°08′29″	80°54′53″	R	15 minutes	1962-Present	NPS	BC
Little Madeira	Little Madeira	25°10′31″	80°37′56″	R	15 minutes	1993-Present	NPS	BC
P-38	NP-P38	25°22′14″	80°50′01″	R	15 minutes	1983-Present	NPS	BC
Terrapin Bay	Terrapin Bay	25°09′24″	80°43′30″	R	15 minutes	1993-Present	NPS	BC
Trout Cove	Trout Cove	25°12′39″	80°31′60″	R	15 minutes	1993-Present	NPS	BC
Upstream Taylor River	Upstream Taylor River	25°13′28″	80°39′11″	R	15 minutes	1993-Present	NPS	BC
Sites shown in figure 10								
Buoy Key	Buoy Key	25°07′15″	80°50′02″	WL,C	15 minutes	1993-Present	NPS	BC
Butternut Key	Butternut Key	25°05′17″	80°31′08″	WL,C	15 minutes	1993-Present	NPS	BC
CY2	CY2	25°19′45″	80°40′58″	WL	15 minutes	1996-Present	NPS	BC
CY3	CY3	25°19′46″	80°45′03″	WL	15 minutes	1996-Present	NPS	BC
East Highway Creek	East Highway Creek	25°14′40″	80°26′28″	WL,C	15 minutes	1996-Present	USGS	BC
Long Sound	Long Sound	25°14′05″	80°27′27″	WL,C,R	15 minutes	1993-Present	NPS	BC
McCormick Creek	McCormick Creek	25°10′03″	80°43′55″	WL,D,C	15 minutes	1995-Present	USGS	MPT
Mud Creek	Mud Creek	25°12′09″	80°35′01″	WL,D,C	15 minutes	1995-Present	USGS	MPT
Nine Mile Pond	NMP	25°15′15″	80°47′54″	WL	15 minutes	1996-Present	NPS	BC
P-46	P46	25°19′11″	80°47′45″	WL	15 minutes	1966-Present	NPS	BC
P-67	P67	25°19′50″	80°39′02″	WL	Daily	1962-Present	NPS	BC
S-175 at L31-W canal	S175	25°25′04″	80°34′25″	D	Daily	1970-Present	SFWMD	BC
S-18C at C-111 Canal	S18C	25°19′50″	80°31′30″	WL,D,C	Daily	1968-Present	USGS	BC
Supplemental Taylor River	Supplemental Taylor River	25°12′41″	80°38′53″	WL,D,C	15 minutes	1998-Present	USGS	MPT
Taylor River	Taylor River	25°11′27″	80°38′21″	WL,D,C	15 minutes	1995-Present	USGS	MPT
Taylor Slough Bridge	TSB	25°24′06″″	80°36′24″	D	Daily	1960-Present	SFWMD	BC
Trout Creek	Trout Creek	25°12′53″	80°32′01″	WL,D,C	15 minutes	1996-Present	USGS	MPT
Upstream of S-18C a C-111 Canal	S18Cu	25°19′50″	80°31′30″	WL	Daily	1985-Present	USGS	BC
West Highway Creek	West Highway Creek	25°14′33″	80°26′50″	WL,D,C	15 minutes	1996-Present	USGS	MPT
Whipray Basin	Whipray Basin	25°04′41″	80°43′39″	WL,C,R	15 minutes	1993-Present	NPS	BC

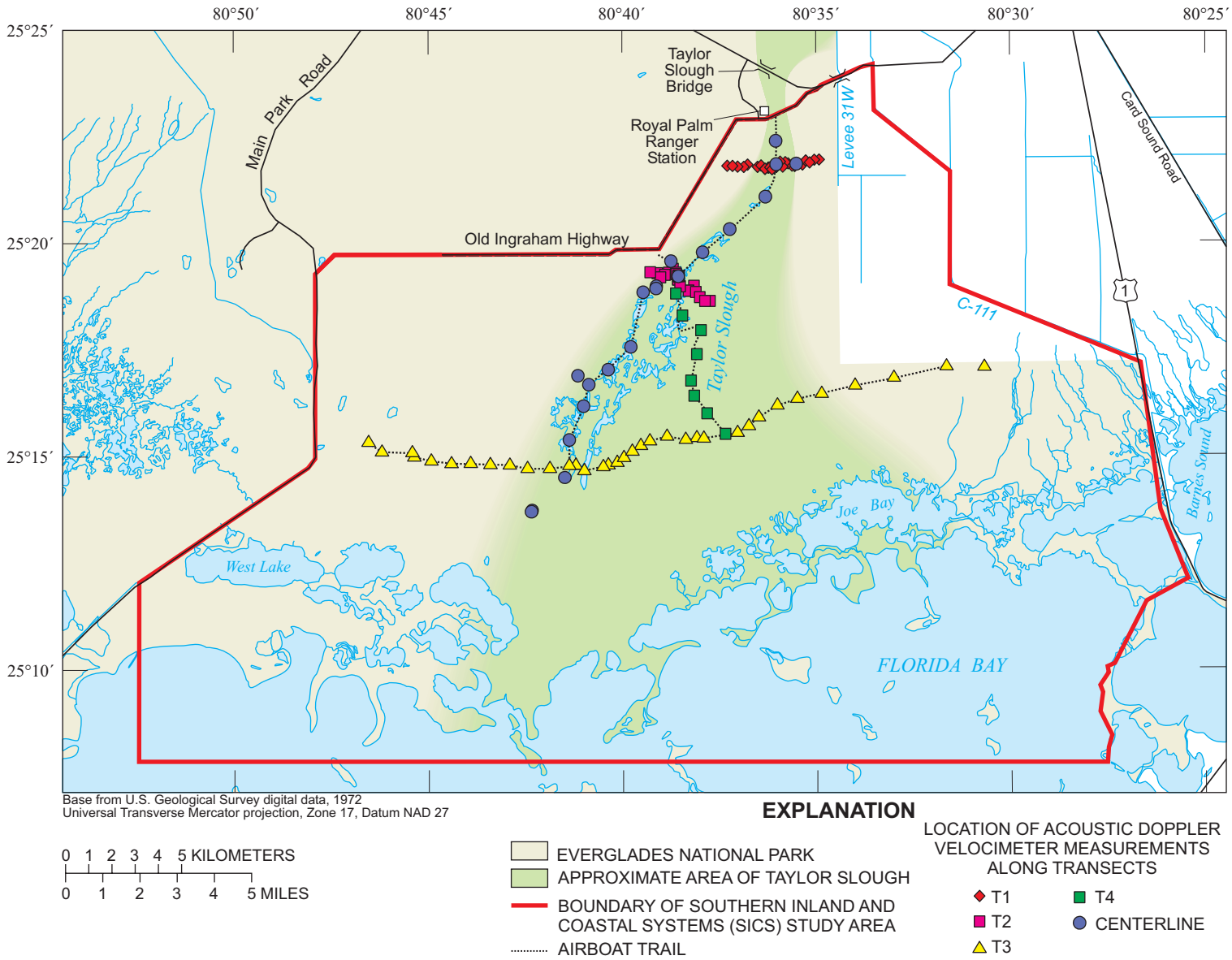

Figure 5. Location of acoustic Doppler velocimeter measurements in the Southern Inland and Coastal Systems (SICS) study area.

The maximum difference in monthly rainfall at the two sites was 17.5 cm in August 1996. In order to improve the spatial representation of rainfall, 15-minute data were collected at a network of 14 rainfall stations (fig. 6), and a kriging algorithm was used to determine rainfall amounts for each cell.

Wind speed and direction were recorded at 15-minute intervals at the Old Ingraham Highway site and at the P33 site, which is located about 29 km north of the Old Ingraham Highway site (fig. 1 and table 1). Winds at these sites are highly correlated (H.L. Jenter, U.S. Geological Survey, oral commun., 1998). As a result, spatially uniform wind speed and direction were used for the study area using measurements at the Old Ingraham Highway site.

Solar radiation data also were collected by a pyranometer at the Old Ingraham Highway and P33 sites (fig. 1 and table 1). Solar radiation can be used as an indicator of evapotranspiration (discussed later). A comparison of solar radiation between the two sites showed a mean absolute difference (MAD) in hourly solar radiation values of 48.5 W/m^2 in 1997, which is 14 percent of the daily mean solar radiation at the Old Ingraham Highway site. Because the Old Ingraham Highway site borders the study area, the pyranometer data from this site are used to represent solar radiation over the entire model domain.

Process Studies in Support of Model Development

A number of investigations and research projects had been (or were) conducted in the SICS area over the course of this study. The investigations ranged from data collection (for example, measurement of ground elevations and flows in tidal creeks) to process studies (for example, studying the relations of wetland vegetation and resistance to flow). Results of many of these investigations were used to construct and test the SICS model and greatly reduced the uncertainty in model parameters (discussed later). The relevant studies are summarized in table 2.

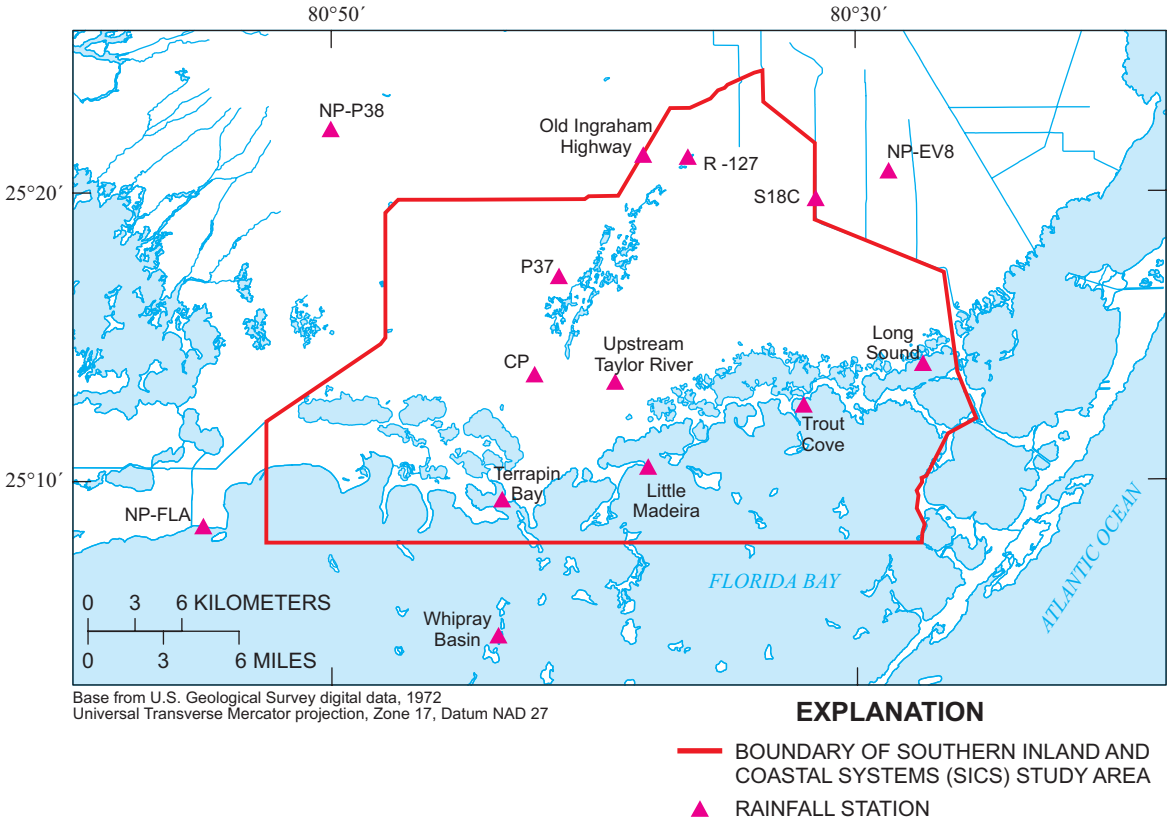

Figure 6. Rainfall data-collection sites.

Table 2. Summary of studies and research investigations used to develop the Southern Inland and Coastal Systems (SICS) model

Reference	Description	Data use in SICS model
Fitterman (1996)	Determination of freshwater-saltwater interface in ground water through airborne electromagnetic methods	Parameter estimation
German (1995)	Two field sites collecting energy-budget information, including rainfall and wind, for computation of evapotranspiration	Hydrologic input to model and model formulation
Halley and Prager (1996)	Mobile salinity measurements in Florida Bay	Model boundary construction
Hansen and DeWitt (1998)	Bathymetry of off-shore areas collected with depth-finder and global positioning system	Model area characterization
Henkle (1996)	Helicopter-based land-elevation measurement for study area at 400-meter spacing	Model area characterization
Jenter (1999)	Determination of wind-friction sheltering term for highly vegetated areas	Model formulation
Jones (1999)	Aerial- and land-based vegetation surveys used to categorize vegetation types	Model area characterization
Lee and Carter (1996)	Laboratory and field studies to relate vegetation type to frictional resistance to flow	Model area characterization
Patino (1996)	Continuous measurement of stage, streamflow, and salinity in five tidal creeks along the southern boundary of the SICS area	Model boundary conditions and model performance testing
Schaffranek and others (1999)	Measurement of wetland flow velocity with mobile acoustic meters	Model performance testing

Model Construction, Calibration, Testing, and Application

The modeling approach consisted of: (1) computational grid development; (2) assembly of data for model boundary conditions and model testing; (3) selection of initial values of model parameters based on results of field and laboratory process studies; (4) model calibration using data from the period September 1-30, 1997; (5) performance testing in which simulation results were compared with data collected from August 1996 to July 1997; (6) sensitivity analysis in which the effects on simulation results of small changes in model parameters and boundary data were evaluated; and (7) model application. Sensitivity analysis included evaluation of the effects of changes in the flow coefficient for coastal creeks, wind-friction coefficient, evapotranspiration rate, wetlands frictional resistance, boundary water levels, tidal function, boundary discharge, salinity, and land elevation on simulation results. The model was applied to quantify the effects of wind and of varying discharges at the Taylor Slough boundary on flows in Taylor Slough and to Florida Bay.

DESCRIPTION OF MODEL STRUCTURE

The two-dimensional, vertically integrated, unsteady flow and transport model SWIFT2D (Leendertse, 1987) was applied to the study area. The model was first developed for applications in Jamaica Bay, N.Y. (Leendertse and Gritton, 1971). Since that time, the model has undergone numerous revisions and updates, including enhancements described in this report for the SICS area application.

The SWIFT2D model was originally designed to simulate flow and transport in vertically well-mixed estuaries, coastal embayments, lakes, rivers, and inland waterways. Westerink and Gray (1991) describe the model as “a very comprehensive modeling package which is based on a staggered alternating-direction implicit solution.” SWIFT2D also includes many features such as time-stepping options, advective term discretization options, transport of passive tracers, coupled salinity transport, flooding and drying, the ability to include hydraulic structures, two alternative bottom friction terms including a form based on the subgrid scale energy level, a parametric expression for turbulence effects, various formulations for horizontal dispersion, and reactions and local inputs for transport.

This section describes the governing equations, the numerical procedures to solve the model equations, model input requirements, and enhancements made to the model for this study.

Governing Equations

Relatively complete mathematical descriptions of the SWIFT2D governing equations are provided in Leendertse (1987), Goodwin (1987), and Bales and Robbins (1995). Those descriptions are not repeated here, but the relevant features of the equations are described for the SICS model.

The basic equations of unsteady, nonuniform, variable density, turbulent fluid motion are formulations of the law of conservation of mass and Newton's second law of motion (conservation of momentum). Conservation of fluid mass is given by the equation of continuity, and conservation of solute mass is expressed by a transport equation. The law of conservation of momentum is given by the Navier-Stokes equation, which is the basic relation expressing Newton's second law for a viscous fluid. These equations apply to a infinitesimal parcel of fluid at an instant in time, but can be simplified by decomposing velocity, pressure, and mass into temporal mean values and turbulent fluctuations and then averaging over a time interval that is long relative to the time scale of the turbulent fluctuations. These three-dimensional equations of motion and transport are further reduced to a set of two-dimensional equations by assuming that vertical accelerations are negligibly small and by integrating the equations over the depth of flow. The resulting equations are nonlinear, time dependent, and retain coupling of motion and transport so that time-varying horizontal density gradients are included in the equations of motion. Because the nonlinear advective and bottom stress terms are retained in the governing equations, the presence of eddies can be simulated and residual circulation can be computed.

The momentum equation describes the balance between fluid acceleration and applied forces. Total acceleration is the sum of local acceleration (temporal), advection of momentum (advective terms), and Coriolis acceleration. Forces acting on the fluid include the horizontal pressure gradient and shear stresses (bottom, surface, and internal). The horizontal pressure gradient consists of the water-surface gradient and the vertically integrated density gradient, which result from horizontal variations in density. Because of this dependence of the momentum balance on salinity (through density), the horizontal density gradient terms couple the momentum equations to the transport equation. The horizontal gradient of atmospheric pressure is assumed to be negligible for the SICS area, and is not included in the model.

Stresses applied at the channel bottom are calculated from a formulation that includes the square of the velocity and a resistance coefficient. This quadratic formulation is essentially a depth-dependent friction relation based on the assumption of a vertical logarithmic profile of horizontal velocity in a steady flow. The equivalent drag coefficient increases with decreasing depth, and the correct vorticity is produced at land boundaries if the shoreline is adequately resolved by the computational grid (Signell and Butman, 1992).

Shear stress exerted by wind at the water surface is typically described as a function of the square of the wind speed. For example, Thomas and others (1990) listed six formulations for computing shear stress at the water surface, five of which are functions of the square of the wind speed. The uncertainty in all of the relations, including the one used in the SICS model, must be considered when determining the value of the empirical coefficient relating stress to wind speed.

Internal stresses are computed from horizontal diffusion terms—one for each coordinate direction (Leendertse, 1987); that is, the product of a horizontal mixing coefficient and the sum of the second derivative of the x- and y-direction velocity gradients. This term includes the effects of viscous stresses, turbulent stresses, subgrid scale momentum transfer, and the horizontal gradient of the cross product of vertical deviations from the vertical mean (a term resulting from the vertical integration of the three-dimensional transport equation). Viscous stresses oppose relative movement between adjacent fluid particles, but are small relative to turbulent stresses. Turbulent stresses represent a momentum flux and are a result of the decomposition of the nonlinear Navier-Stokes equations. Momentum transfer that occurs at horizontal scales greater than the computational grid length is resolved by the model through the velocity field, but momentum transfer that occurs at the subgrid scale must be described empirically. This subgrid scale momentum transfer, which becomes less important as the computational cell size decreases, is also included in the horizontal diffusion term.

SWIFT2D uses a formulation for the horizontal mixing coefficients that is a function of the kinematic viscosity (used to compute viscous stress), horizontal gradient of the vertical vorticity, and an unadjusted horizontal mixing coefficient (Leendertse, 1987). The kinematic viscosity is spatially and temporally invariant for the model domain, as are the unadjusted horizontal mixing coefficients (one for each coordinate direction). Vorticity is computed from the velocity field.

The vertically integrated transport equation includes terms for advection, dispersion, sources, and sinks. The dispersion coefficient in each horizontal direction is assumed to equal the sum of a dispersion in the direction of flow and an isotropic dispersion. The dispersion coefficient in the direction of flow is computed from a relation (Elder, 1959) that includes the depth of flow, velocity, the Manning coefficient, and a coefficient relating dispersion to flow properties, which is a user-defined value. The isotropic dispersion coefficient also is specified by the user and includes the effects of wind, waves, molecular diffusion, subgrid-scale effects, and vertical integration of the transport equation.

The final equation required by the model is an equation of state relating water density to water temperature and salinity. Because water density varies only slightly with temperature, temperature is assumed to be uniform and constant throughout the model domain.

In summary, the governing equations are as follows: (1) a vertically integrated continuity equation, (2) a vertically integrated longitudinal momentum equation, (3) a vertically integrated lateral momentum equation, (4) a vertically integrated transport equation, and (5) an equation of state relating salinity and density of water. These five equations are solved simultaneously at each timestep for the five unknowns: (1) water level, (2) vertically integrated longitudinal velocity, (3) vertically integrated lateral velocity, (4) vertically integrated salinity, and (5) vertically integrated density.

Numerical Solution Technique

The governing differential equations cannot be solved analytically. Instead, the equations are solved using a procedure that replaces the continuous differentials in the equations by finite-difference expressions. The finite-difference equations are applied at specified, equally spaced, computational points in the model domain and are solved at successive timesteps to provide a close approximation of the time history of water level, flow velocity, and salinity within the model domain.

The finite-difference equations are solved on a space-staggered grid (fig. 7). This grid results in an efficient solution because velocity points are located between water-level points for solution of the continuity equation (Leendertse, 1987). A complete description of the finite-difference formulations for each of the four governing conservation equations is given by Leendertse (1987).

The alternating-direction implicit (ADI) method is used to solve the governing equations. This method uses a splitting of the timestep to obtain a multidimensional implicit solution which provides second-order accuracy. The advantage of the ADI method over other implicit schemes is that solution of each set of algebraic finite-difference equations requires only the inversion of a tridiagonal matrix (Roache, 1982). The stability and convergence characteristics of the ADI technique as applied to the SWIFT2D governing equations are presented by Leendertse (1987). Although the method is unconditionally stable, there are some practical limitations to the magnitude of the timestep (Roache, 1982), particularly for model domains having irregular boundaries (Weare, 1979) or complex bathymetries (Benque and others, 1982).

Model Input Requirements

Six types of input information are required to execute the SICS model: (1) initial conditions, (2) boundary conditions, (3) physical properties of the system, (4) model parameter values, (5) orientation of the coordinate system, and (6) model options. Initial conditions are required to define the water level, velocity, and salinity in each computational cell prior to initiation of a simulation. Except as noted below, initial water surface must be level, and the initial velocities are usually set to zero. Initial salinity values can be uniform or can vary from computational cell to computational cell. Better results are obtained more quickly when initial conditions specified in the model closely match prototype conditions. The model also can be restarted using results saved from a previous simulation as initial conditions, but this option was not used in the SICS application. When the model is restarted using results from a previous simulation as initial conditions, the initial water surface need not be level.

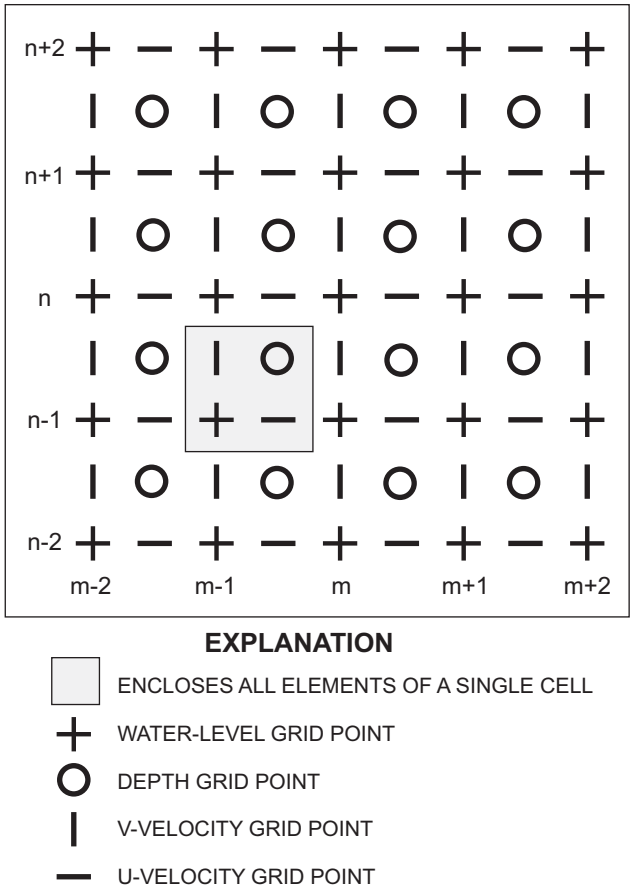

Figure 7. Space-staggered grid used in SWIFT2D.

Information on boundary conditions is required at each computational timestep throughout the simulation period. Lateral boundaries can be open (flow passes through the boundary in either direction) or closed (no flow through the boundary). Time-varying boundary conditions for flow or water level and salinity must be established at the open boundaries to describe inflows and outflows to the model domain.

Physical properties of the system are described at land surface and water surface. The bottom conditions are described by the land-surface elevation, a resistance coefficient, and ground-water inflow in each computational cell. The land-surface elevation and the resistance coefficient remain constant during a simulation period, but ground-water inflow is time varying. The water-surface boundary condition consists of the spatial and time-varying wind field, evapotranspiration, and rainfall inputs. A spatially uniform wind field was used for the SICS model application, whereas evapotranspiration and rainfall varied throughout the model domain, as subsequently described.

Several regional model parameters must be specified prior to each simulation. These parameters include air density, latitude of the study area (a single value for the entire area), kinematic viscosity of water, wind-stress coefficient, the unadjusted horizontal mixing coefficients, the isotropic mass dispersion coefficient, a coefficient that relates mass dispersion to flow properties, a resistance coefficient for each computational cell and for tidal creeks, and marginal depth. The first three parameters (air density, latitude, and kinematic viscosity) are easily specified for the SICS area, assuming that the air and water temperature do not vary substantially during the simulation period. The other parameters are known with less certainty, but results from process studies were used to establish these parameters as subsequently described.

A marginal depth, which is used to identify when a computational cell is “wet” and when the cell is “dry,” must be specified. When the water depth is less than one-half the marginal value, the computational cell is assumed to be dry and is removed from the flow and transport computations. The marginal depth effectively represents the fact that vegetation and microtopography completely impede flow for very shallow water. Likewise, in the evapotranspiration computations, as the water depth goes to zero, the volume of water available for evapotranspiration reaches zero when the water depth reaches one-half the marginal value (the same depth at which the computational cell is removed from the flow calculations).

The orientation of the coordinate system must be specified. At long open boundaries, the governing equations are solved by assuming: (1) the velocity that is parallel and adjacent to the boundary is zero; and (2) the gradient of velocity perpendicular to the boundary is zero. Consequently, to improve model performance near open boundaries, the x-axis is ideally, if feasible, aligned with the predominant longitudinal axis of the study area so that the y-axis is parallel to the upstream and downstream boundaries.

There are three primary user-controlled model options. Two options permit the user to specify the type and frequency of model output. The form of the numerical scheme used for solution of the advective terms in momentum equations also can be selected. Choices for the numerical scheme include: (1) omitting the advective terms; (2) the Arakawa (1966) method, which results in the conservation of vorticity and vorticity squared in the simulation; and (3) the Leendertse (1987) method, which is computationally

simpler than the Arakawa method but does not conserve vorticity. The second (Arakawa method) option was used for the SICS model.

Enhancements for Everglades Application

Several enhancements to the SWIFT2D model were made to adequately simulate key hydrologic processes for the SICS application. The following features were added to the model: (1) time-varying areal gains (rainfall or ground-water discharge) and losses (ground-water recharge), (2) spatially detailed computation of evapotranspiration, (3) spatially varying wind-sheltering coefficient, and (4) flexibility for computational cells adjacent to flow barriers. These and other minor code modifications are discussed in this section. A list of the original SWIFT2D routines that were modified to create the computer code used for the SICS application is given in appendix I.

Rainfall as a Time-Varying Point Source

The original SWIFT2D "rainfall" code has the option of designating time-varying point sources and sinks in specific computational cells. The computational algorithm simply adds or subtracts the volume per timestep from the appropriate cell. For the SICS application, it is desirable to have such a specified input applicable to all cells in the computational domain to represent the effects of rainfall. A subroutine created for SWIFT2D reads in rainfall information at the same time interval specified for the tidal input data. For each time interval, a flag specifies whether rainfall occurs during the time interval. If rainfall does occur, a grid of rainfall values is read in and applied to every active cell (wet cell within the computational domain).

The concentration of all constituents in rainfall inflow to each cell is assumed to be zero. Following the addition of water to a cell from rainfall, the constituent concentration within each cell is recalculated based on the ratio of added volume from the input to total cell volume. Some limitations to this approach for treating rainfall inputs are described as follows:

- There are no inputs to dry cells, which conceptually is equivalent to assuming that rainfall to dry areas infiltrates and does not run off to wet cells. This assumption has not been tested, but seems reasonable for the flat terrain of the SICS area. However, ground-water discharge to the study area is likely affected by the infiltration.
- Rainfall with nonzero constituent concentration are not represented. For the SICS application, however, the only constituent included in the simulations is salinity, and the salinity of rainfall is generally negligible.

Spatially Detailed Evapotranspiration Calculations

Evapotranspiration is the primary mechanism by which water leaves the Everglades (Duever and others, 1994). Evapotranspiration rates depend on vegetation characteristics (rainfall interception and leaf area), net solar radiation, wind (advection and turbulent transport), relative humidity, and plant-available water capacity which is a function of rooting depth, soil hydraulic properties, and water depth (Zhang and others, 2000). The SICS model represents the spatial variation in vegetation and water depth at the computational grid scale (305 × 305 m), and data do not exist on smaller scales to represent evapotranspiration, which can depend strongly on water depth and vegetation at the same scale. Enhancements were made to SWIFT2D to include evapotranspiration in the calculations and to include this process at the scale of the computational grid.

Evapotranspiration at a particular location in the Everglades can be reasonably represented by a formulation that is a function of water depth and solar radiation (German, 1999). Research is continuing to improve evapotranspiration predictions by including vegetation type as variable in the formulation (German, 2000b). The formulation developed by German (1999), described later, was used to calculate evapotranspiration for the SICS model.

The evapotranspiration volume is determined for each computational cell during each computational timestep, and this volume is removed from the model domain. Constituent concentrations in the computational cell are adjusted for the change in water volume. In reality, evapotranspiration continues even when the water level is below land surface, with water extracted from the unsaturated zone and shallow ground-water system. However, the SICS model represents surface water only, so evapotranspiration that withdraws water from below land surface is not represented in the model. When the water depth is less than the user-defined marginal depth, the evapotranspiration rate is multiplied by a factor of:

$$(2 \times \text{depth} - \text{marginal depth})/\text{marginal depth}.$$

With this equation, the evapotranspiration rate reaches zero when the depth reaches one-half the marginal depth (the same depth at which the dry computational cell is removed from the flow calculations).

There are three limitations to the evapotranspiration calculation used in the SICS model. First, water lost from below the ground surface through evapotranspiration is not included in the calculations, so the surface water required to resaturate the soil is not accounted for in the simulations. Second, the evapotranspiration rate is actually a function of the available energy in the water rather than solar radiation. The pyranometer measurement of solar radiation is a useful areal indicator of local solar radiation and available energy. However, because solar radiation becomes zero at sunset when significant heat energy remains in the water, there is a tendency in the model to underestimate evapotranspiration at sunset. Likewise, evapotranspiration is generally overestimated near sunrise when solar radiation is heating the water. However, over a daily cycle, the total evapotranspiration volume, which is on the order of 0.3 cm, generally is accurately predicted. Finally, the evapotranspiration algorithm in the SICS model was based on measurements in the study area and may not be applicable to other areas.

Wind-Sheltering Coefficient

Because SWIFT2D was originally developed for open-water applications, a spatially uniform surface wind stress was applied to the entire model domain. However, highly vegetated areas, such as the wetlands in the SICS area, shelter the water surface from the wind (Reid and Whitaker, 1976), effectively reducing the wind stress at the water surface. The work of Jenter (1999) supports this idea that emergent vegetation has a substantial sheltering effect on water-surface wind forcing. This reduction of wind stress at the water surface was simulated in this study by using a wind-sheltering coefficient, which is a simple linear multiplier of wind speed. Wind-sheltering coefficients have been successfully used in other hydrodynamic models to account for the effects of seasonal variation in vegetation along the shoreline of a reservoir (Cole and Buchak, 1995).

Preliminary results from research on the effects of wetland vegetation on wind stress at the water surface (Jenter, 1999) suggest that a spatially uniform sheltering coefficient can be applied to areas with emergent vegetation. The SWIFT2D model was modified by adding a simple algorithm for efficiently applying the wind-sheltering coefficient. This sheltering coefficient is applied to all computational cells having a Manning's coefficient greater than 0.1, which is based on the assumption that the high Manning's coefficient indicates the presence of emergent vegetation, which is true for the SICS application. This approach simplifies model input by avoiding the need to define a separate array of cell-by-cell wind-sheltering coefficients. For cells with no emergent vegetation, the wind-sheltering coefficient was 1.0.

Computational Cells Adjacent to Flow Barriers

In the original version of SWIFT2D, computations ceased if a computational cell adjacent to a flow barrier in the direction of flow became dry. When the adjacent computational cells are wet, the flow barrier acts as a levee or weir. However, barriers are used in the SICS model to represent the coastal embankment which, in the natural system, has adjacent high ground that is dry under some conditions. Hence, an enhancement was required to allow computations to continue even if computational cells adjacent to barriers were dry. The code was modified to provide the constraint that there was no flow over or through a barrier at locations where computational cells on either side of the barrier were dry. Flow is allowed to enter a cell adjacent to a barrier from other directions. There is no storage of constituents at the barrier when the cell adjacent to the barrier is dry. This modification resulted in a reasonable representation of the coastal embankment.

This enhancement does not, however, cover all possible conditions that can occur at a barrier. For example, consider the condition in which cells on both sides of a barrier are initially dry and one cell becomes wetted as a result of inflow. Because of the previously described algorithm, no flow can occur across or through the barrier. The dry cell remains artificially dry and can only be rewetted from another cell on the same side of the barrier as the dry cell. This situation does not occur in the application of the SICS model, but users should be aware of such a limitation in other SWIFT2D applications.

Other Code Modifications

Several other minor modifications were made to the original SWIFT2D code for the SICS area application:

- The code was modified to set the wind friction to zero in computational cells adjacent to a water-level boundary. This modification helps prevent numerical oscillations at the boundary: a situation observed in other model applications (R.W. Schaffranek, U.S. Geological Survey, oral commun., 1999).
- Print routines were modified so that: (1) simulated constituent concentrations at selected locations can be printed at the same time interval as water levels and discharges, and (2) simulated water levels and velocities are printed to a different file than the remainder of the simulation output. The output units for the simulated velocities also were given increased precision to accommodate the low velocities in the SICS area.
- The original version of SWIFT2D would not operate properly if more than one barrier was present in a column of computational cells. The code was modified to allow multiple barriers to be specified per column.

CONSTRUCTION, CALIBRATION, TESTING, AND APPLICATION OF FLOW AND TRANSPORT MODEL

Implementation of the SWIFT2D model for the SICS study area required: (1) development of the computational grid, (2) specification of boundary conditions, and (3) identification of values for model parameters. Each of these steps is described in the subsequent sections along with model calibration, testing, and application results.

Computational Model Domain

The model domain is irregularly shaped and contains 9,738 computational cells (fig. 8). The computational cells are 305 m square, so the total area of the model domain is 905.8 km^2. The maximum north-south extent of the domain is 29.90 km (98 computational cells), and the maximum east-west extent is 45.14 km (148 computational cells). The 305-m square grid cells provide good resolution of the study area, and do not require unreasonable computer resources to perform simulations. The Florida Bay open boundary of the model was positioned a sufficient distance from the freshwater-saltwater mixing zone to minimize the problems associated with gradient type boundary conditions.

As previously described, land-surface elevations were measured at about 400-m spacings (Desmond and others, 2000). A linear distance-weighted four-point interpolation of the 400-m (1,312 ft) spaced data was used to assign land-surface elevations to each computational cell of the 305-m SICS grid (fig. 9).

The spatial characteristics of the Buttonwood Embankment (fig. 8) vary at a scale that is much smaller than the computational cell size. Rather than attempting to assign relatively high land-surface elevations to computational cells along the embankment, which would result in poor resolution of the embankment, flow barriers were used to represent the embankment (fig. 8). In cells where the embankment is diagonal to the cell, the embankment is represented by a series of north-south and east-west flow barriers within the cell. The location of the embankment was derived from field observations aided by USGS 1:24,000 scale topographic maps. All creeks flowing through the embankment are defined as cuts in the flow barriers (fig. 8). Elsewhere, creeks are defined as solitary flow barriers with the sill elevations at the creek bottom. (Creek dimensions were presented earlier in the topography section.)

Boundary Conditions

Boundary conditions are supplied at the water surface and at lateral boundaries. These boundary conditions are described in this section.

Water-Surface Boundary

The “rigid lid” assumption, in which the water surface in each computational cell moves vertically, but no deformation of the level water surface in the cell occurs, is used at the water-surface boundary. This implies that high-frequency wind waves are not included in the simulations. As previously described, evapotranspiration and rainfall volumes are computed for each computational cell during each timestep, and these volumes are removed (evapotranspiration) or added (rainfall) to the computational cells.

Wind conditions are represented as spatially uniform over the model domain, and data from the Old Ingraham Highway site (fig. 1 and table 1) were used to define the wind field. Measured fluctuations in wind conditions at less than an hourly timescale typically do not reflect regional patterns. Therefore, a moving average wind speed was used for the boundary. For each

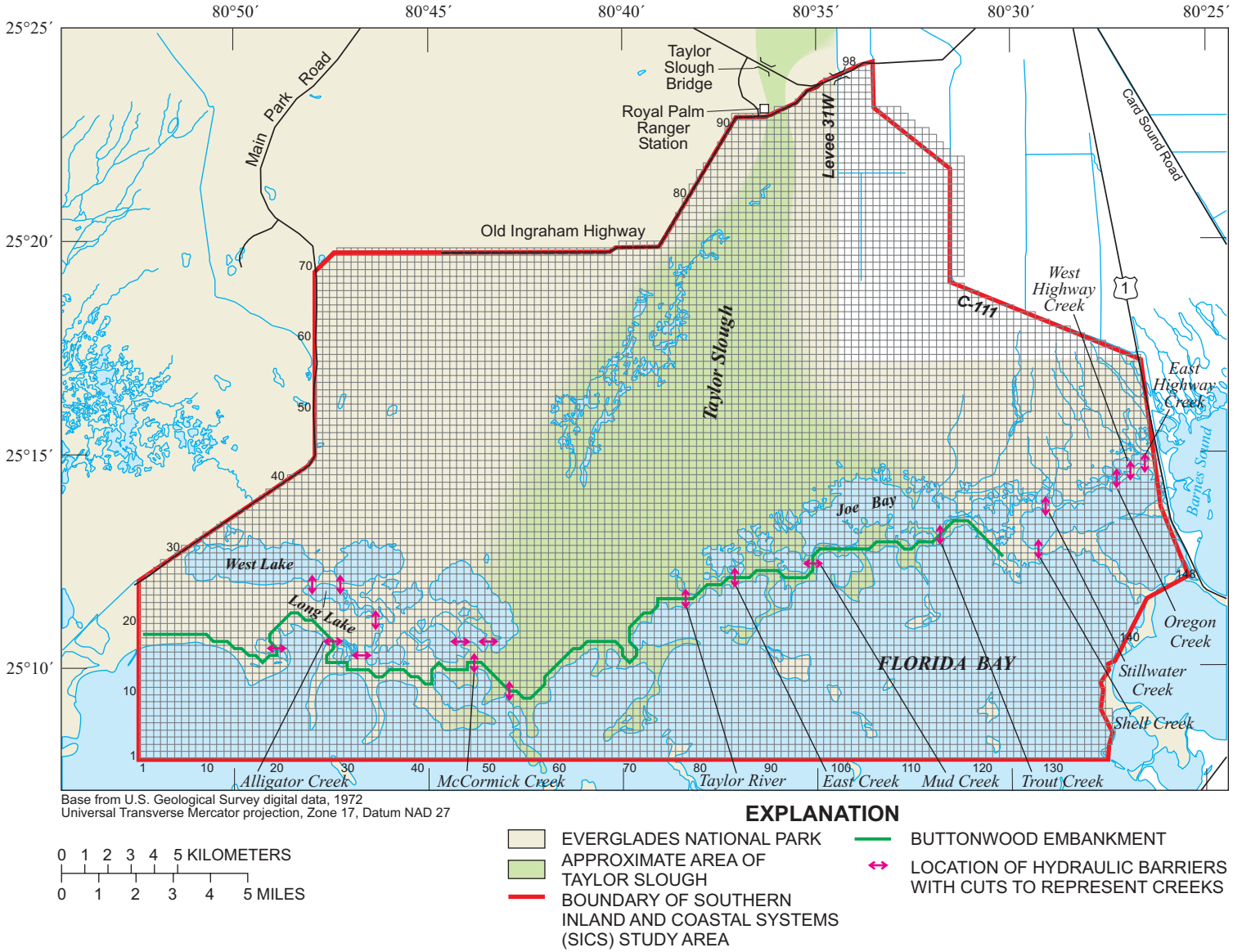

Figure 8. Model grid, location of embankment barriers, and location of creeks in the study area.

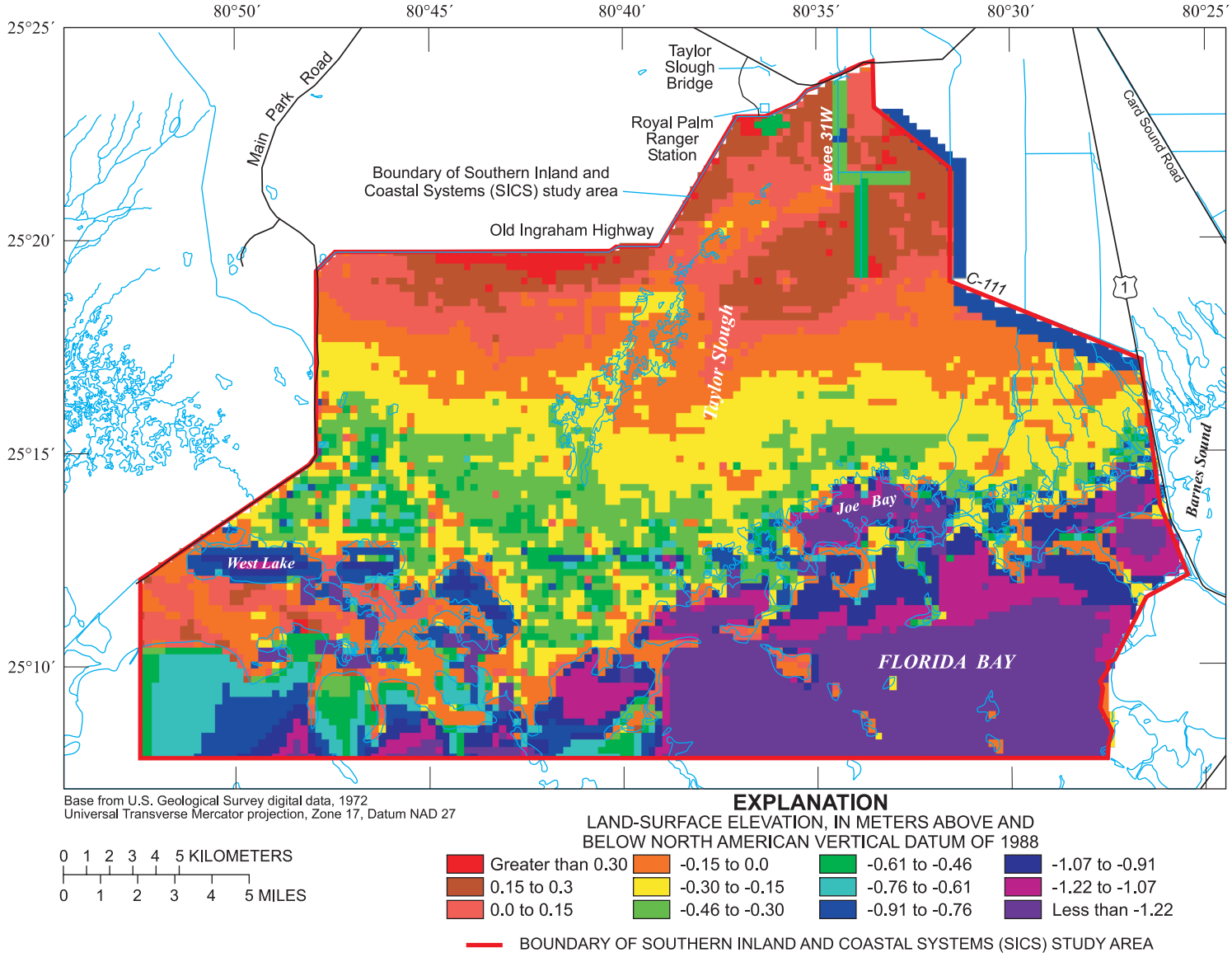

Figure 9. Land-surface elevation in grid cells.

computational timestep, the east and north components of the wind speed were averaged over a 5-hour period centered on the timestep. This temporal smoothing yields a realistic regional wind field (H.L. Jenter, U.S. Geological Survey, oral commun., 1999).

Wind measurements were made 2.4 m above land surface, but the wind drag coefficient, C_d, is applicable to wind speeds measured at a height of 10 m above land surface. Wind speeds measured at 2.4 m were converted to speeds at 10 m by the equation (Chadwick, 1996):

$$\frac{W}{W_m} = \frac{\ln\left(\frac{z}{z_o}\right)}{\ln\left(\frac{z_m}{z_o}\right)}, \qquad (2)$$

where W is the wind speed at the desired height, W_m is the wind speed at measured height, z is the desired height above the land surface of 10 m, z_m is the measured height of 2.4 m, and z_o is the roughness height. Assuming that z_o = 1 m, then equation 2 reduces to $W = 2.5W_m$.

Lateral Boundaries

Lateral boundaries are defined as open (having free exchange of water and salt across the boundary) or closed (having no flow across the boundary). Open boundaries can be described by a time series of discharge or water level, with discharge boundary conditions generally providing more realistic simulation results. The SICS model lateral boundaries are identified in figure 10.

Inflow at Taylor Slough bridge is computed with a stage-discharge relation (Everglades National Park, written commun., 1999) from the Taylor Slough bridge site. Discharge entering from the north into L-31W, released from hydraulic gate structure S-175, is provided by the SFWMD using a stage-discharge rating at S-175.

Dynamics of the flows entering the wetlands from the section of C-111 Canal between hydraulic control structures S-18C and S-197 (fig. 10) are of great interest and are under investigation (Schaffranek, 1996; Schaffranek and Ball, 2000). The S-18C discharge is provided by the USGS, and S-197 is usually closed. When S-197 is occasionally opened, flow is provided by the SFWMD. The levee on the southern side of the section of C-111 has been removed to promote delivery of additional water to the easternmost area of the ENP wetlands (fig. 1) (Ball and Schaffranek, 2000a). The discharge entering the wetlands along C-111 is assumed to be the difference in flows at S-18C and S-197. Field observations by the USGS and ENP indicate that the northerly flows through several culverts that line this section of the canal are minimal due to the higher topography on the northern side of the canal. Within the model, the canal discharge to the model domain is placed in an artificial topographic low along the boundary of the SICS area adjacent to C-111 (fig. 9) to allow uniform flow distribution along the entire section of C-111 between S-18C and the US-1 boundary of the SICS flow model just upstream of S-197. Evapotranspiration losses from this boundary are simulated in the same manner as for the rest of the model domain.

The lateral boundary along C-111 Canal in the northeastern part of the model domain actually represents ground-water interaction through the levee with C-111 Canal. The ground-water interaction between the L-31W and C-111 Canals north of S-18C (fig. 10) is considered important. Specifically, when water levels in the C-111 Canal are higher than the land elevation west of the levee, leakage through and under the levee supplies water to the wetlands west of the levee, supplementing the wetland ponding. Although SWIFT2D is a surface-water model, the ground-water interaction of the wetlands with the C-111 Canal can be approximated. Water levels at the boundary cells north of S-18C and east of the levee are assigned measured S-18C water levels for boundary condition treatment. The frictional coefficient for the model cells within the boundary is set to represent flow resistance equivalent to the hydraulic conductivity through and under the levee. In this way, leakage though and under the levee is represented as flow through these boundary cells. At lower water levels in the C-111 Canal, the simulated leakage would tend to dry the boundary cells. Under these conditions, the model would represent no exchange through and under the levee.

The boundary along Old Ingraham Highway and southward along part of Main Park Road (fig. 10) experiences overtopping and occasional culvert flow. Flow measurements have been made by ENP at the culverts along Main Park Road (fig. 10), which includes the western Old Ingraham Highway boundary, but none have been made on the rest of Old Ingraham Highway nor have overtopping flows been measured. Due to the

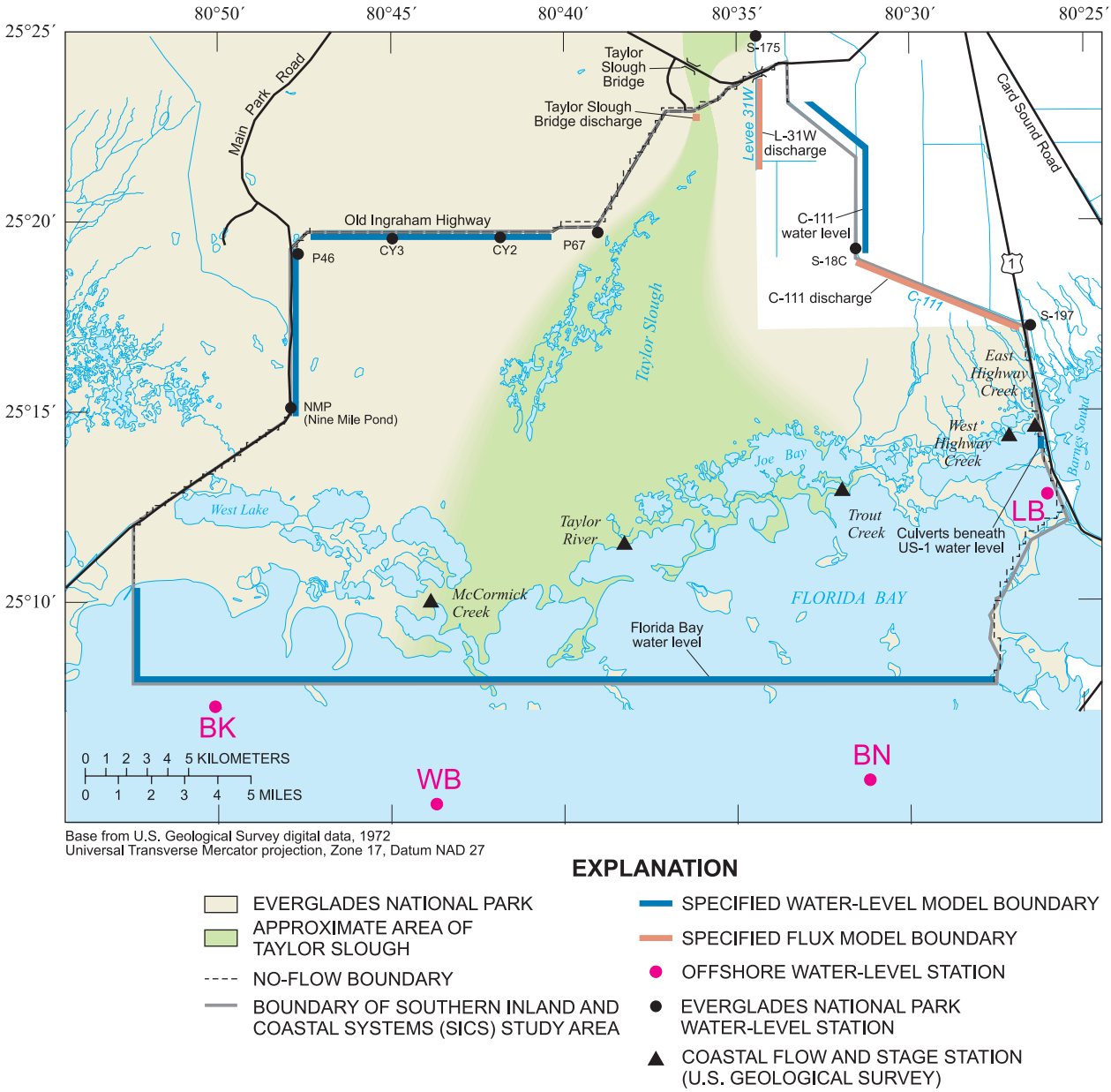

Figure 10. Model boundaries and data-collection sites used to determine discharge, conductivity, and water-level boundary conditions.

scarcity of these flow data, the model boundary was constructed using water-level data from five ENP field sites (NMP, NP46, CY2, CY3, and NP67) shown in figure 10. These sites provide data on stage along the south and east side of Old Ingraham Highway (fig. 10). Because Old Ingraham Highway is just outside the model domain defined by these stage sites, it was not necessary to simulate flow in the culverts under the highway.

The Old Ingraham Highway and Main Park Road boundary is designed in three segments. Boundary cell water levels were linearly interpolated between each pair of adjacent sites. Segments are from: NMP to NP46, NP46 to CY3, and CY3 to NP67. This approach is justified by the fact that station CY2 had water-level values very close to those obtained by a linear interpolation from CY3 to NP67. Water levels along this boundary were set to zero when field sites measured water levels below the land surface.

Field measurements indicate that the culverts on Old Ingraham Highway south of NMP carry negligible flow (Stewart and others, 2000), which is also true for the section of Old Ingraham Highway northeast of NP67. Hence, these boundaries were established as no-flow boundaries. Flows are not available for the culverts under US-1. Therefore, this boundary was specified with a measured water level at nearby West Highway Creek (fig. 10).

The open boundary along the southern part of the model has a specified water-level condition designed to closely match measured water levels in Florida Bay and at coastal creeks. In order to determine if there is a significant diurnal tide signature at the coastal water-level stations (fig. 2), a spectral analysis was performed on the water-level data from selected sites. The spectrum is the Fourier transform of the autocovariance function α_τ, which is computed from the field data by:

$$\alpha_\tau = \frac{\sum_{t=1}^{t_{max}} (z_t - \bar{z})(z_{t+\tau} - \bar{z})}{t_{max} - 1}, \qquad (3)$$

where t_{max} is the total time of the data set, z_t is the water level at time t, $\bar{z}$ is the mean water level, and $z_{t+\tau}$ is the water level at a later time $(t + \tau)$. The spectrum Γ_ω is then calculated from the autocovariance function by the equation (Lumley and Panofsky, 1964):

$$\Gamma_\omega = \frac{1}{2\pi} \frac{\sum_{\tau=1}^{\tau_{max}} \cos(\omega\tau)\alpha_\tau}{\tau_{max}}, \qquad (4)$$

where ω is the frequency. At frequencies (ω) that have more significant autocovariance values, the value of the spectrum is higher. Thus, the spectrum shows dominant frequencies of fluctuations. A spectrum calculated for downstream water levels at structure S-21 along the shore of Biscayne Bay (fig. 1) shows a strong lunar tidal signature (fig. 11). The sharp peak in the spectrum at one-half day (12 hours) indicates the lunar tidal cycle. In comparison, the spectra at McCormick Creek (fig. 12) and Trout Creek (fig. 13) do not show this lunar tide signature. The water-level fluctuations at these coastal creek outlets to Florida Bay are not subject to a standard lunar tide and instead are probably influenced more by wind.

The southern SICS model boundary lies between the water-level data collected at the coastal flow stations at McCormick Creek, Taylor Creek, and Trout Creek and offshore ENP stations BK, WB, and BN (fig. 10). An average of these water levels from these seven stations was used to define the boundary. The average is used for the entire boundary to avoid numerical oscillations that can occur when small lateral water-level differences are forced along long open boundaries (R.W. Schaffranek, U.S. Geological Survey, oral commun., 2000).

Salinity must be defined at all open boundaries. All the discharge open boundaries are located inland and were assigned a salinity value of zero. Flow through the culverts beneath US-1 is assumed to have the salinity recorded at East Highway Creek (fig. 10). Salinity data measured at offshore ENP stations BK, WB and BN (fig. 10) were used for the southern boundary. Salinity was linearly interpolated between sites BK and WB and between sites WB and BN.

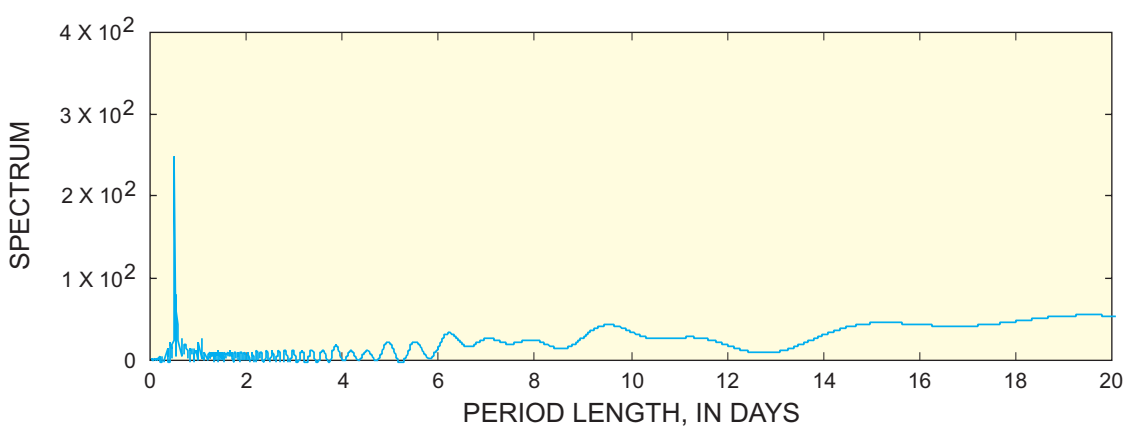

Figure 11. Spectral function of stage downstream of structure S-21.

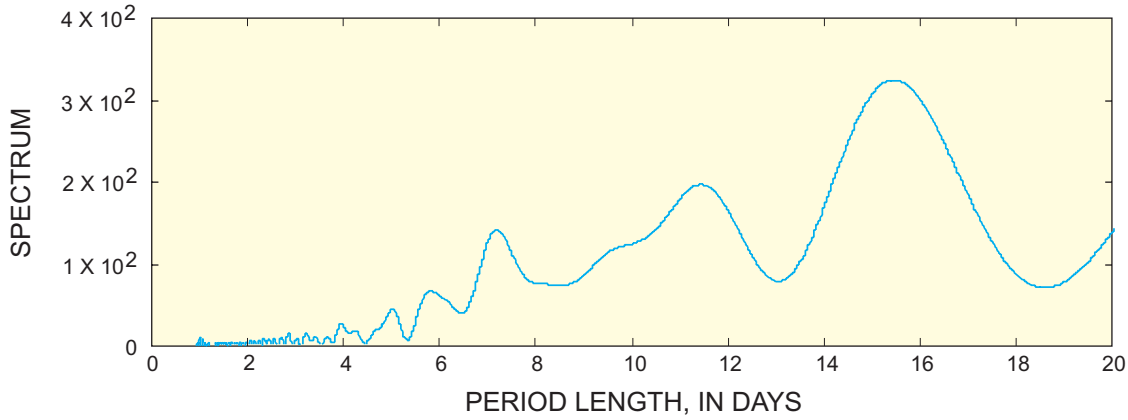

Figure 12. Spectral function of stage at McCormick Creek.

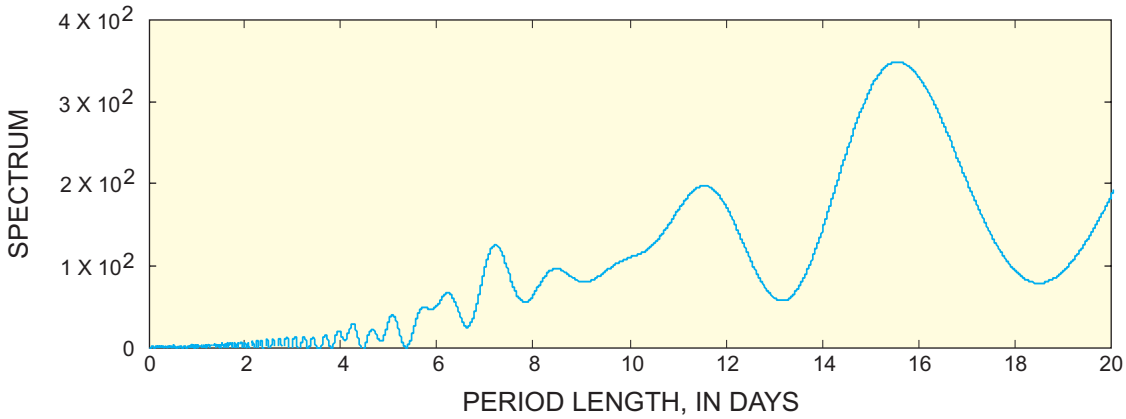

Figure 13. Spectral function of stage at Trout Creek.

Salinity west of site BK was assumed to be equal to site BK values. Likewise, salinity east of site BN was assumed to be equal to values measured at site BN. All of the salinity values were then translated north and applied at the model boundary.

Model Parameters

Implementation of the SWIFT2D model for the SICS study area required specification of values for critical model parameters. This section describes the various model parameters including computational control parameters, wind coefficients, evapotranspiration, frictional resistance both in vegetated marshes and coastal creeks, and the dispersion coefficient for the transport equation.

Computational Control Parameters

Control of the computational simulations requires specification of an integration timestep, selection of a frequency for reevaluation of depth-dependent Chezy coefficients, and assignment of parameters for the wetting and drying algorithm. A 7.5-minute computational timestep of one-half the data-collection interval, was used. The Courant number was less than 4 for this timestep size.

The numerical solution in the SICS model does not allow the computation of depth-dependent Chezy friction factors from the specified Manning coefficients at times when the grid nodes are checked for drying and flooding. For this application, new Chezy values are computed every 45 minutes, and drying and flooding are checked every 30 minutes; therefore, the resultant Chezy computations are delayed one timestep only every 90 minutes.

A Chezy value cannot be computed from the assigned Manning coefficient when the water depth in a cell is less than the marginal value, so the Chezy value must be assigned in those cases. As previously discussed, the user-supplied value for marginal depths in dry cells was set to 0.10 m. The residual depth values for dry cells, at which higher Chezy resistance values are assigned, is intended both to approximate the naturally occurring drop in flow velocities to zero at the bottom and to suppress the potential growth of local numerical instabilities that can develop in complex shallow water bodies. If a wetland cell has a Manning's n of about 0.4, and the water depth is at the marginal value of 0.10 m, the Chezy value is about 3. However, in areas of the model which are open water and have a Manning's n of 0.02, the Chezy value is 60 at the marginal depth. Because virtually all flooding and drying occurs in the wetlands, an average Chezy value of 5 is specified for cells with depths less than the marginal depth.

Wind Coefficients

The coefficient for the wind-friction term, C_d, in the momentum equation has historically ranged from 1.5×10^{-3} for light winds to 2.6×10^{-3} for heavy winds (Wilson, 1960). A research project is underway to better define this coefficient and the effects of emergent vegetation (Jenter, 1999). A slightly lower value (1.2×10^{-3}), identified for winds less than 36 m/s (Large and Pond, 1981), was found to work well in the model. The wind-sheltering coefficient, S_w, for emergent vegetation (as previously discussed) is described by Reid and Whitaker (1976). Best estimates of S_w range from 0.1 to 0.5; a value of 0.33 is used in the model. Jenter and Duff (1999) suggest that the Reid and Whitaker (1976) values are reasonable for the SICS area wetlands.

Evapotranspiration

Results of research to parameterize evapotranspiration in southern Florida wetlands were used to compute evapotranspiration in the SICS model (German, 1995). The Priestly-Taylor equation relates evapotranspiration to available energy (Linsley and others, 1982, p. 162-163):

$$ET = \alpha \frac{\delta[R_n - G - M]}{H_L(\delta + \gamma)} , \qquad (5)$$

where ET is evapotranspiration, α is the site coefficient, δ is the slope of the saturation-vapor-pressure curve, R_n is the net radiation exchange, G is the soil heat flux, M is the rate of heat storage above the soil and below the point where R_n is observed, H_L is the latent heat of evaporation, and γ is the Bowen ratio coefficient.

Substantial site-specific information is needed to use equation 5. Comparison of a number of sites near the model area indicates that the coefficient α can be expressed as a function of solar radiation, χ, in watts per square meter and water depth, d, in meters (German, 1999):

$$\alpha = 1.036 - 0.000388\chi + 0.4564d - 03.3342d^2 . \qquad (6)$$

No strong correlation between α and vegetation type was found by German (2000a; 2000b) in the sets of data available from nine evapotranspiration sites, suggesting that a general formulation is valid for all vegetation types in the model domain.

Whereas most of the parameters in equation 5 are site specific and difficult to measure, χ in equation 6 is assumed to be spatially uniform at the scale of the model. Therefore, regression analysis was used to estimated ET from α and χ. Hourly data from 1996 at the Old Ingraham Highway site and the P-33 site (fig. 1) were used in the analysis; data were used only when measured water levels were above land surface. Although located north of the study area, the P-33 site has vegetation and hydrology similar to the SICS area. Two forms of the regression were used: (1) ET as a function of $\alpha\chi$ and χ, (equation 5 suggests a multiplicative relation between α and available energy), and (2) ET as a function of α and χ. The two prediction equations are:

$$ET = -1.32 \times 10^{-5}\alpha\chi + 2.73 \times 10^{-5}\chi + 2.56 \times 10^{-3} \qquad (7)$$

and

$$ET = -2.30 \times 10^{-3}\alpha + 1.70 \times 10^{-5}\chi + 1.79 \times 10^{-4} . \qquad (8)$$

Both equations had a correlation coefficient ρ of 0.79 and were statistically significant at $p < 0.01$.

Given that neither equation has a stronger correlation, the multiplicative relation of α and χ in equation 7 was used. A time series of pyranometer readings χ are input from the evapotranspiration data set to the model to compute an effective cell-by-cell evapotranspiration value. The coefficient α is computed for each cell by equation 6, and the evapotranspiration rate computed by equation 7 is applied to the cell for the timestep as described in the evapotranspiration computation section.

Frictional Resistance — Vegetation

One of the most important flow-controlling terms in virtually all hydraulic models is the resistance to flow or frictional resistance. Unfortunately, very little information exists in the literature to guide selection of appropriate values for friction coefficients in vegetated wetlands, such as in the SICS study area. Because of the importance of this term, field and laboratory research was performed to determine the effective frictional resistance to water flow through differing Everglades vegetation types (Lee and others, 1999). Extensive hydraulic measurements (velocity, depth, hydraulic gradient, and so forth) were made in a laboratory flume containing transplanted marsh vegetation. Field measurements of velocity, depth, and vegetation type and density were also made in conjunction with point measurements of the hydraulic gradient using a portable pipe manometer at many locations in the study area (Lee and others, 2000a). The results indicated that flow regimes in the study area are not fully turbulent flow and are normally within the transition region between laminar and turbulent flow (Lee and others, 2000b). Because the Manning equation was formulated for fully turbulent flow and the SICS flow is transitional, an effective Manning's *n* was calculated for use in the equations developed for SWIFT2D.

Preliminary results show high values for Manning's *n* with little variation among vegetation types. For sawgrass, 14 measurements gave an average Manning's *n* of 0.43 $s/m^{1/3}$ with a range from 0.23 $s/m^{1/3}$ to 0.60 $s/m^{1/3}$. For rush, four measurements gave an average Manning's *n* of 0.46 $s/m^{1/3}$ with a range from 0.36 to 0.57 $s/m^{1/3}$. For mixed rush/sawgrass, six measurements gave an average Manning's *n* of 0.38 $s/m^{1/3}$ with a range from 0.26 to 0.61 $s/m^{1/3}$. The range of average values for different vegetation types is 0.08 $s/m^{1/3}$ (J.K. Lee, U.S. Geological Survey, written commun., 1998). According to Schaffranek and others (1999), the average values of Manning's *n* for different sawgrass densities are 0.42 to 0.48 $s/m^{1/3}$; a range for different densities of 0.06 $s/m^{1/3}$. The range of variation within each type is larger than both the average range between vegetation types as well as the range between densities within the same type. Acknowledging that measurement variation exceeded type variation, average values for each type were used: 0.43 $s/m^{1/3}$ for sawgrass, 0.46 $s/m^{1/3}$ for rush, and 0.38 $s/m^{1/3}$ for mixed rush/sawgrass. These values were used as a guide for the model based on vegetation types identified in figure 4. Many areas that did not clearly fall into one of these vegetation types were assigned a Manning's *n* of 0.4. Open-water areas were given a nominal value of 0.02. This areal distribution of Manning's *n* coefficients is shown in figure 14.

Due to microtopography and vegetation, the effective flow resistance factor for a model cell varies with the flow depth. Research is underway to identify the hydraulic factors that affect the frictional resistance and to determine resistance as a function of flow depth and velocity (Jenter, 1999). No final conclusions have been drawn as to the most suitable form of the resistance factor variation. However, when upscaling frictional resistance from point measurements at the field scale to represent resistance of an entire model grid, microtopography has the capability of increasing the effective frictional resistance at lower water depths. The variation in topography creates sinuosity in flow, increasing the flow resistance experienced at shallow depths. Based on this functionality, a form is proposed and used in the SICS model to represent the variation of Manning's *n* with depth:

$$n_{eff} = n_{ref}(d_{ref}/d)^{power}, \qquad (9)$$

where

n_{eff}	is the effective Manning's *n*,
n_{ref}	is the reference Manning's *n* from preliminary field estimates,
d_{ref}	is the reference water depth,
d	is water depth, and
$power$	is the exponent that represents nonlinear characteristics of the relationship.

The parameter d_{ref} would theoretically be the water depth at which the previously mentioned field value n_{ref} was measured. Numerical experiments with the SICS model indicated that best results were obtained with $d_{ref} = 0.6$ m and $power = 2$. The values of these coefficients would logically depend on the topographic and vegetative features of the application region.

Flow Coefficient — Coastal Creeks

Resistance coefficients are also needed for the coastal creeks that convey water to Florida Bay. The approach used to establish reasonable resistance coefficient values for the SICS model included numerical experiments to adjust coefficients to closely match computed and measured creek flow in five creeks. Field confirmation of these values was then obtained

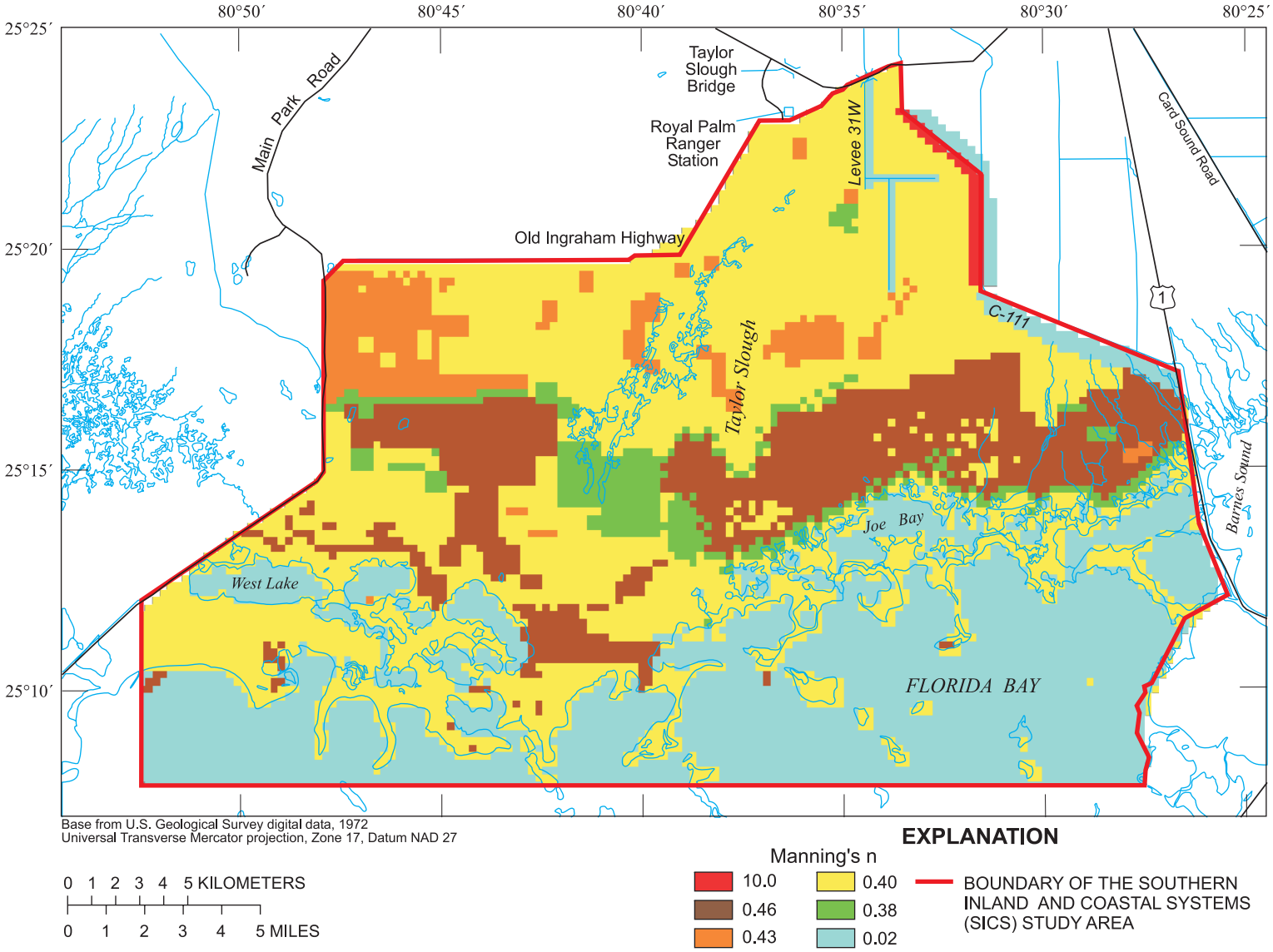

Figure 14. Manning's *n* values used in the model.

in one creek by measuring sufficient information to compute Manning's n for 1 year. The values were also compared to those available in the literature.

The regions where coastal creeks cross the Buttonwood Embankment (fig. 2) are represented in the SICS model as cuts in barrier cells. The flow condition that occurs almost exclusively in the cuts is submerged weir flow. The hydraulic barrier equation defining this flow condition in the model is (Leendertse, 1987, p. 34):

$$Q = C_r B d \sqrt{2g\Delta h}, \tag{10}$$

where Q is discharge in the stream, C_r is a flow coefficient term of the stream segment, B is stream width, d is depth, g is gravitational acceleration, and Δh is head drop across the embankment. Equation 10 is similar to a weir flow equation. The Manning equation for this assumed rectangular cross section is:

$$Q = \frac{\lambda}{n} B d^{5/3} \sqrt{\frac{\Delta h}{L}}, \tag{11}$$

where λ is 1 in metric units and 1.49 in English units, and L is the stream length.

Combining equations 10 and 11 gives:

$$n = \frac{\lambda d^{2/3}}{C_r \sqrt{2gL}}. \tag{12}$$

Equation 12 can then be used to estimate Manning's n from the model calibrated C_r value. Values of C_r were calibrated to match measured flows for the five creeks where discharge data were available. Results are presented in table 3 along with the stream lengths, L, estimated from USGS topographic quadrangle maps. Values of L were not allowed to exceed 610 m (the width of two cells) because the section of the stream crossing the embankment is represented in the model as occurring between the cell immediately upstream of the barrier and the cell immediately downstream. Effective Manning's n values are computed from equation 12 using an average creek depth of 1.5 m. West Highway Creek has a substantially lower n than the others creeks, and field observations indicate this creek has the least vegetation. The range of n values for the creeks, other than West Highway Creek, is generally considered to be valid for heavily vegetated reaches (French, 1985, p. 129).

Manning's n for a coastal creek can be inferred from the measured creeks to be about 0.1 (table 3). For the creeks where discharge was not measured, values of C_r were estimated using equation 12. These values assume that the Manning approximation is valid, and the frictional resistance is similar to the average of the measured creeks.

As a further investigation of the flow coefficients for the coastal creeks, a supplemental continuous water-level and discharge monitoring station was installed 3.22 km upstream from the original coastal station on Taylor River (fig. 2). The measured discharge and water-level differences between the original station and the upstream station were used to determine n from Manning's equation for daily average data from July 31, 1999 to August 1, 2000. The computed Manning's n for each day was averaged for the period and yielded a mean value of Manning's n of 0.121 s/m$^{1/3}$ with a standard deviation of 0.078 s/m$^{1/3}$. The value of n determined by using equation 12 and calibrating the model to measured flows was 0.152 s/m$^{1/3}$ at Taylor River. Thus, the difference between the Manning's n value obtained by calibrating the model to measured flows and that obtained directly from field measurements is less than the standard deviation of the field measurements.

Although the Manning equation for surface water applies for turbulent flow and Darcy's law for ground water applies for laminar flow, Merritt (1996) found it useful to approximate overland flow with Darcy's law in a ground-water model. In this study, an

Table 3. Stream friction terms and lengths and Manning's n

[C_r, friction term of the stream segment; n, Manning's coefficient]

Site name	C_r	Length (meters)	Effective n
McCormick Creek	0.10	610	0.121
Taylor River	.08	610	.152
Mud Creek	.07	488	.194
Trout Creek	.25	146	.099
West Highway Creek	.35	219	.058
Alligator Creek	.08	610	.1*
East Creek	.10	390	.1*
Shell Creek	.08	610	.1*
Stillwater Creek	.08	610	.1*
Oregon Creek	.08	610	.1*
East Highway Creek	.08	610	.1*

* Estimated vlue.

analogous technique is used to represent the ground-water interactions with the C-111 Canal in a surface-water model. Fish and Stewart (1991) indicate a hydraulic transmissivity in the area between the L-31W and C-111 Canals of about 56,000 m^2/d. Equating the Manning equation with Darcy's law yields the following:

$$\frac{\lambda}{n} d^{\frac{5}{3}} \sqrt{S_f} = TS_f, \qquad (13)$$

where λ is Manning's constant (1.49 in English units, 1 in metric units), d is overland flow depth adjacent to the canal, S_f is surface-water slope, and T is aquifer transmissivity.

Solving equation 13 with an average flow depth of 0.1 m, a water slope of 0.0005, and a transmissivity of 56,000 m^2/d = 0.648 m^2/s yields a Manning's n of 1.5. Raising the flow depth to 0.3 m raises Manning's n to 9.3, and a flow depth of 0.6 m yields a Manning's n of 29.5. With this level of uncertainty and unusually high values of n, an order of magnitude value for n of 10 was assigned to cells that represent ground-water flow between the C-111 Canal and the model domain.

Dispersion Coefficient

The transport of salt and other constituents in the model is affected by the dispersion coefficient in the transport equation. The magnitude of the dispersion coefficient is scale dependent; the larger the water body, the larger the coefficient. The effective dispersion coefficient is on the order of meters squared per second in open channels, whereas its magnitude is hundreds of meters squared per second in estuaries (Fischer and others, 1979). In application of the dispersion coefficient in a numerical model, the length scale of significance is the cell size. Additionally, numerical diffusion can result from solution approximations in numerical models. This creates an additional dispersion component because concentrations at the end of a timestep must be assigned to the two closest computational nodes rather than at an exact physical location (Fischer and others, 1979). The horizontal dispersion coefficient, D, is calculated as:

$$D = \frac{0.5(\sigma_{i+1}^2 - \sigma_i^2)}{\Delta t}, \qquad (14)$$

where σ^2 is the variance of the constituent concentration distribution. In the case of the SICS model, if the mean velocity $\bar{u} \approx 0.05$ m/s, which would be an unusually high value considering the field measurements (Tillis, 2001), then the ratio of the distance traveled in one timestep $u\Delta t$ to the grid size Δx is about 0.07. This means that at the end of the timestep, mass originating at the edge of the cell has moved to an average location $x = 0.07\Delta x$. The mass must be reassigned to node locations: 0.93 fraction to $x = 0$ and 0.07 fraction to $x = \Delta x$. Thus, at the end of the timestep, 0.93 fraction of the mass is at a distance $0.07\Delta x$ from x, and 0.07 fraction of the mass is at a distance $0.93\Delta x$ from x. The increase in variance that is solely due to this numerical process is:

$$\sigma^2 = 0.93(0.07\Delta x)^2 + 0.07(0.93\Delta x)^2 = 0.065\Delta x^2. \qquad (15)$$

This yields a numerical dispersion of $D = (1/2)0.065$ $(305\ m)^2/450s = 6.7\ m^2/s$. With a lower mean velocity of $\bar{u} = 0.01$ m/s typically found in the wetlands, numerical dispersion is reduced to 1.5 m^2/s. Numerical dispersion is much smaller than the physical dispersion described in the next section.

Calibration

The model was calibrated by adjusting computational control parameters over reasonable ranges to produce the best match between computed and measured values of velocity flow and salinity for the calibration period. The calibrated model was subsequently applied to a different time period to verify or assure that the determined parameter values apply for conditions other than those used for calibration.

The calibration period was chosen to coincide with a time of intensive measurement of flow velocities in the wetlands. The 1-month simulation period was September 1-30, 1997. Results from September 22 to 25 were used for comparison with field velocity data, which corresponds to one of four field measurement efforts conducted from July 1997 to July 1998. A 17-day warm-up period (August 15-31, 1997) was used to allow effects of errors in the initial conditions to dissipate from the model.

Extensive field research in the study area has reduced the uncertainty in values to use for a number of parameters in the SICS model. The parameters with greatest uncertainty are the flow coefficients of the coastal creeks and the field-scale dispersion coefficients. The flow coefficients of the coastal creeks were calibrated to the values as presented in table 3 by matching measured and simulated flow at the coastal creeks, flow velocities and water velocities in the wetlands, and coastal salinities.

Salinity dispersion is most noticeable near the coast. The dispersion coefficient that produced the best match between measured and simulated salinities was 10 m^2/s (fig. 15). This result indicates that the numerical dispersion is a smaller part of the effective dispersion. The calibrated model dispersion coefficient is not as large as documented in field-scale estuary studies because the coefficient in the model applies to individual computational cells.

The coastal creek outlets where the point field conductivity measurements were taken had large spatial gradients in salinity. Salinity distributions from the calibration simulation are shown in figure 16; some salinity intrusion into the subembayments is apparent. This spatial variability in salinity presents difficulties in comparing point measurements and computed mean cell salinities as shown in figure 15. Nonetheless, considering these difficulties, measured and computed

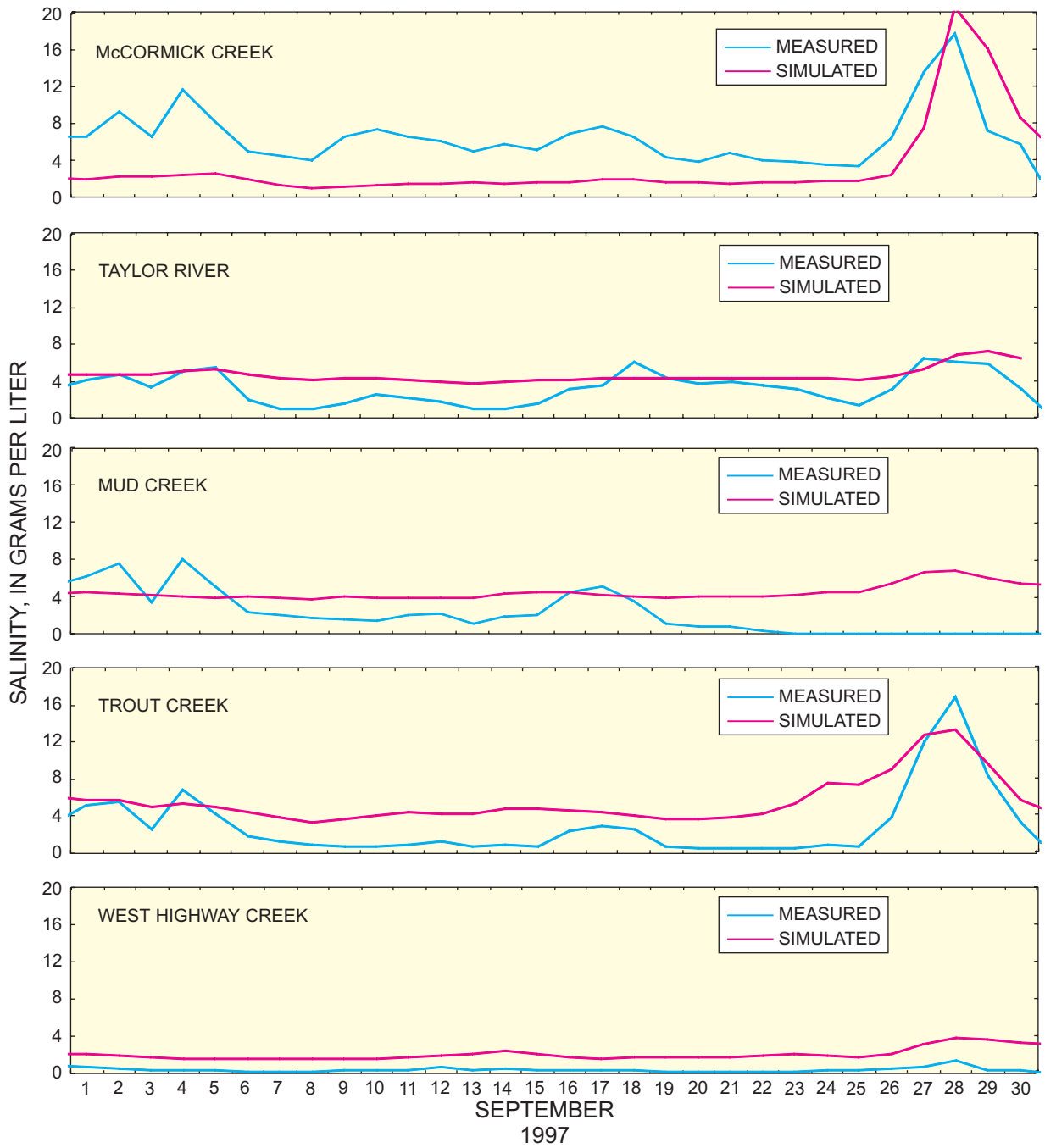

Figure 15. Measured and computed salinities at coastal creeks for calibration simulation in September 1997.

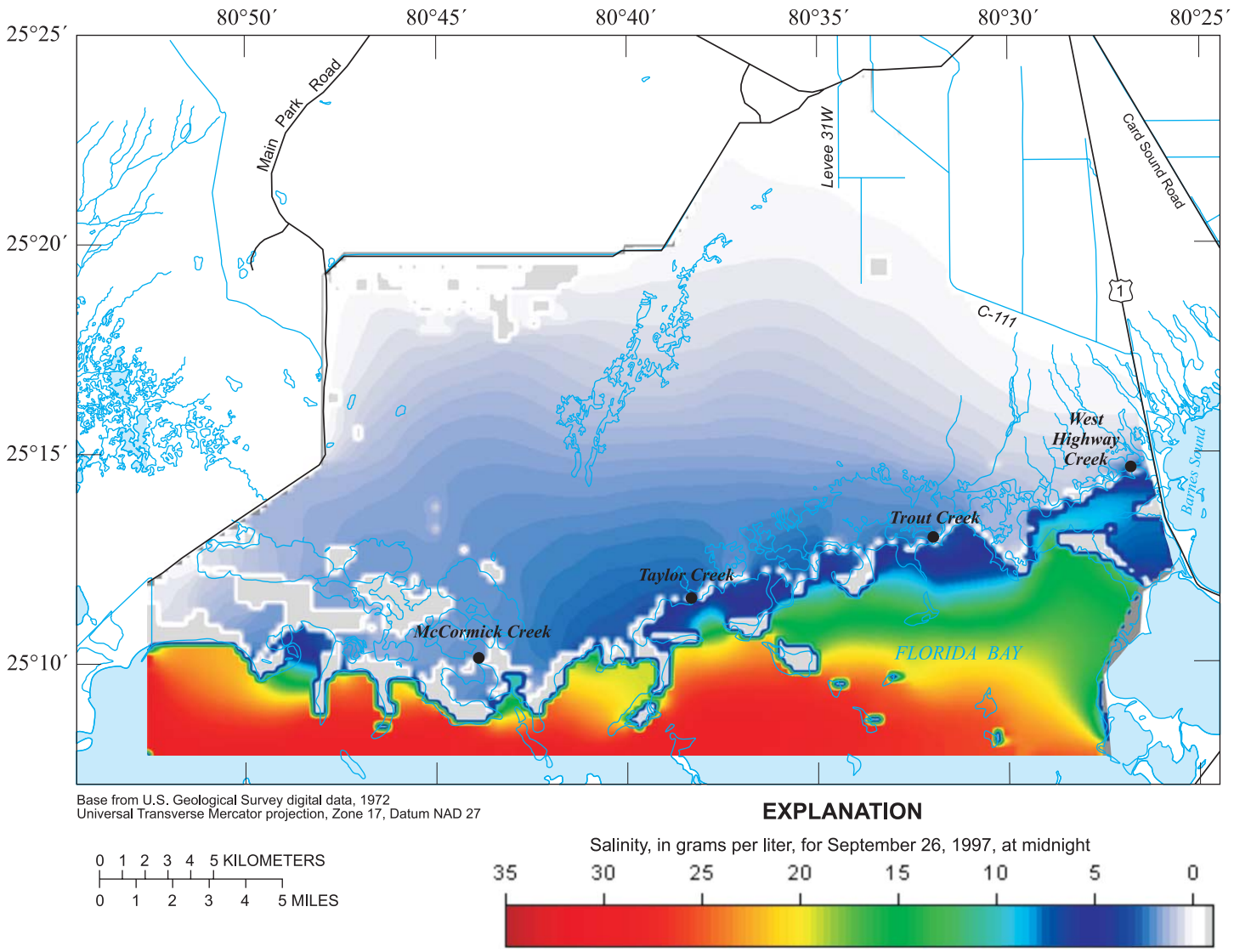

Figure 16. Salinity distributions from the calibration simulation.

salinities shown in figure 15 are in reasonable agreement. The average errors in salinity for this 1-month period for these five creeks in figure 15 are: -3.32 ppt for McCormick Creek, 1.40 ppt for Taylor River, 2.25 ppt for Mud Creek, 2.56 ppt for Trout Creek, and 1.62 ppt for West Highway Creek.

Measured and computed flows at the coastal creeks are shown in figure 17. Positive flow is toward Florida Bay. The measured creek flows were well reproduced by the model as shown in figure 17. The largest observed flows, both positive and negative, occurred at Trout Creek (fig. 17). The statistical agreement between measured and computed flows is discussed later in this report.

Although the general direction and magnitudes are similar, substantial differences exist between measured and computed wetland flow velocities as shown in figure 18. It should be noted that the measured values are point values measured over a 2- to 5-minute period, whereas the computed values are presented as daily averages for the cell area. Short-timescale variations in flow direction are created by wind fluctuations, causing instantaneous measurements to differ from daily averages. The high, multidirectional flows near Old Ingraham Highway (fig. 18, September 22, 1997) are a boundary effect, but are indicative of higher velocities in shallower depths. Further examination of computed and measured wetland flow velocities is made in the next section. Additional data collection is underway using continuous measuring field sites.

The USGS crews measured flows along Main Park Road, which enters the study area along Old Ingraham Highway (fig. 1), during September 22-26, 1997, and obtained an average of 4.53 m^3/s (excluding Taylor Slough bridge). The total volume rate produced by the SICS model was 5.29 m^3/s inflow along the entire Old Ingraham Highway model boundary on September 24, 1997 (Tillis, 2001), which represents a good match of flow magnitude and direction.

Testing

This section describes results of model testing. First, model verification is described in which the calibrated model is applied with a different set of boundary input than used for calibration, and with no adjustment of model input parameters. The extent of agreement between computed and measured results serves as an indicator of model accuracy and the degree of confidence to place in subsequent simulations. Results of sensitivity testing also are described in which several input variables are systematically varied one at a time. The differences between computed output (water level, flow, velocity, and salinity) before and after input variation are a measure of model sensitivity to the parameter being changed. It is desirable that output be minimally sensitive to parameter variations. In cases where this is not so, additional effort is needed to increase accuracy of input as much as possible.

The verification simulation run encompasses the period from August 1996 to July 1997. This time period also was used by the U.S. Army Corps of Engineers in the development of boundary conditions for inland and Florida Bay models. Including a 16-day warm-up period, the model run starts on July 15, 1996, and finishes July 31, 1997.

Verification

The model parameters developed for the calibration simulation were used in the verification simulation to represent the flow regime in the wetlands and along the coast. Results of the 1-year verification simulation are shown at monthly intervals on plate 1. The higher land-surface elevations are most apparent as dry areas at intermediate water levels, such as on August 1, 1996. At high water levels, such as on September 1, 1996, the Joe Bay area receives water from Taylor Slough, the L-31W Canal, and the C-111 Canal. However, at low-water levels, such as on February 1, 1997, simulations indicate that Joe Bay appears to receive little water from inland areas. Simulated flow velocities to the West Lake area are very low (pl. 1), even when the area north of West Lake is fully inundated. The West Lake area seems to be relatively disconnected hydraulically and insensitive to flows from the Taylor Slough basin. Results shown on plate 1 compared well with water-level maps generated by spatially interpolating levels from field measurement stations (Ball and Schaffranek, 2000b).

The close agreement between measured and computed flow volumes in the coastal creeks is an important indicator of SICS model capability to simulate real flow dynamics in the area. Measured and computed flows at the five monitored creeks are shown in figure 19. The best agreement between measured and computed values for most of the creeks occurs between October and May—the dry season in southern Florida. This would tend to indicate that the controlling phenomena in the dry season are represented in the model better than those in the wet season. The phenomena particular to the wet

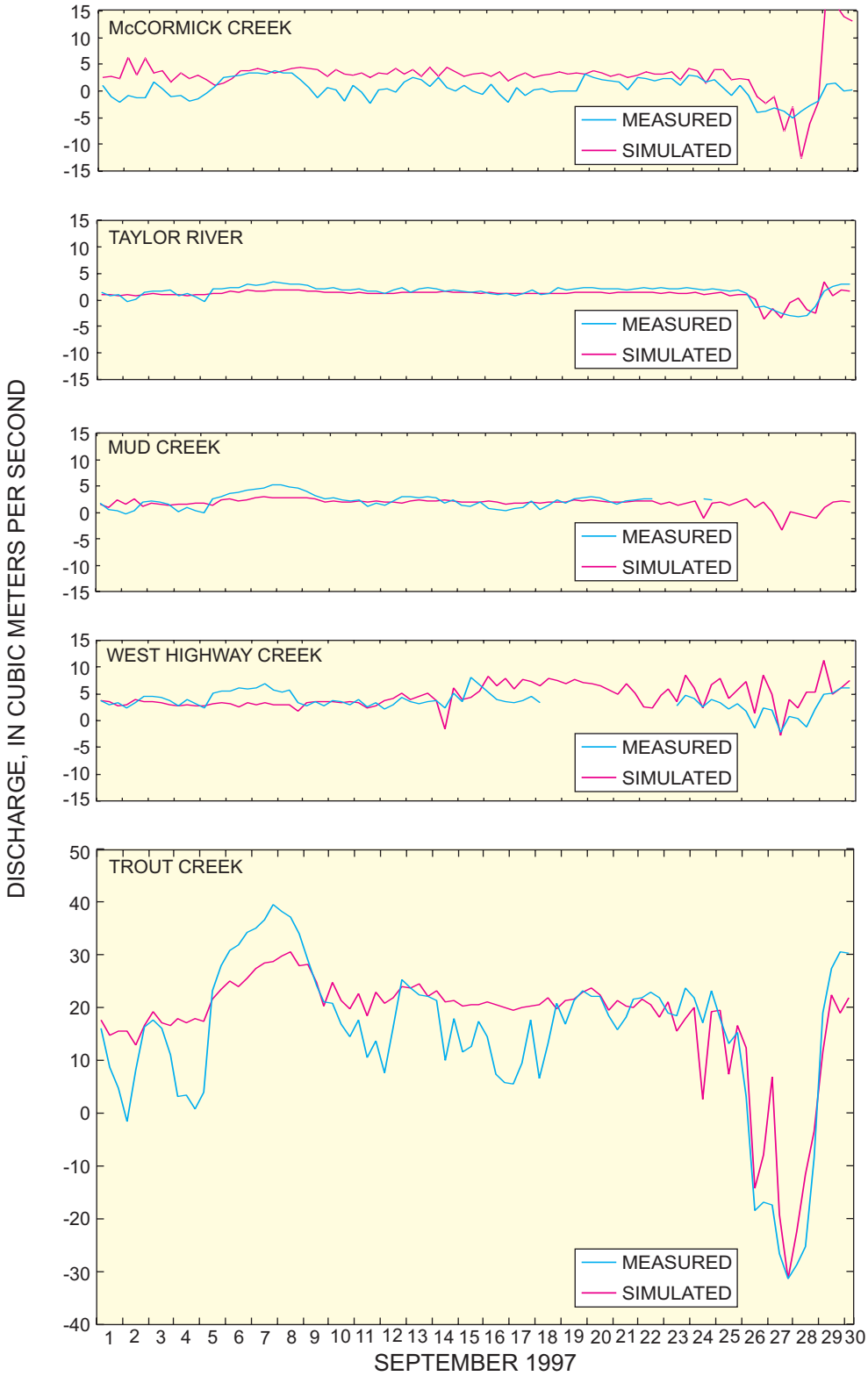

Figure 17. Measured and computed flows at coastal creeks for calibration simulation in September 1997.

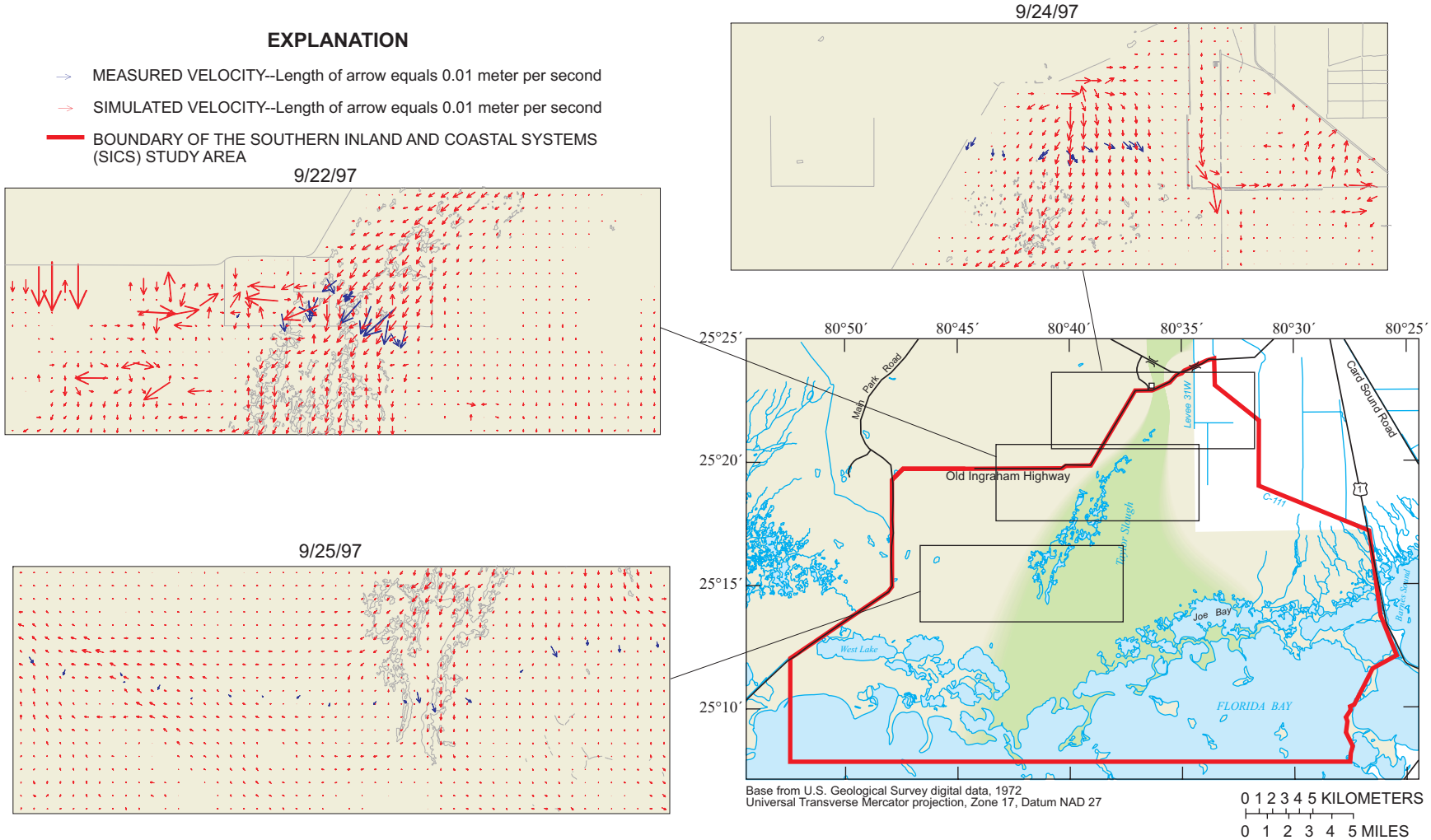

Figure 18. Wetland flow velocities for calibration simulation, September 22, 24, and 25, 1997.

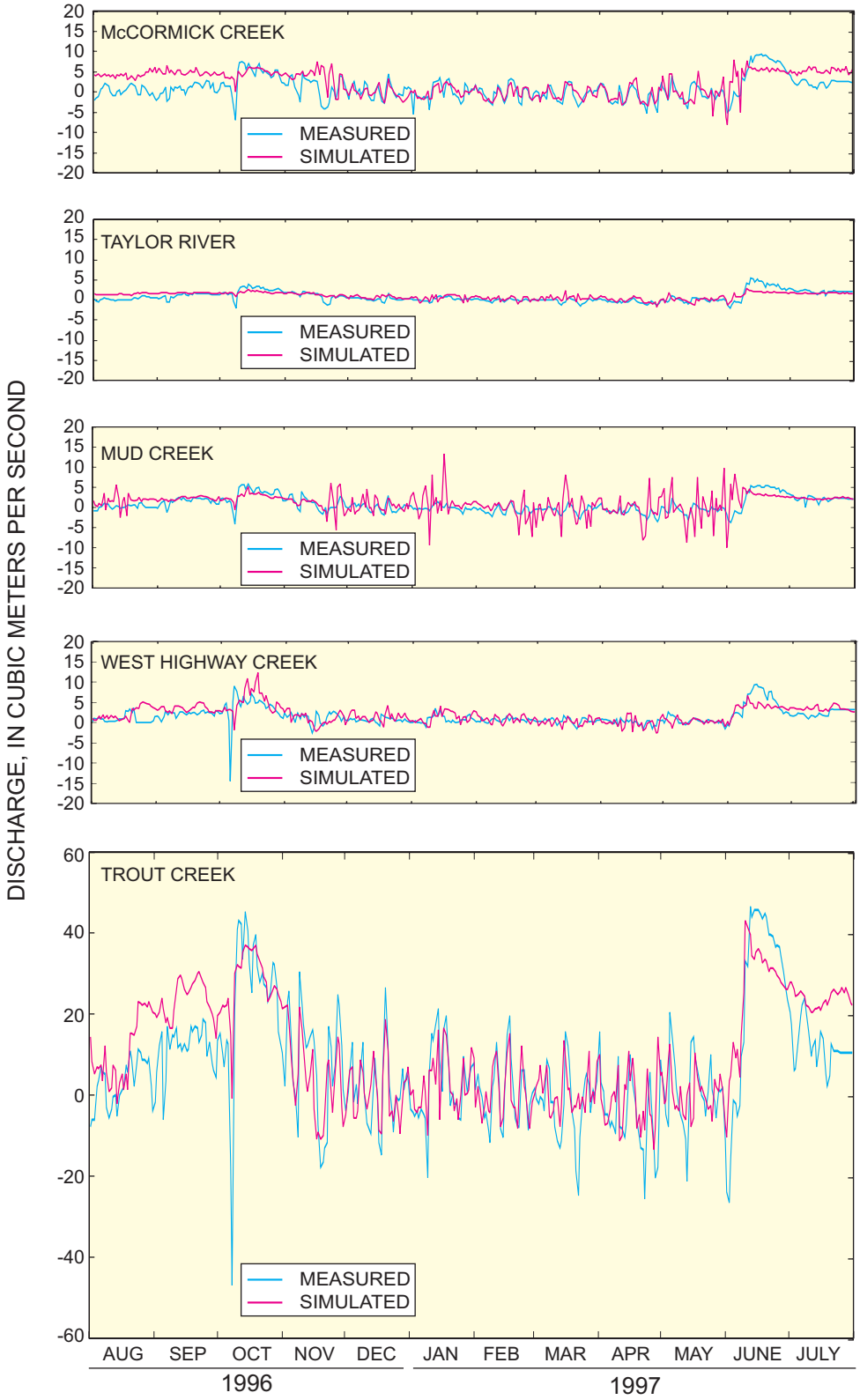

Figure 19. Measured and computed creek flows for verification simulation, August 1996 to July 1997.

season are: more inflow from surface-water sources, higher rainfall rates, and higher water levels with a corresponding difference in frictional resistance.

The ratio of the root mean square difference (RMSD) between measurements and simulations to the standard deviation σ of the measurements is used to describe the ability of the model to reproduce the field measurements. The RSMD is the square root of the mean of the differences between measured and simulated values for a selected period. The standard deviation of the measured data is a representation of the variability in the data, with greater variability indicating more difficulty in producing accurate simulations. Thus, the ratio RMSD/σ should be a good dimensionless measure of the ability to fit versus the difficulty in fitting; the lower the value, the better the model performance.

The best model performance for creek flow simulation was at Trout Creek, where RMSD/σ = 0.673. This is fortunate because, as the highest flow outlet to Florida Bay, Trout Creek is the most important of the creek flows to represent well. The worst value for RMSD/σ is 1.329 at Mud Creek. Flows from this creek may be more difficult to represent because it is connected to a small-scale set of lakes that may not be adequately delineated by the model grid. Other values of RMSD/σ were 0.711 at Taylor River, 0.981 at West Highway Creek, and 1.072 at McCormick Creek.

The highest water-level gradients occur along the coast (pl. 1). For example, on December 1, 1996, the model produced a 0.14-m water-level drop across the embankment at Taylor River (fig. 2). No gradient measurements were available along the coast for this simulation period; however, on February 28, 1998, water-surface elevation measurements were taken at the USGS station at the mouth of Taylor River and at an ENP station about 3.22 km upstream of the station at the mouth. Measurements taken over a 45-minute period revealed an average water-level drop of 0.18 m between stations. This measured difference indicates that the relatively high water-surface gradients simulated by the model can (and probably do) occur along the coast.

A comparison was made between the verification simulation results and the measured water levels in the wetlands, and results are shown on plate 2. The simulated values do not include ground-water levels below a dry cell, so the computed line terminates when the cell becomes dry and the stage is 0.0, but the measured data continue below land surface under these conditions. Occasionally, cells in the model become wet briefly when measured data show levels are below land surface (see P67 on pl. 2). This is a transient phenomenon, however, and the volume associated with those wet cells is small. The agreement between measured and computed is within 0.03 m for most of the simulation time at most of the stations. Under almost all conditions, including wetting and drying, the difference between simulations and measurements is less than 0.1 m.

Velocity measurements were made in the wetlands during July 29-31, 1997, which was near the end of the verification period. The comparison of simulated velocities with field measurements is shown on plate 3. The velocity vectors compare velocities measured at the noted times with those computed during the period between 3 hours before and 3 hours after the measurement time. This accounts for the fact that the majority of the small-scale variation in velocities is due to wind forcing, and a 5-hour averaging period is used for the wind values. Moreover, the simulated vectors shown on plate 3 are a spatial average of 10 computational cells—the measurement cell and the nine cells that bound that cell. Field values do, however, have the same general magnitude and direction as simulated values.

Monthly simulated salinity distributions are shown on plate 4. During dry periods, such as from December 1, 1996, to April 1, 1997, salinity intrusion occurs in Joe Bay and in the subembayments (for example, Monroe Lake shown in fig. 2) north of McCormick Creek. In Joe Bay, salinities usually are greater than 4 g/L and can be as high as 7 g/L (pl. 4). The high salinity gradient seen at the coastline is indicative of the effect of the Buttonwood Embankment as a barrier to salinity intrusion inland. The only salinity intrusion occurs when reversals in creek flows occur; the reversals are caused by wind as discussed later.

Sensitivity Analysis

The purpose of the sensitivity analysis is to identify the response of the SICS model to variations in input parameter values and boundary conditions. This helps identify the input error that may contribute to most of the output uncertainty. The sensitivity analysis is performed using the verification simulation period, which includes an extensive output data set (1 year) with a wide variety of flow conditions. The sensitivity analysis was conducted by increasing and decreasing the input values an arbitrary amount and observing the effects on simulated coastal creek flows. These creek

flows are integrators of all upstream effects in the model, are sensitive to variations in bay water levels, and are the quantity of most interest to Florida Bay scientists, which makes them ideal for this purpose.

The flow coefficients for the coastal creeks are of interest in the sensitivity analysis because of the lack of field data for this parameter. The dispersion coefficient was not tested because it has no direct effect on flow rate. Other important parameters investigated are the wind-friction term, evapotranspiration rate as a function of solar radiation, Manning's *n* values, boundary-value water levels, boundary-value discharges, and land-surface elevations. The sensitivity to a sinusoidal tide at the western model boundary and the effect of salinity on flows were also tested.

Subjective criteria were used to determine a reasonable range of parameter values for sensitivity testing. The effective Manning's *n* values for the coastal creeks (table 3) varied about ±50 percent among creeks, so this range was used for Manning's *n* testing.

A wind-friction coefficient of 1.2×10^{-3} is used in the model. Due to the high uncertainty in determining this value and the wind-sheltering coefficient, a ±100 percent variation in the wind-friction coefficient was used.

The best fit evapotranspiration relation (eq. 7) has a correlation coefficient of about 80 percent, indicating that 80 percent of the observed variability in evapotranspiration can be explained by the independent variables in equation 7. Thus, the sensitivity of the model to evapotranspiration variations was assessed by varying the only input variable, solar radiation χ, by ±10 percent.

As previously discussed, ranges of Manning's *n* values for vegetative frictional resistance were determined from field measurements. The range of average values for different vegetation types was given as 0.08 $s/m^{1/3}$. Based on this, the sensitivity analysis uses a range of 0.10 $s/m^{1/3}$ (±0.05 $s/m^{1/3}$).

Boundary water levels along Florida Bay and for the culverts under US-1 are determined from coastal stations, which should be accurate to 0.015 m. To ensure an adequate range, a variation of ±0.03 m is used for the sensitivity analysis. Of major concern for Everglades restoration is the effect of varying flow at Taylor Slough bridge on wetland flows and flows to the coast. The flows at Taylor Slough bridge were varied ±50 percent for the sensitivity analysis.

Errors in land-surface-elevation measurements can be quantified. Applying a constant elevation difference to all of the cells in the model is a straightforward process. However, an 0.03-m rise in all the cells is equivalent, in a relative sense, to lowering the water-level boundaries by 0.03 m. To avoid essentially repeating the sensitivity analysis for water-level boundaries, an analysis is needed that is more representative of the type of error found in measuring land-surface elevations. Sensitivity analysis of land elevations is somewhat different than for other parameters because flow can be substantially affected by differences in elevations between cells. Random variance is added to the land-surface elevation data by use of the turning bands algorithm (TBA) as described by Tompson and others (1989). The random application of perturbations is not as applicable with other parameters, including the evapotranspiration rate and Manning's *n*, because flow is substantially affected by net changes in the parameter model wide.

Thirty-two trials were used in the sensitivity analysis of land-surface elevation. The TBA was used to generate 30 two-dimensional random fields, all with a mean of zero and a standard deviation of 0.15 m, which was the stated uncertainty in the helicopter-based elevation measurements (Desmond and others, 2000). The correlation scale was set to 0.1 of the cell size, so that the perturbations were uncorrelated between cells. For each of the 30 realizations, the random field was then added to the elevation data set, the model was run, and the statistics were computed. The arithmetic average of the statistics from all the simulations indicates the sensitivity of the model to land-surface elevation perturbations.

Three statistical measures were used to describe the difference in coastal creek discharge between verification and sensitivity runs. These statistics are the RMSD, mean absolute difference (MAD), and mean difference (MD). The RMSD is the square root of the mean of the squares of all the differences between verification and sensitivity discharge values. The MAD is the mean of all the absolute values of the differences, whereas MD is the mean of the differences, which allows positive and negative values to offset. Each of these statistics states the difference between the flows produced by the verification and sensitivity run in a different way. The RMSD shows the average difference, with no offsetting of positive and negative differences, and the effects of outliers are exaggerated. The MAD also shows the average differences in instantaneous

discharge with no offsetting differences, but all data points affect the mean equally. The MD is similar to the MAD, but it does allow positive and negative values to offset. If creek flows from verification and sensitivity model runs are shifted in time, the MAD and RMSD cause large differences whereas the MD does not. Any input parameter variation that has a major effect on output will be detected by one of these three statistical measures.

Results of model sensitivity to changes in selected parameters are presented in table 4. Most table segments give three statistical measures of the difference between computed flows in five coastal creeks for this verification simulation, with and without the labeled sensitivity modifications. The first segment in table 4 gives the same statistical measures of flow differences between the verification run and measured creek flows.

Table 4. Results of sensitivity analysis

Each chart segment gives three statistical measures of the difference in flows at each of five creeks discharging to Florida Bay. Each chart segment compares creek flow model results for the verification simulation with either field data, the first segment, or subsequent computed creek flows from simulations having indicated modifications to input data. Acronyms: RMSD, root mean square difference; MAD, mean absolue difference; MD, mean difference. Values are shown in cubic meters per second]

Statistic	McCormick Creek	Taylor Creek	Mud Creek	Trout Creek	West Highway Creek
Compared to Field Data					
RMSD	2.887	0.945	2.593	9.824	2.092
MAD	2.190	.725	1.758	7.656	1.420
MD	1.195	.210	.412	3.231	.377
Creek Conductances Plus 50 Percent					
RMSD	2.119	.875	2.477	5.423	1.312
MAD	1.616	.633	1.604	3.573	1.012
MD	.824	.353	.138	1.104	.639
Creek Conductance Minus 50 Percent					
RMSD	2.092	.716	2.749	10.374	1.646
MAD	1.769	.611	1.788	4.608	1.199
MD	- .861	- .398	- .221	-3.069	- .605
Wind Friction Term Plus 100 Percent					
RMSD	1.759	.670	2.895	2.519	1.320
MAD	1.168	.389	1.770	1.895	.977
MD	.097	.020	- .304	- .122	- .473
Wind Friction Term Minus 100 Percent					
RMSD	1.485	.425	2.149	3.869	2.583
MAD	.944	.258	1.271	2.675	1.421
MD	.005	.055	.053	.419	.601
Solar Radiation Plus 10 Percent					
RMSD	1.289	.786	2.995	1.253	.824
MAD	.768	.310	1.555	.717	.583
MD	- .024	- .046	- .144	- .415	.058
Solar Radiation Minus 10 Percent					
RMSD	1.277	.438	3.558	1.490	.792
MAD	.790	.251	1.719	.875	.529
MD	.067	.086	.165	- .019	.018

Table 4. Results of sensitivity analysis (Continued)

Each chart segment gives three statistical measures of the difference in flows at each of five creeks discharging to Florida Bay. Each chart segment compares creek flow model results for the verification simulation with either field data, the first segment, or subsequent computed creek flows from simulations having indicated modifications to input data. Acronyms: RMSD, root mean square difference; MAD, mean absolue difference; MD, mean difference. Values are shown in cubic meters per second]

Statistic	McCormick Creek	Taylor Creek	Mud Creek	Trout Creek	West Highway Creek
Manning's *n* Plus 0.05					
RMSD	1.286	.409	2.624	10.357	.895
MAD	.799	.243	1.469	4.204	.594
MD	.161	.042	.057	-3.779	.203
Manning's *n* Minus 0.05					
RMSD	1.130	0.389	2.735	6.007	0.692
MAD	.704	.225	1.467	1.540	.502
MD	.069	.037	.153	- .410	- .074
Florida Bay Boundary Water Levels Plus 0.1					
RMSD	2.441	.616	4.622	5.009	.798
MAD	1.631	.381	2.447	2.570	.572
MD	- .231	- .175	.216	- .117	.003
Florida Bay Boundary Water Levels Minus 0.1					
RMSD	1.755	.791	2.398	1.569	.828
MAD	1.319	.375	1.375	1.053	.567
MD	- .317	.066	.184	- .410	.021
Sinusoidal Tide Function at Western Boundary with Amplitude 0.30 meter					
RMSD	1.507	.397	3.532	10.460	.691
MAD	1.009	.230	1.629	4.569	.496
MD	- .017	.059	.263	-4.082	- .031
Taylor Slough Bridge Discharges Plus 50 Percent					
RMSD	1.256	0.364	4.337	1.063	.743
MAD	.750	.211	1.987	.755	.519
MD	.030	.021	.022	.314	.105
Taylor Slough Bridge Discharges Minus 50 Percent					
RMSD	1.339	.402	2.405	.925	.824
MAD	.853	.215	1.377	.618	.551
MD	.040	.002	- .084	- .233	- .041
Density Effects of Salinity Neglected					
RMSD	1.224	1.211	2.400	1.090	2.743
MAD	.793	.336	1.353	.659	1.568
MD	- .054	.113	- .092	- .132	.247
Land-Surface Elevation Standard Deviation 0.15 meter					
RMSD	1.130	.389	2.735	6.007	.692
MAD	.704	.225	1.467	1.540	.502
MD	.069	.037	.153	- .410	- .074

The RMSD, MAD, and MD parameters are summed for all five creeks, and the sensitivity modifications are ranked by impact on the statistical measures as presented in table 5. Summarizing these results qualitatively, simulation results are most sensitive to the flow coefficients for the coastal creeks, followed by the frictional resistance of the wetlands (Manning's *n*), and the wind friction. The magnitude of the perturbations in the input parameters was based on the uncertainty of the parameters. Therefore, the high sensitivity of the coastal creek flow coefficient is due, in part, to the large variation in input perturbation, which represents the high uncertainly in field data.

Table 5. Summary of sensitivity tests for coastal creeks

[RMSD, root mean square difference; MAD, mean absolute difference; MD, mean difference; %, percent; values are shown in cubic meters per second]

Statistic	Parameter name	Parameter modification	Sum of statistics for all coastal creeks
RMSD	Creek flow coefficient	Decreased by 50%	17.58
	Manning's *n*	Increased by 0.05	15.57
	Creek flow coefficient	Increased by 50%	12.21
	Manning's *n*	Decreased by 0.05	10.95
	Wind-friction term	Set to 0.0	10.51
MAD	Creek flow coefficient	Decreased by 50%	9.98
	Creek flow coefficient	Increased by 50%	8.44
	Manning's *n*	Increased by 0.05	7.31
	Wind-friction term	Set to 0.0	6.57
	Wind-friction term	Set to 0.0024	6.20
MD	Creek flow coefficient	Decreased by 50%	5.15
	Manning's *n*	Increased by 0.05	4.24
	Creek flow coefficient	Increased by 50%	3.06
	Wind-friction term	Set to 0.0	1.13
	Wind-friction term	Set to 0.0024	1.02

Model Application Examples

In this section, some examples are given to demonstrate how the SICS model can be applied to better understand water and salinity dynamics in the marsh and coastal and near-shore areas adjacent to northeastern Florida Bay (fig. 1, study area). The first example shows how details of flows and flow differences can be estimated in regions of special interest and where flows are not measured. The next example shows various patterns of computed water levels, water distribution, and salinity throughout the SICS area under different wind and water inflow conditions.

The final part of this section describes a tool to allow application of the SICS model in concert with future evaluations of proposed CERP alternatives. With this tool, results of possible CERP flows provided north of the SICS area can be converted to a realistic estimate of flow input to the SICS model, allowing simulation of marsh and coastal changes due to the specific CERP alternative being evaluated.

Flow Estimates at Unmeasured Locations

Flows to the coast of the SICS area are of great interest to resource managers and planners as Everglades restoration options are evaluated. The application of the SICS model allows both the estimation of flows at locations where field measurements are not made, as well as at measured sites for hypothetical scenarios. As with the coastal creeks, quantification of flow into Joe Bay and other embayments is needed to develop a better understanding of flow-related processes in the SICS area and to provide boundary conditions for future models of Florida Bay.

Joe Bay (fig. 2) is a prominent feature of the shoreline encompassed by the SICS model. It is situated immediately north of the Buttonwood Embankment and in a position to receive water inflow from the surrounding marsh before discharging primarily through Trout Creek (fig. 20. Flow measurements (figs. 17 and 19) indicate that Trout Creek discharge from Joe Bay is a predominant source of freshwater to northeastern Florida Bay.

The SICS model was used to identify the sources and relative magnitudes of these sources of water to Joe Bay under high- and low-water conditions. Estimates of flows to Joe Bay across the six cross-sectional segments partially encircling the bay were

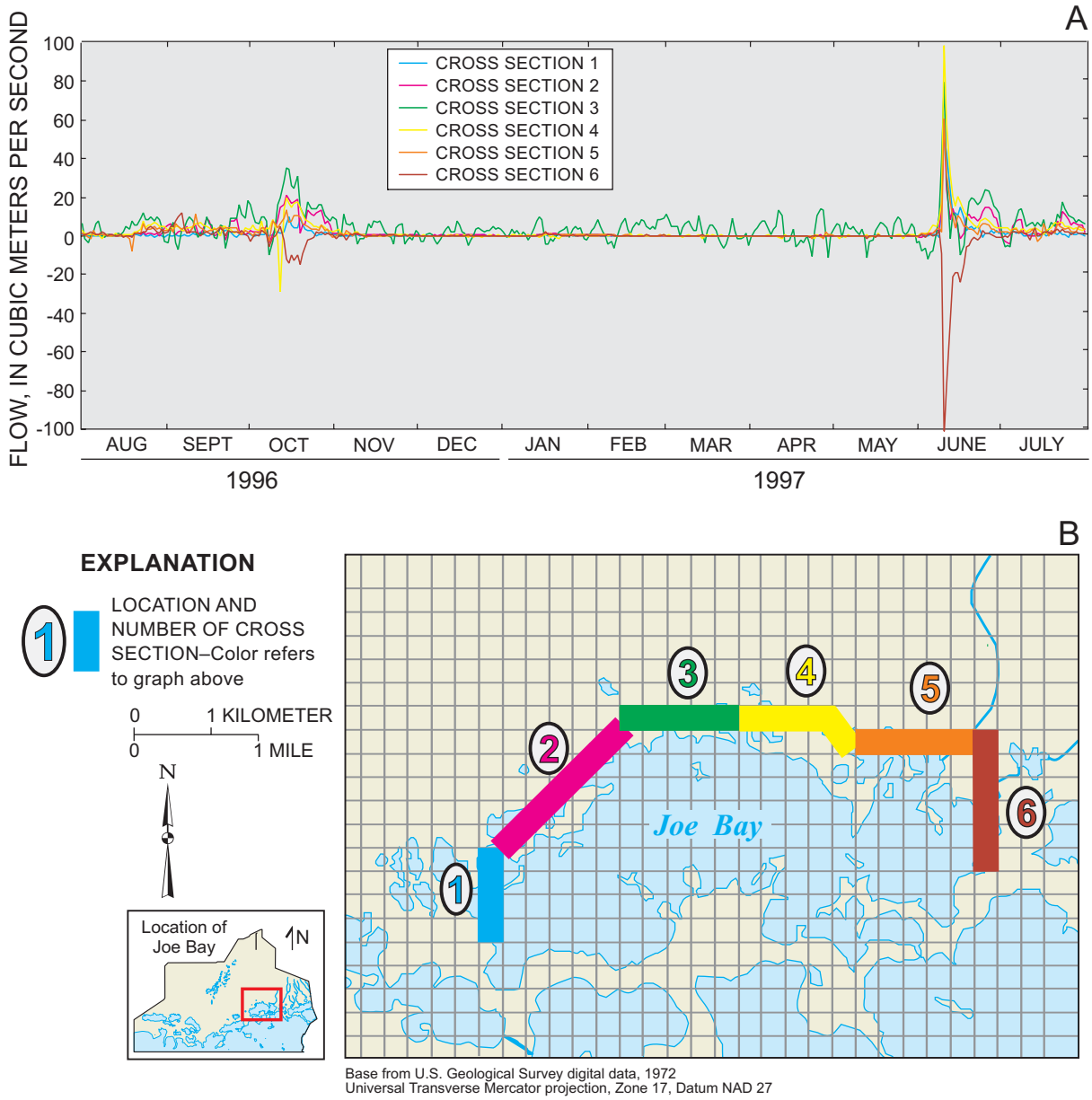

Figure 20. (A) Model-computed flows at each section for verification simulation and (B) map showing flow cross sections for Joe Bay.

computed for the period August 1996 to July 1997, and the results are also shown in figure 20. All flows into Joe Bay are defined as positive. Flow through segments 1 to 5 was predominately occurring into Joe Bay during the simulation period, but flow across segment 6 was in both directions, with greater flows out of the bay during high water-level conditions.

Continuous field measurements of flow were not made at Alligator Creek, East Creek, Stillwater Creek, Oregon Creek, and Shell Creek (fig. 2) as part of this study. Thus, model-computed flows at these creeks (fig. 21) become a useful estimate of their contributions to Florida Bay. The magnitude of the computed flows at these creeks is similar to that of the other creeks where continuous flow measurements were made as discussed earlier in this report (fig. 19), and the error of these estimates should be similar to those given in the first segment of table 4.

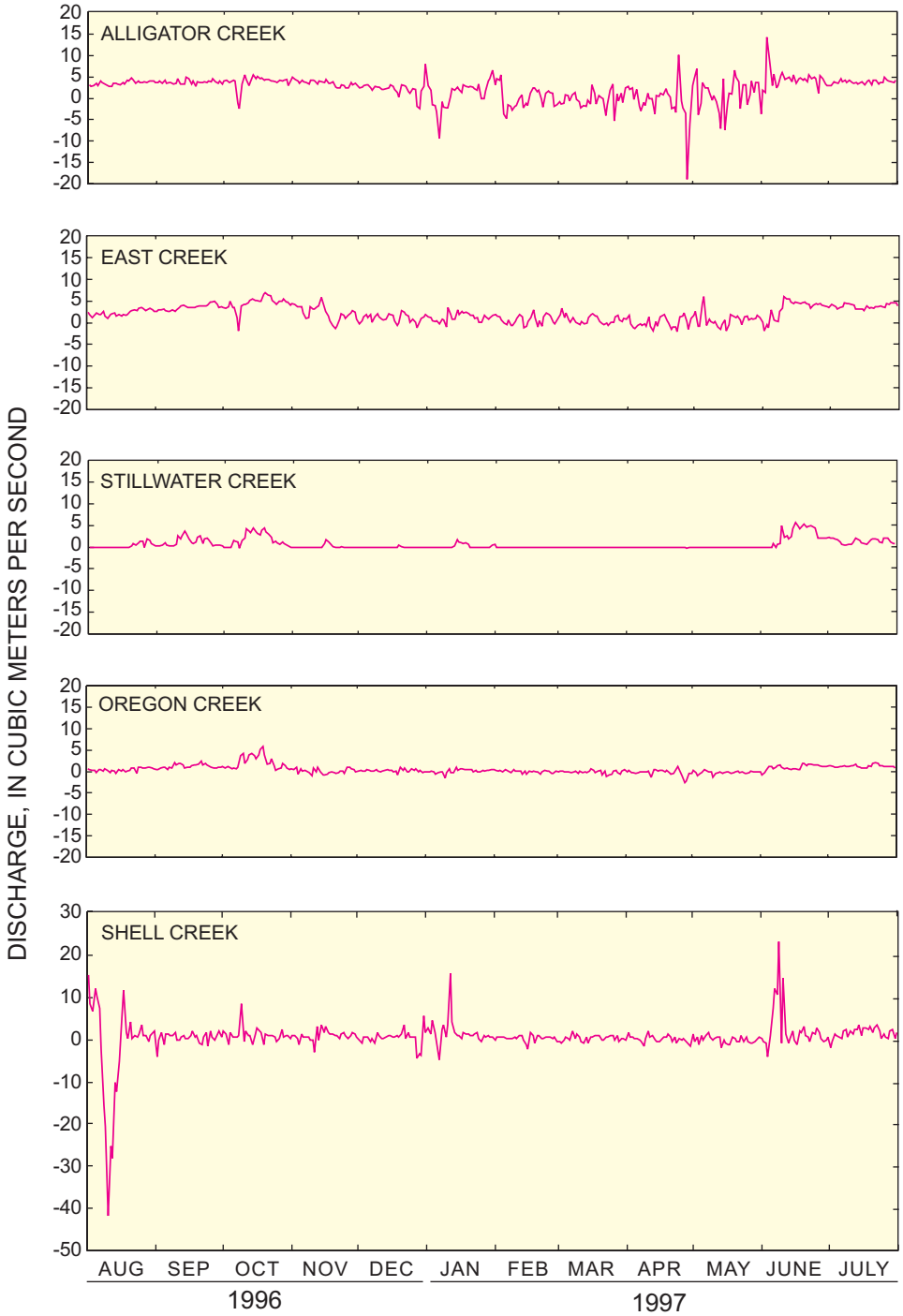

Figure 21. Model-computed flows at selected coastal creeks for verification simulation, August 1996 to July 1997.

Water Ponding and Salinity Distribution for Different Inflow and Wind Conditions

The ability of the SICS model to compute ponding of water during low-flow conditions in the marsh and overall water and salinity distribution under a range of conditions is of great value in determining which CERP alternatives best meet restoration objectives. The illustrations on plate 5 show the relative importance of two input variables, wind and Taylor Slough flow, on computed water levels and ponding for typical high- and low-water conditions. The top two frames show the water levels computed in the SICS area for a high-water condition on September 1, 1996, and a low-water condition 3 months later. These are snapshot excerpts from a simulation run from August 1, 1996, to July 31, 1997, and the simulations include measured wind and Taylor Slough bridge flows as input. Marsh water levels range from about +0.5 m to about -0.2 m below NAVD 88 for September 1, 1996, and from about 0.3 m above to about -0.2 m below NAVD 88 for December 1, 1996.

To illustrate the effect of wind on computed water levels, a second model simulation was conducted for the same time period with the wind input set to zero and all other input unchanged. Snapshots of water levels on the same 2 days (September 1 and December 1, 1996) were then compared to the originals, and their differences are shown in the middle tier of frames on plate 5.

The high water-level difference map (September 1, 1996) shows large areas of very little change, particularly in the western part of the SICS area. There is some minor increase in water levels greater then 0.02 m in the northern and northeastern parts of the area and some localized increases concentrated near the shoreline in the eastern part of the SICS area. Lack of wind in this case seems to have had minimal effects on water levels and water distribution. For the low water-level condition (December 1, 1996), there were some areas of increased ponding in the absence of wind relative to the original simulation.

Wind forcing on wetland flow directions can be observed in the study area (pl. 1); however, the most dramatic effects are on flows to the coast. The measured discharges at Trout Creek, the largest coastal outflow (Hittle, 2000), and also model-computed discharges with and without wind effects are shown in figure 22. Flow reversals in the creeks are only evident in the model simulations when wind is included. Because Florida Bay boundary water levels are the same for each simulation with and without wind, flow reversals are not due to tidal variations in Florida Bay, but by seiching in the subembayments or wetlands caused by wind forcing.

Of greater relevance to Everglades restoration is the effect that changing flows at Taylor Slough bridge (a primary water input to the SICS area) may have on Everglades conditions. The bottom tier of frames on plate 5 shows how increasing Taylor Slough bridge flows by 50 percent affects water levels during high- and low-water conditions.

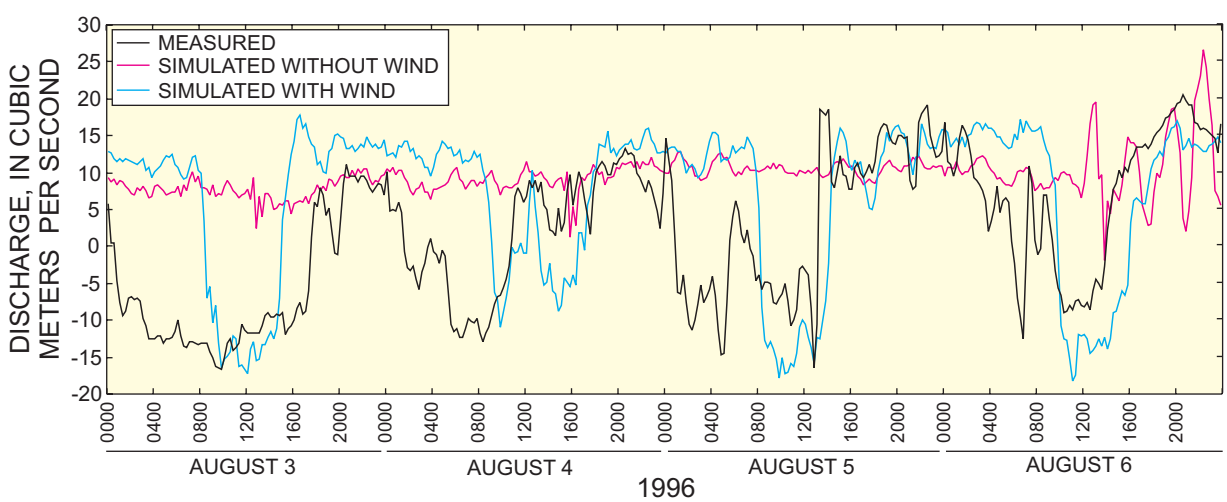

Figure 22. Differences in computed flow at Trout Creek with and without wind effects for verification simulation.

The changes for both high- and low-water conditions are striking, but in different ways. For high-water conditions, water levels in a large area near the Taylor Slough bridge are raised by 0.02 to 0.03 m due to increased water flow. This increase appears to radiate outward from the source and causes substantial increases in the Joe Bay area and in the downstream area of Taylor Slough relative to baseline conditions. For low-water conditions, water-level increases are not greatest near the point of increased flow. Rather, a large area of increased ponding (+0.02 to +0.04 m) is created in the central region of Taylor Slough. This is most likely the remnant of increased flow in the wetter times.

In general, wind seems to reduce ponding during low-water periods and has small effects during high water. Increases in Taylor Slough bridge flow appears to generally increase water levels throughout the SICS area and particularly near the bridge for high water levels.

Similar to illustrations on plate 5, the top two frames on plate 6 show salinity distributions computed in the SICS area for a high-water condition on September 1, 1996, and a low-water condition on December 1, 1996. As previously mentioned, these are snapshots from a 1-year simulation (August 1, 1996, to July 31, 1997) and include measured wind and Taylor Slough bridge flows as input. Color gradations for all frames on plate 6 show marsh salinities varying from near zero inland to about 5 g/L at the coast and varying from about 10 to more than 30 g/L in Florida Bay. Dispersion coefficients, which are estimated in the model, have a greater effect on salinity distributions in regions of high salinity gradients than regions of lower salinity gradients.

The distribution of marsh and Florida Bay salinity varies substantially between high- and low-water conditions, but the effects of wind (middle two frames) and increased Taylor Slough bridge flows (bottom two frames) are less noticeable than the effects of water-level condition on salinity. The absence of wind results in some increased salinity intrusion into the marsh compared to the baseline condition. The situation is mixed for low-water conditions; there is less intrusion for the no-wind condition in the eastern part of the marsh and some greater salinity intrusion in the central marsh relative to the baseline condition. These different responses are likely due to varying antecedent wind patterns. An increase in inflow of 50 percent at Taylor Slough bridge causes very little change in salinity distribution for both high- and low-water conditions.

Perhaps the most interesting observation regarding salinity distributions is that salinity intrusion into the marsh is significantly greater under high-water conditions than low-water conditions. This is counter-intuitive because, in most other instances of relatively higher freshwater flow in wet seasons, salt is forced downstream resulting in reduced intrusion. The dry time, December 1, 1996, follows a particularly wet October, so the area was still flushed of salinity. The wet time, September 1, 1996, still retains some of the salinity intruded in the previous dry time. This demonstrates the importance of considering antecedent conditions. The low-water condition shown on December 1, 1996, followed the heavy rainfall events in October 1996. Both salinity and water level are fixed at the lower boundary. This artificially constrains the system from the southern boundary some distance north.

Using SICS Model for Restoration Testing

In order to utilize the SICS model to evaluate restoration scenarios, the boundary conditions must be altered to allow inclusion of operational changes outside the SICS model area. The need is to define the flows at Taylor Slough bridge to reflect the strong influence of pumpage at station S-332 (fig. 1). One method of incorporating changes in operations at S-332 with SICS boundary inflows at Taylor Slough bridge is to use a multiple regression analysis to relate the important variables between the two sites.

A multiple regression analysis consists of relating a dependent variable to a set of quantitative independent variables. A first-order regression was used in this study, which includes all independent variables, but does not include any cross-products or exponents, and assumes that the effects of the independent variables are additive and do not interact with each other. The general formula used to represent this regression is as follows (Ott, 1993, p. 566):

$$y_i = \beta_0 + \beta_1 x_1 + \beta_2 x_2 + ... + \beta_i x_i + \varepsilon \qquad (16)$$

where y_i is the dependent variable, β_0 is the y-intercept (the expected value of y when each x is zero), $\beta_0 ... \beta_i$ are partial slopes (expected change in y for a unit increase in x), $x_1 ... x_i$ are independent variables, and ε is the error term.

An array of different statistics can be calculated when running a multiple regression, including the R_p value, standard error, sum of squares, mean square, t-statistic, and p-values (Helsel and Hirsch, 1992, p. 108-124). One of the most significant of these terms to the SICS model analysis is the R_p value. This value is the

Pearson Product Moment correlation coefficient, a dimensionless index that ranges between +1 and -1, and reflects the extent of a linear relation between the different data sets. The formula used to calculate R_p is as follows (Ott, 1993, p. 475):

$$R_p = \frac{n_i \sum XY - \sum X \sum Y}{\sqrt{[n_i \sum X^2 - (\sum X)^2][n_i \sum Y^2 - (\sum Y)^2]}} , \quad (17)$$

where n_i is the number of data points, X is the independent set of observations, and Y is the dependent set of observations.

The northern boundary of the SICS model area is defined by discharges at Taylor Slough bridge. A relation had to be established between flows at the bridge and a nearby S-332 flow-control structure to use the model for operational purposes. This relation was accomplished by performing a multiple regression on flows at Taylor Slough bridge with respect to pumping and rainfall rates at S-332. The regression yielded an R_p value of 0.83, which indicates a good relation (fig. 23) and demonstrates that pumping rates at S-332 and daily rainfall rates can be used to estimate daily flows at the Taylor Slough bridge.

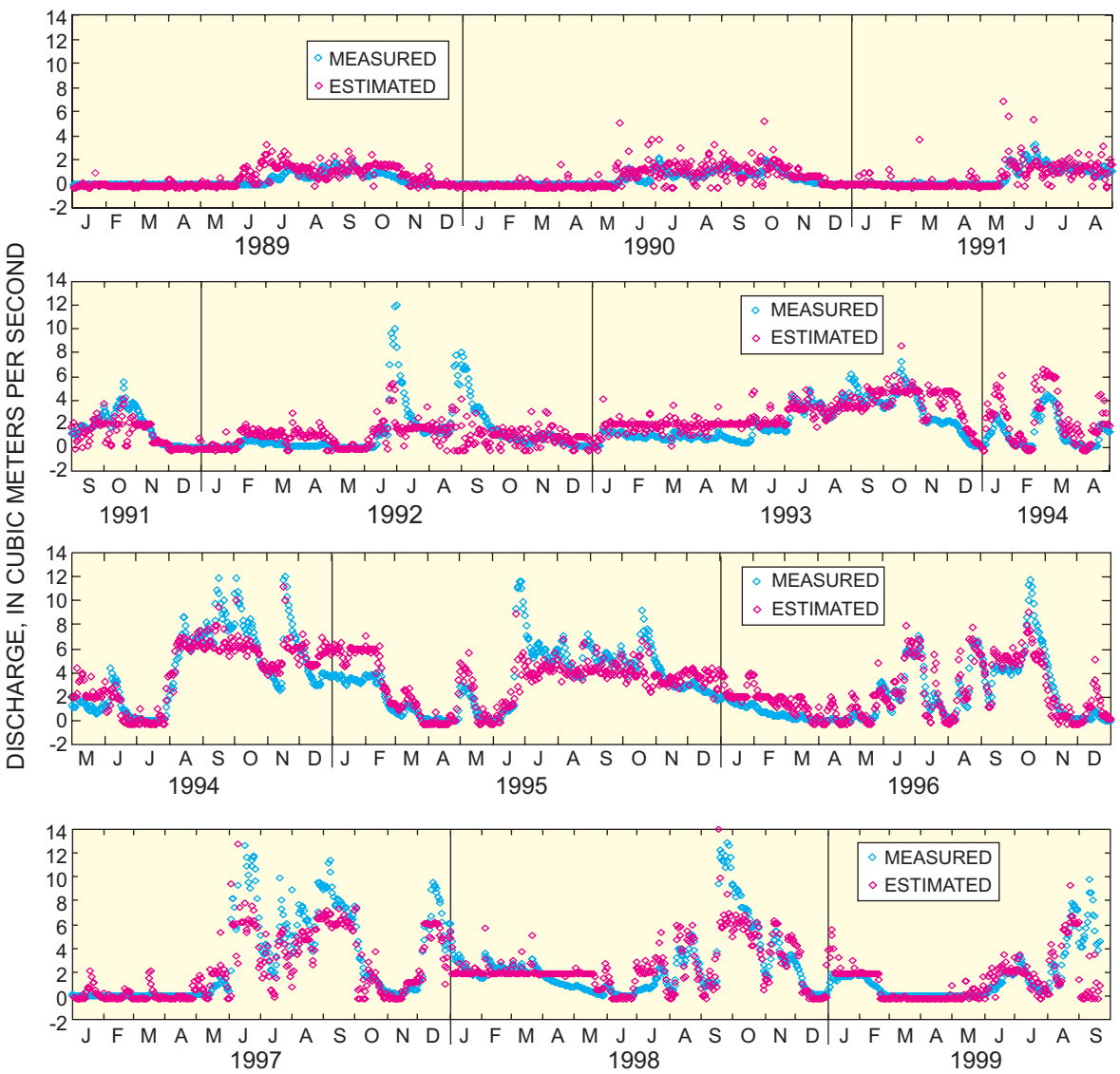

Figure 23. Measured and estimated daily mean flows for Taylor Slough bridge, 1989-99.

CONCLUSIONS

To understand flow conditions along the coastal areas of Florida Bay, a two-dimensional dynamic surface-water model was developed and applied to the region encompassing the wetlands at southern ENP and the subtidal embayments of northern Florida Bay. The model has the capability to simulate drying and flooding, wind forcing, land barriers, and the transport of salinity that affects density. Model modifications were made to allow areal variations in rainfall, cell-by-cell computation of evapotranspiration, and a wind-sheltering coefficient for emergent vegetation. Process studies yielded input values for land-surface elevations and bathymetry, frictional resistance terms, evapotranspiration computation, location of ground-water inflows, and flow data for the coastal creeks and wetlands. Results of studies relating wetland vegetation types to frictional resistance were combined with areal mapping of vegetation to develop Manning's *n* terms for the model. A least-squares best-fit technique was used to relate the pertinent parameters to evapotranspiration rates for this area. This information was used to simulate two periods: a 1-month calibration simulation and a 1-year verification simulation. Measured coastal creek flows and unit discharges measured in the wetlands were used for comparison with simulations and for model calibration.

The calibration simulation demonstrated the ability of the model to reproduce coastal flows, unit discharges in the wetlands, and coastal salinities. The verification simulation produced long-term coastal flow volumes at creeks and elsewhere. The varying distribution of flows at high- and low-water conditions was also represented. Numerical experiments showed that flow reversals at the coastal creeks are primarily due to wind forcing and not due to variations in tidal level. Flows into Joe Bay are primarily from Taylor Slough during low-water periods. The highest water-level simulated gradients occur along the coast where the coastal embankment confines overland flow to the creeks. This finding is supported by limited field measurements.

A sensitivity analysis was performed on the major input parameters of the model. Results of the sensitivity analysis indicate that the parameters need to be better defined. The flow coefficient of the coastal creeks was the most critical parameter needing further study. Other parameters needing study are the frictional effects of wetland vegetation and wind.

The sensitivity analysis included scenarios in which wind was neglected as a forcing function, and the inflows at the northern boundary of Taylor Slough were varied. Wetland water levels and salinity mixing at the coast are significantly affected by wind. Higher and lower inflows through Taylor Slough bridge do not have a significant effect on coastal area water levels, but water-level effects are seen nearer to the bridge.

To utilize the SICS model for evaluating the hydrologic response to proposed restoration scenarios, a multiple-regression analysis was applied to relate the SICS boundary flows from Taylor Slough bridge to pumpage at S-332, a pump station north of the SICS area. This allows boundary flows at Taylor Slough bridge to be estimated from operations at S-332.

REFERENCES CITED

Arakawa, A., 1966, Computational design of long-term numerical integration for the equations of fluid motion: Part I. Two-dimensional incompressible flow: Journal of Computational Physics, v. 1, no. 1, p. 119-143.

Bales, J.D., Fulford, J.M., and Swain, E.D., 1997, Review of selected features of the Natural System Model, and suggestions for application in south Florida: U.S. Geological Survey Water-Resources Investigation Report 97-4039, 42 p.

Bales, J.D., and Robbins, J.C., 1995, Simulation of hydrodynamics and solute transport in the Pamlico River Estuary, North Carolina: U.S. Geological Survey Open-File Report 94-454, 85 p.

Ball, M.H., and Schaffranek, R.W., 2000a, Flow-velocity data collected in the wetlands adjacent to Canal C-111 in south Florida during 1997 and 1999: U.S. Geological Survey Open-File Report 00-56, 56 p.

——— 2000b, Regional simulation of inundation patterns in the south Florida Everglades: U.S. Geological Survey Program on the South Florida Ecosystem: 2000 Proceedings of the Greater Everglades Ecosystem Restoration (GEER) Conference, December 11-15, 2000: U.S. Geological Survey Open-File Report 00-449.

Beccue, Shirley, 1999, Endangered species: Everglades National Park: Public Affair Office summary, accessed August 20, 2003, at http://www.nps.gov/ever/eco/danger.htm

Benque, J., Cunge, J., Fevillet, and others, 1982, New method for tidal current computations: American Society of Civil Engineers Journal of the Waterways, Ports, and Coastal Ocean Division, v. 108, p. 396-417.

Brion, L.M., Senarath, Sharika, Lal, Wasantha, and others, 2000, Concepts and algorithms for an integrated surface water/groundwater model for natural areas: Proceedings of the Greater Everglades Ecosystem Restoration (GEER) Science Conference, Naples, Florida, December 11-15 2000, p. 280.

Carter, Virginia, Rybicki, N.B., Reel, J.T., and others, 1999, Classification of vegetation for surface-water flow models in Taylor Slough, Everglades National Park: Proceedings of the 3rd International Symposium on Ecohydraulics, Salt Lake City, Utah, July 13-16 1999.

Chadwick, Helen, 1996, Module 1 (Meteorology), Section 3, The structure of the wind: wind energy training course: De Montfort University, 6 p., accessed September 9, 2003, at http://www.iesd.dmu.ac.uk/wind_energy/wetc132.html .

Cole, T.M., and Buchak, E.M., 1995, CE-QUAL-W2-A two-dimensional, laterally averaged, hydrodynamic and water quality model, version 2.0 user manual: Vicksburg, Miss., Instruction Report EL-95-1, U.S. Army Engineer Waterways Experiment Station, 57 p., app.

Craighead, F.C., and Holden, M., 1965, A preliminary report on the closure of the culverts along the mangrove area of the Flamingo Highway and some observations on the effects of changing water levels on wildlife and plants: Research Pamphlet 43-C, Everglades National Park, Homestead, Fla., 32 p.

Deangelis, D.L., 2000, Across Trophic-Level Systems Simulation (ATLSS) Program: U.S. Geological Survey Program on the South Florida Ecosystem: 2000 Proceedings of the Greater Everglades Ecosystem Restoration (GEER) Conference, December 11-15, 2000: U.S. Geological Survey Open-File Report 00-449.

Desmond, G.B., Cyran, Edward, Caruso, Vince, and others, 2000, Topography of the Florida Everglades: U.S. Geological Survey Program on the South Florida Ecosystem: 2000 Proceedings of the Greater Everglades Ecosystem Restoration (GEER) Conference, December 11-15, 2000: U.S. Geological Survey Open-File Report 00-449.

Duever, M.J., Meeder, J.F., Meeder, L.C., and McCollom, J.M., 1994, The climate of south Florida and its role in shaping the Everglades ecosystem *in* S.M. Davis and J.C. Ogden, eds., Everglades–The ecosystem and its restoration: Delray Beach, Fla., St. Lucie Press, p. 225-248.

Elder, J.W., 1959, The dispersion of marked fluid in turbulent shear flow: Journal of Fluid Mechanics, v. 5, p. 544-560.

Fischer, H.B., List, J.E., Koh, R.C.Y., and others, 1979, Mixing in inland and coastal waters: New York, N.Y., Academic Press, p. 126-127, 263.

Fish, J. E., and Stewart, Mark, 1991, Hydrogeology of the surficial aquifer system, Dade County, Florida: U.S. Geological Survey Water-Resources Investigation Report 90-4018, 53 p.

Fitterman, D.V., 1996, Geophysical mapping of freshwater/saltwater interface in Everglades National Park, Florida: U.S. Geological Survey Fact Sheet FS-173-96, 4 p.

Fitterman, D.V., and Deszcz-Pan, Maria, 1998, Helicopter EM mapping of saltwater intrusion in Everglades National Park, Florida: Exploration Geophysics, v. 29, p. 240-243.

——— 1999, Geophysical mapping of saltwater intrusion in Everglades National Park, Proceedings of the 3rd International Symposium on Ecohydraulics, Salt Lake City, Utah, July 13-16 1999.

French, R.H., 1985, Open channel hydraulics: New York, N.Y., McGraw-Hill, 129 p.

German, E.R., 1995, Regional evaluation of evapotranspiration in the Everglades: U.S. Geological Survey Fact Sheet FS-134-95, 5 p.

——— 1999, Regional evaluation of evapotranspiration in the Everglades: Proceedings of the 3rd International Symposium on Ecohydraulics, Salt Lake City, Utah, July 13-16 1999.

——— 2000a, Regional evaluation of evapotranspiration in the Everglades: U.S. Geological Survey Water-Resources Investigations Report 00-4217, 48 p.

——— 2000b, Regional evaluation of evapotranspiration in the Everglades: U.S. Geological Survey Program on the South Florida Ecosystem: 2000 Proceedings of the Greater Everglades Ecosystem Restoration (GEER) Conference, December 11-15, 2000: U.S. Geological Survey Open-File Report 00-449.

Goodwin, C.R., 1977, Circulation patterns for historical, existing, and proposed channel configurations in Hillsborough Bay, Florida (Section 1-4): Proceedings of the 24th International Navigation Congress: Permanent International Association of Navigation Congresses, Brussels, Belgium, 13 p.

——— 1987, Tidal-flow, circulation, and flushing changes caused by dredge and fill in Tampa Bay, Florida: U.S. Geological Survey Water-Supply Paper 2282, 88 p.

——— 1991, Tidal-flow, circulation, and flushing changes caused by dredge and fill in Hillsborough Bay, Florida: U.S. Geological Survey Water-Supply Paper 2376, 49 p.

——— 1996, Simulation of tidal-flow, circulation, and flushing of the Charlotte Harbor estuarine system, Florida: U.S. Geological Survey Water-Resources Investigations Report 93-4153, 92 p.

Halley, R.B., and Prager, E.J., 1996, Sedimentation, sea level rise, and circulation in Florida Bay: U.S. Geological Survey Fact Sheet FS-156-96, 4 p.

Hansen, Mark, and DeWitt, Nancy, 1998, Modern and historical bathymetry of Florida Bay: U.S. Geological Survey Fact Sheet FS-96-98, 5 p.

Harvey, J.W., Choi, Jungyill, and Mooney, R.H., 2000a, Hydrologic interaction between surface water and ground water in Taylor Slough, Everglades National Park: U.S. Geological Survey Program on the South Florida Ecosystem: 2000 Proceedings of the Greater Everglades Ecosystem Restoration (GEER) Conference, December 11-15, 2000: U.S. Geological Survey Open-File Report 00-449.

Harvey, J.W., Jackson, J.M., Mooney, R.H., and Choi, J., 2000b, Interactions between ground water and surface water in Taylor Slough and Vicinity, Everglades National Park, south Florida: Study Methods and Appendixes: U.S. Geological Survey Open-File Report 00-483, 67 p.

Helsel, D.R., and Hirsch, R.M., 1992, Statistical Methods in Water Resources: New York, N.Y., Elsevier, 522 p.

Henkle, Charles, 1996, South Florida high-accuracy elevation data collection project: U.S. Geological Survey Fact Sheet FS-162-96, 3 p.

Hittle, C.D., 2000, Quantity, timing, and distribution of freshwater flows into northeastern Florida Bay: U.S. Geological Survey Program on the South Florida Ecosystem: 2000 Proceedings of the Greater Everglades Ecosystem Restoration (GEER) Conference, December 11-15, 2000: U.S. Geological Survey Open-File Report 00-449.

Holmes, C.W., Robbins, John, Halley, Robert, and others, 2000, Sediment dynamics of Florida Bay mud banks on a decadal time scale: U.S. Geological Survey Program on the South Florida Ecosystem: 2000 Proceedings of the Greater Everglades Ecosystem Restoration (GEER) Conference, December 11-15, 2000: U.S. Geological Survey Open-File Report 00-449.

Jenter, Harry, 1999, Laboratory experiments for evaluating the effects of wind forcing on shallow waters with emergent vegetation: Coastal Ocean Processes Symposium: A Tribute to William T. Grant: Woods Hole Oceanographic Institution Technical Report, 15 p.

Jenter, H.L., and Duff, M.P. 1999, Locally-forced wind effects on shallow waters with emergent vegetation: Proceedings of the 3rd International Symposium on Ecohydraulics, Salt Lake City, Utah, July 13-16 1999.

Jones, J.W., 1999, Land characterization for hydrologic modeling in the Everglades: Proceedings of the 3rd International Symposium on Ecohydraulics, Salt Lake City, Utah, July 13-16 1999.

Large, W.G., and Pond, S., 1981, Open ocean momentum flux measurements in moderate to strong winds: Journal of Physical Oceanography, v. 11, p. 324-336.

Lee, J.K., and Carter, Virginia, 1996, Vegetation affects water movement in the Florida Everglades: U.S. Geological Survey Fact Sheet FS-147-96, 5 p.

Lee, J.K., Carter, Virginia, and Rybicki, N.B., 1999, Determining flow-resistance coefficients in the Florida Everglades: Proceedings of the 3rd International Symposium on Ecohydraulics, Salt Lake City, Utah, July 13-16, 1999.

Lee, J.K., Jenter, H.L., Lai, V.C., and others, 2000a, A pipe manometer for the determination of very small water-surface slopes in the Florida Everglades: U.S. Geological Survey Program on the South Florida Ecosystem: 2000 Proceedings of the Greater Everglades Ecosystem Restoration (GEER) Conference, December 11-15, 2000: U.S. Geological Survey Open-File Report 00-449.

Lee, J.K., Roig, L.C., Jenter, H.L., and Visser, H.M., 2000b, Determination of resistance coefficients for flow through submersed and emergent vegetation in the Florida Everglades: U.S. Geological Survey Program on the South Florida Ecosystem: 2000 Proceedings of the Greater Everglades Ecosystem Restoration (GEER) Conference, December 11-15, 2000: U.S. Geological Survey Open-File Report 00-449.

Lee, J.K., Schaffranek, R.W., and Baltzer, R.A., 1989, Convergence experiments with a hydrodynamic model of Port Royal Sound, South Carolina: Proceedings of the 1989 National Hydraulic Engineering Conference, New York, N.Y., p. 434-441.

——— 1994, Simulating effects of highway embankments on estuarine circulation: Journal of Waterway, Port, Coastal, and Ocean Engineering, v. 120, no. 2, p. 199-218.

Leendertse, J.J., 1987, Aspects of SIMSYS2D, a system for two-dimensional flow computation: Santa Monica, Calif., Rand Corporation Report R-3572-USGS, 80 p.

——— 1988, A summary of experiments with a model of the Eastern Scheldt: Santa Monica, Calif., Rand Corporation Report R-3611-NETH, 41 p.

Leendertse, J.J., and Gritton, E.C., 1971, A water-quality simulation model for well-mixed estuaries and coastal seas: Volume 2, Computation Procedures: New York City Rand Institute, Report R-708-NYC, 53 p.

Leendertse, J.J., Langerak, A., and de Ras, M.A.M., 1981, Two-dimensional tidal models for the Delta Works: Transport models for inland and coastal waters: Proceedings of the Symposium on Predictive Abilities: New York, N.Y., Academic Press, p. 408-450.

Lin, H.C., Talbot, C.A., Richards, D.R., and others, 2000, Development of a multidimensional modeling system for simulating canal, overland, and groundwater flow in south Florida: Waterways Experiment Station, Vicksburg, Miss., U.S. Army Corps of Engineers report.

Linsley, R.K. Jr., Kohler, M.A., and Paulhus, J.L.H., 1982, Hydrology for engineers: New York, N.Y., McGraw-Hill, p.162-163.

Lumley, J.L., and Panofsky, H.A., 1964, The structure of atmospheric turbulence: John Wiley, New York.

MacVicar, T.K., VanLent, Thomas, and Castro, Alvin, 1984, South Florida Water Management Model documentation report: South Florida Water Management District Technical Publication 84-3, 123 p.

McAdory, R.T., and Kim, K.W., 1998, Field and model studies in support of the evaluation of impacts of the C-111 Canal on regional water resources, south Florida, Part IV: Florida Bay hydrodynamic modeling, U.S. Army Corps of Engineers, Waterways Experiment Station.

Merritt, M.L., 1996, Simulation of the water-table altitude in the Biscayne aquifer, southern Dade County, Florida, water years 1945-89: U.S. Geological Survey Water-Supply Paper 2458.

Miller, R.L., Bradford, W.L., and Peters, N.E., 1988, Specific conductance: theoretical considerations and application to analytical quality control: U.S. Geological Survey Water-Supply Paper 2311.

North Carolina Geographic Information Coordinating Council, 1999, Official method for horizontal reference conversions: Position Paper 99-01, GIS Technical Advisory Board, 4 p.

Nuttle, W.K., 1995, Dynamics of groundwater, surface water, and salinity related to the mangrove/marsh ecotone: assembled historical data sets: Prepared for Global Climate Change Research Program, South Florida Biogeographic Region.

Ott, R.L., 1993, An introduction to statistical methods and data analysis: Calif., Duxbury Press, p. 475, 566.

Patino, Eduardo, 1996, Gaging flows in northeastern Florida Bay: U.S. Geological Survey Fact Sheet FS-130-96, 5 p.

Reid, R.O., and Whitaker, R.E., 1976, Wind-driven flow of water influenced by a canopy: Journal of the Waterways, Harbors, and Coastal Engineering Division, v. 102, no. WW1, p. 61-77.

Ridderinkhof, H., and Zimmerman, J.T.F., 1992, Chaotic stirring in a tidal system: Science, v. 258, p. 1107-1111.

Riley, J.P., and Skirrow, G., eds., 1975, Chemical oceanography: New York, N.Y., Academic Press, v. 5, p. 340.

Roache, P.J., 1982, Computational fluid dynamics: Albuquerque, N.M., Hermosa Publishers, 446 p.

Robbins, J.C., and Bales, J.D., 1995, Simulation of hydrodynamics and solute transport in the Neuse River Estuary, North Carolina: U.S. Geological Survey Open-File Report 94-511, 85 p.

Rose, P.W., Flora, M.D., and Rosendahl, P.C., 1981, Hydrologic impact of L-31W on Taylor Slough, Everglades National Park: South Florida Research Center Report T-612.

Russell, G.M., and Goodwin, C.R., 1987, Simulation of tidal flow and circulation patterns in the Loxahatchee River Estuary, southeastern Florida: U.S. Geological Survey Water-Resources Investigations Report 87-4201, 32 p.

Schaffranek, R.W., 1986, Hydrodynamic simulation of the Upper Potomac Estuary: Proceedings of the Water Forum 86: World Water Issues in Evolution, American Society of Civil Engineers: New York, N.Y., v. 2, p. 1572-1581.

——— 1996, Coupling models for canal and wetland interactions in the south Florida ecosystem: U.S. Geological Survey Fact Sheet FS-239-96, 8 p.

Schaffranek, R.W., and Ball, M.H., 2000, Flow velocities in wetlands adjacent to C-111 Canal in south Florida, U.S. Geological Survey Open File Report 00-449, p. 45-47.

Schaffranek, R.W., and Baltzer, R.A., 1988, A simulation technique for modeling flow on floodplains and in coastal wetlands: Proceedings of the 1988 National Hydraulic Engineering Conference, American Society of Civil Engineers: New York, N.Y., p. 732-739.

——— 1990, Horizontal density-gradient effects on simulation of flow and transport in the Potomac estuary: Proceedings of the 1990 National Hydraulic Engineering Conference, New York, N.Y., p. 1251-1256.

Schaffranek, R.W., Ruhl, H.A., and Hansler, M.E., 1999, An overview of the Southern Inland and Coastal Systems Project of the U.S. Geological Survey South Florida Ecosystem Program: Proceedings of the 3rd International Symposium on Ecohydraulics, Salt Lake City, Utah, July 13-16 1999.

Signell, R.P., and Butman, B., 1992, Modeling Tidal Exchange and Dispersion in Boston Harbor: Journal of Geophysical Research, v. 97, p. 15591-16606.

Smith, N.P. 2001, Wind-forced interbasin exchanges in Florida Bay: Proceedings of the 2001 Florida Bay Science Conference, Key Largo, Fla., April 23-26 2001.

Smith III, T.J. 1998, Imperiled wetlands: review of mangroves and salt marshes: Nature, no. 395, p. 131-132.

Stewart, Dave, 1997, A GIS interface for environmental systems analysis: application to the south Florida ecosystem: U.S. Geological Survey Fact Sheet FS-193-97, 5 p.

Stewart, M.A., Bhatt, T.N., Fennema, R.J., and Fitterman, D.V., 2000, The road to Flamingo, an evaluation of flow pattern alterations and salinity intrusion in the lower Glades, Everglades National Park, National Park Service Report, 36 p.

Swain, E.D., 1999, Numerical representation of dynamic flow and transport at the Everglades/Florida Bay interface: Proceedings of the 3rd International Symposium on Ecohydraulics, Salt Lake City, Utah, July 13-16 1999.

Swain, E.D., Howie, Barbara, and Dixon, Joann, 1996, Description and field analysis of a coupled ground-water/surface-water flow model (MODFLOW/BRANCH) with modifications for structures and wetlands in southern Dade County, Florida: U.S. Geological Survey Water-Resources Investigation Report 96-4118, 67 p.

Thomas, L., Cartwright, J.C., and Wakeling, D.P., 1990, Lidar Observation of the Horizontal Orientation of Ice Crystals in Cirrus Clouds, Tellus v. 42B, p. 211-216.

Tillis, G.M., 2001, Measuring Taylor Slough boundary and internal flows, Everglades National Park, Florida: U.S. Geological Survey Open-File Report 01-225, 16 p.

Tompson, A.F.B., Ababou, Rachid, and Gelhar, L.W.,1989, Implementation of the three-dimensional turning bands random field generator: Water Resources Research, v. 25, no. 10, p. 2227-2243.

U.S. Army Corps of Engineers, 1992, Modified water deliveries to Everglades National Park, Central and Southern Florida Project, Part 1, Agricultural and Conservation Areas, Supplement 54, General Design Memorandum and Environmental Impact Statement.

——— 1999, Central and southern Florida comprehensive review study: Final integrated feasibility report and programmatic environmental impact statement, April 1999.

Van Lent, T.J., Snow, R.W., and James, Fred, 1998, An examination of the Modified Water Deliveries Project, the C-111 Project and the Experimental Water Deliveries Project: Hydrologic analyses and effects on endangered species: Everglades National Park Technical Report, 232 p.

Weare, T.J., 1979, Errors arising from irregular boundaries in ADI solutions of the shallow-water equations: International Journal for Numerical Methods in Engineering, v. 14, p. 921-931.

Westerink, J.J., and Gray, W.G., 1991, Progress in surface water modeling: Reviews in geophysics (supplement): U.S. National Report to International Union of Geodesy and Geophysics, 1987-90, p. 210-217.

Wilson, B.W., 1960, Note on surface wind stress over water at low and high wind speeds: Journal of Geophysical Research, v. 65, no., 10, p. 3377-3382.

Zhang, L., Dawes, W.R., and Walk, G.R., 2000, The response of mean annual evapotranspiration to vegetation changes at catchment scale: Water Resources Research, v. 37, p. 701-708.

APPENDIX I – SWIFT2D SUBROUTINES MODIFIED FOR SOUTHERN INLAND AND COASTAL SYSTEMS (SICS)

SWIFT2D.F: Modified input of point discharges to allow areal gains and losses as user input and areal computation of evapotranspiration.

SEPU.F: Modified input of point discharges to allow areal gains and losses as user input and areal computation of evapotranspiration. Sheltering coefficient applied for wind forcing in vegetated areas. Wind forcing not applied to cells adjacent to water-level boundary.

SEPV.F: Modified input of point discharges to allow areal gains and losses as user input and areal computation of evapotranspiration. Sheltering coefficient applied for wind forcing in vegetated areas. Wind forcing not applied to cells adjacent to water-level boundary. Error fixed to allow multiple barriers to function properly in the same grid column.

DIFU.F: Modified to allow concentrations of constituents to be affected by areal recharge and evapotranspiration. Defined zero concentration of all constituents at barriers when barriers run dry.

DIFV.F: Modified to allow concentrations of constituents to be affected by areal recharge and evapotranspiration. Defined zero concentration of all constituents at barriers when barriers run dry.

TIDAL.F: Modified input of point discharges to allow areal gains and losses as user input and areal computation of evapotranspiration.

TIMSMO.F: Modified input of point discharges to allow areal gains and losses as user input and areal computation of evapotranspiration.

BARENU.F: Modified to stop flow across a barrier if an adjacent grid cell runs dry.

BARENV.F: Modified to stop flow across a barrier if an adjacent grid cell runs dry.

SLUCEU.F: Modified to allow grid cells adjacent to barriers to run dry without ending the simulation.

SLUCEV.F: Modified to allow grid cells adjacent to barriers to run dry without ending the simulation.

FLOW.F: Modified so that constituent concentration at selected points is printed at the same time interval as water levels and discharges.

OUT.F: Modified so that grid values of water level and velocities are printed to a different file than the remainder of the output. Printed velocities are multiplied by 10^3 rather than 10^2, which is better for the low velocities in this application.

APPENDIX II – EXCERPT FROM INPUT FILE HIGHLIGHTING AREAL GAINS AND LOSSES

```
RUN NUMBER 1
WETLANDS        15 JUL ‘96  98/ 8/2517:23:39 IDPV514
   7.5  15.0   0.0      329190999999  120.999999 1440. 1440. 1440. 1440.
999999999999999999   15.   45.   30.999999   60.999999999999999999    0.
     0     0     2     0     0     5     1     0     0     0     0     0
     7     3     4     4     0     4
     1
     0     1     1     1     0     0     0     0     0
     1     0     0     0     0     0     0
 2160 10800 19440 28080 36720 45360 54000 62640 71280 79920 88560 97200
1058401144801231201317601404001490401576801663201749601836001922402008 80
2095202181602268002354402440802527202613602700002786402872802959203045 60

   148    98     1    14     0     9     0     3     5     5     0     1
    94   122
              0.5                                   1
25.000   0.0 1000.  2.55   0.0   0.3    1.  1.00   0.5   1.0   5.0 300.0
    32.2  0.0012 0.00237  1.9362  1.0000    14.3  1000.0    0.97  0.0023
FR80      35SPRO           1.0   1.0
    25     1   0.0  13.0  20.0  14.0K/HR             5
   4.0 170.0  2.00 121.0 163.0  1.25  74.0  89.0  1.00 122.0 103.0  1.00
   1.0   2.0   2.0   2.0   2.0
     1     1     2   0.5   1.0 -0.40 -0.40  0.25   1.0   0.0     1     1

    25.0  1.0250   0.698   1.0
    1   57   36 CP
    2  109   78 EVER4
    3  100   58 EVER5A
    4   69   45 E146
    5   98   97 E158
    6  142   52 EP12R
    7  139   57 EP1R
    8  123   55 EPGW
    9  120   61 EVER6
   10  110   65 EVER7
   11   74   73 NP67
   12   62   56 P37
   13   89   81 R127
   14   81   66 TSH
    1   90   90 TSB <------------------ FLOW FROM TAYLOR SLOUGH BRIDGE
    2  -68  -70 Old Ingraham <--------- RAINFALL AT OLD INGRAHAM HIGHWAY
    3 -105  -36 Joe Bay <--------------- RAINFALL AT JOE BAY
    4  100   88 L-31W <---------------- FLOW FROM L-31W CANAL
    5   27   45 west culverts <-------- FLOW THROUGH CULVETS ON WEST BOUNDARY
    6  120   64 C-111 <---------------- FLOW FROM C-111 CANAL
    7  -80  -72 GW Leakage <----------- POINT OF PEAK GROUND-WATER INFLOW IN NORTHERN AREA
    8  -80  -26 no GW Leakage <-------- POINT OF NO GROUND-WATER INFLOW IN SOUTHERN AREA
    9    0    0 Pyranometer <---------- TIME SERIES OF PYRANOMETER SOLAR ENERGY
    1   93   31   36 Joe Bay 1
    2   98   36   40 Joe Bay 2
    3  116   34   39 Joe Bay 3
```